Western Graduate&PostdoctoralStudies

Western University
Scholarship@Western

Electronic Thesis and Dissertation Repository

2-15-2018 9:30 AM

The Role Of FER Kinase In Human Melanoma Growth and Invasion

Shinthujah Arulanantham, *The University of Western Ontario*

Supervisor: Dagnino, Lina, *The University of Western Ontario*

A thesis submitted in partial fulfillment of the requirements for the Master of Science degree in Physiology and Pharmacology

© Shinthujah Arulanantham 2018

Follow this and additional works at: https://ir.lib.uwo.ca/etd

Part of the Medical Cell Biology Commons

Recommended Citation

Arulanantham, Shinthujah, "The Role Of FER Kinase In Human Melanoma Growth and Invasion" (2018). *Electronic Thesis and Dissertation Repository*. 5272.
https://ir.lib.uwo.ca/etd/5272

This Dissertation/Thesis is brought to you for free and open access by Scholarship@Western. It has been accepted for inclusion in Electronic Thesis and Dissertation Repository by an authorized administrator of Scholarship@Western. For more information, please contact wlswadmin@uwo.ca.

Abstract

Feline sarcoma-related (FER) kinase is a ubiquitous non-receptor tyrosine kinase overexpressed in many cancer types. It promotes proliferation, migration and metastasis in prostate, lung and ovarian carcinoma cells, respectively. However, the biological roles of FER in human metastatic melanoma have not been explored. I used a doxycycline-inducible, lentivirus-based shRNA approach to silence FER kinase expression in the 131/4-5B1 human melanoma (hereafter termed 5B1) cells. I determined fewer FER-deficient 5B1 cells in the S-phase of the cell cycle and reduced motility of FER-deficient 5B1 cells, suggesting that FER promotes 5B1 cell cycle transit and migration. *In vivo* chorioallantoic membrane (CAM) studies demonstrate that FER-deficient 5B1 cells have an increased capacity to invade into CAM mesoderm and that both FER-expressing and FER-deficient tumours acquire endothelial cells within the tumour. My study outlines a novel role for FER kinase in 5B1 cell proliferation, migration and invasion.

Keywords

FER kinase, metastatic human melanoma, proliferation, migration, chorioallantoic membrane, invasion

Co-Authorship Statement

All of the experiments presented in this thesis were conducted by me with the exception of the lentiviral transductions performed by Dr. Iordanka Ivanova, egg cracking procedures performed by Danielle Johnston and Taylor Freeman, rhodamine-labelled lectin injections performed by Dr. Mario Cepeda and tumour tissue sectioning performed by Kevin Barr.

Acknowledgments

First and foremost, I would like to thank my supervisor, Dr. Lina Dagnino for being a constant source of knowledge and support. From the moment I first stepped into the lab as a 4th year thesis student, up until my very last edit, I haven't stopped learning. Thank you for teaching me that there is no such thing as a failed experiment, but rather there is something to be learned from every experiment. I now understand the placement of hyphens and the difference between fluorescent and fluorescence. Thank you for being patient with me and for your numerous letters. You understood my full potential and therefore challenged me to reach new heights.

Next, I would like to thank Dr. Iordanka Ivanova. I started with minimal expertise in wet lab research, however, with your patience and guidance, I have acquired different skill sets and can proficiently perform various assays and techniques. Thank you for the many hours we've spent planning experiments and next steps. You taught me to critically analyze challenges and reassured me that some solutions required more digging than others. Thank you for being a constant source of support and for sharing your passion for research with me.

Thank you to the members of my advisory committee, Dr. John Di Gugielmo and Dr. Silvia Penuela. Despite your busy schedules, you made time to meet with me every 3 to 4 months to ensure I was on track and was occupying my time in the most efficient manner to complete my experiments. Thank you for all the insightful feedback and kind words of encouragement! A special thanks to the members of the Penuela lab for all the help you provided me throughout my CAM experiments. Thank you for the numerous eggs you cracked for me, and for fitting my experiments into your busy schedules.

Next, I would like to thank the present and former members of the Dagnino Lab. My big sister, Mell, thank you for always being there for me, for listening to my stories and rants, and providing the best advice and support! You were excited and optimistic for me even when I wasn't. Your 'beautiful' voice and bubbly personality has made me laugh more times than I can count. Thank you for being weird with me :). Kevin, sectioning all those tumours was quite the task (to say the least), thank you so much for helping me out and for all your witty remarks as I stained yet another set of sections. Morgan, thank you for listening to my endless tales, tackling mounting tumours for the first time with me and for being clumsier than me. Miki, in the short timespan I've gotten to know you, we have become such great friends, thank you for being such amazing company during our microscope times. Ran, thank you for all your suggestions and well-thought input anytime I came to you and for being the one who stuck around lab as late as I did. Hannah, thank you for telling me how nice my hair was at least 3 times a week and for all your witty, clever remarks. Lastly, thank you Eddie (unofficial member) for all your support and impromptu visits, especially during all those laborious section staining evenings.

Last but not least, thank you to all my friends who have been the absolute best support system. You made sure I was sane, you picked up every phone call and responded to every message with words of encouragement and positivity. I am forever grateful for you all! Finally, thank you to my parents, Arul and Uma, for all your support and for being so patient with me during this journey, I truly appreciate it!

Table of Contents

Abstract i

Co-Authorship Statement ii

Acknowledgments iii

List of Tables viii

List of Figures ix

List of Appendices xi

List of Abbreviations xii

Chapter 1 1

1 Introduction 1

1.1 Melanocytes as the cells of origin of melanoma 1

1.2 Driver genetic mutations in melanoma 4

1.3 Other common genetic mutations found in melanoma 8

1.4 Melanoma progression and clinical staging 9

1.5 Current therapies for melanoma 12

1.6 Preclinical models used to study metastatic melanoma 16

1.6.1 Human melanoma cell lines 16

1.6.2 The chick chorioallantoic membrane (CAM) model 17

1.6.3 Mouse melanoma models 18

1.7 FER kinase 21

1.7.1 The FES family of non-receptor tyrosine kinases 21

1.7.2 FER kinase protein-protein interactions 24

1.7.3 The role of FER kinase in human tumours 26

1.8 Rationale, hypothesis and aims 29

Chapter 2 31

2 Materials and methods 31
2.1 Reagents 31
2.2 Materials 33
2.3 Antibodies 35
2.4 Preparation of poly-L-lysine (PLL)-coated glass coverslips 37
2.5 Preparation of poly-HEMA coated dishes 37
2.6 Laminin 332 matrix production, collection and coating procedures 37
2.7 Cell culture and doxycycline treatments 38
2.8 Analysis of cell proliferation 40
2.9 Apoptosis and anoikis analysis 41
2.10 Cell motility assays 41
2.11 Immunoblot analysis 42
2.11.1 Preparation of cell lysates 42
2.11.2 Polyacrylamide gel electrophoresis and immunoblot analysis 42
2.12 Immunofluorescence microscopy 44
2.13 Chorioallantoic Membrane (CAM) experiments 45
2.13.1 Chicken embryo incubation 45
2.13.2 Tissue sectioning 46
2.13.3 Immunohistochemistry analyses 46
2.14 Statistical analyses 47
Chapter 3 48
3 Results 48
3.1 Characterization of Control and FER 9 human melanoma cells 48
3.2 Effects of FER knockdown on cell proliferation 52
3.3 Effect of FER kinase silencing on 5B1 susceptibility to anoikis 60
3.4 Effects of FER knockdown on random 5B1 cell motility 60

3.5 The chicken chorioallantoic membrane (CAM) *in vivo* tumour xenograft model to study tumour invasion 65

3.6 Comparison of 5B1 tumour growth in Matrigel and Cultrex 72

3.7 Analysis of 5B1 cell invasion into the CAM mesoderm 74

3.8 Effect of FER kinase silencing on 5B1 cell invasion into the CAM mesoderm... 74

Chapter 4 88

4 Discussion 88

4.1 Summary 88

4.2 FER kinase modulates cell cycle progression 88

4.3 5B1 cell susceptibility to anoikis 90

4.4 FER is necessary for normal 5B1 cell migration on laminin 332 91

4.5 The study of 5B1 melanoma tumour formation using the *in vivo* chicken chorioallantoic membrane model 93

4.6 FER kinase and 5B1 melanoma cell invasion into the CAM 94

4.7 FER kinase effects on endothelial cell localization to 5B1 tumours 98

4.8 Future directions 99

4.9 Limitations to the study 99

4.10 Concluding remarks 101

References 104

Appendices 122

List of Tables

Table 2.1: Reagents 31

Table 2.2: Materials 33

Table 2.3: Antibodies 35

Table 3.1: Characteristics of excised tumours 84

List of Figures

Figure 1.1. Schematic of the epidermis 2

Figure 1.2. MAPK signaling pathway 6

Figure 1.3. PI3K signaling pathway 7

Figure 1.4. T-cell inactivation by tumour cells 15

Figure 1.5. FER kinase protein domains 22

Figure 3.1. FER kinase knockdown of Control and FER 9 cells 49

Figure 3.2. Melanocytic lineage confirmation of GFP-positive 5B1 cells 51

Figure 3.3. Duration of FER kinase knockdown after dox removal in 5B1 cells 54

Figure 3.4. Effect of FER kinase silencing on 5B1 expression of Ki67 57

Figure 3.5. Effect of FER kinase silencing on 5B1 cells in S-phase 59

Figure 3.6. FER kinase knockdown on 5B1 cell susceptibility to anoikis 61

Figure 3.7. 5B1 migration on different extracellular matrices 64

Figure 3.8. Effect of FER kinase knockdown on 5B1 motility 67

Figure 3.9. Illustration of the chicken chorioallantoic membrane (CAM) used to measure 5B1 cell invasion 71

Figure 3.10. Capacity of Matrigel and Cultrex matrices to support 5B1 tumour growth 73

Figure 3.11. Systematic analysis of 5B1 cell invasion into the CAM mesoderm 76

Figure 3.12. Analysis of 5B1 invasion into the CAM mesoderm in ten sections of a FER-expressing tumour 79

Figure 3.13. Analysis of 5B1 invasion into the CAM mesoderm in ten sections of a FER-deficient tumour 83

Figure 3.14. Effect of FER kinase on 5B1 cell invasion into the CAM mesoderm..... 85

Figure 3.15. Effect of FER kinase on endothelial cell localization to the tumour..... 87

List of Appendices

Appendix A: Additional representative fluorescence micrographs depicting Control and FER 9 cell invasion into the CAM mesoderm 122

Appendix B: Additional representative fluorescence micrographs depicting endothelial cell localization to FER 9 tumours. 123

List of Abbreviations

Abbreviations	Full Name
ARP	Actin-related protein
ATP	Adenosine triphosphate
BRDU	Bromodeoxyuridine
CAM	Chorioallantoic membrane
CDK4	Cyclin-dependent kinase 4
CDKN2A	Cyclin-dependent kinase inhibitor 2A
CSD	Chronically sun-damaged
CTLA-4	Cytotoxic T-lymphocyte-associated antigen 4
DOX	Doxycycline
DG	Dystroglycan
ECM	Extracellular matrix
EGF	Epidermal growth factor
EGFR	Epidermal growth factor receptor
EMT	Epithelial-mesenchymal transition
FACS	Fluorescence activated cell sorting
FBS	Fetal bovine serum
FER	Feline sarcoma-related
FES	Feline sarcoma/Fujinami avian sarcoma oncogene homolog
GAB1	GRB2-associated-binding protein 1

GEF	Guanine nucleotide exchange factor
GFP	Green fluorescent protein
GM-CSF	Granulocyte-macrophage colony-stimulating factor
GPCR	G protein-coupled receptor
GTP	Guanosine triphosphate
H&E	Hematoxylin and eosin
HGF/SF	Hepatocyte growth factor/scatter factor
IL-6	Interleukin 6
IRS1	Insulin receptor substrate 1
LCA	Lens culinaris agglutinin
LPS	Lipopolysaccharide
mAb	Monoclonal antibody
MAPK	Mitogen-activated protein kinase
MC1R	Melanocortin 1 receptor
MCL-1	Myeloid cell leukemia-1
MHC	Major histocompatibility complex
MITF	Microphthalmia-associated transcription factor
MMP	Matrix metalloproteinase
MSH	Melanocyte stimulating hormone
mTOR	Mammalian target of rapamycin

NF1	Neurofibromin 1
NF-κB	Nuclear factor kappa B
PARP1	Poly [ADP-ribose] polymerase 1
PBS	Phosphate-buffered saline
PD1	Programmed death-1
PDGF	Platelet-derived growth factor
PDGFR	Platelet-derived growth factor receptor
PFA	Paraformaldehyde
PI3K	Phosphoinositide 3-kinase
PIP_2	Phosphatidylinositol-(3,4)-P_2
PIP_3	Phosphatidylinositol-(3,4,5)-P_3
PKA	Protein kinase A
PLL	Poly-L-lysine
PMEL	Premelanosome
POMC	Pro-opiomelanocortin
PP1α	Protein phosphatase 1α
PTEN	Phosphatase and tensin homolog
PTP1B	Protein tyrosine phosphatase 1B
PVDF	Polyvinylidene difluoride
RAC1	Ras-related C3 botulinum toxin substrate 1

RB	Retinoblastoma protein
RhoGDI	Rho GDP-dissociation inhibitor
ROS	Reactive oxygen species
RTK	Receptor tyrosine kinase
SDS-PAGE	Sodium dodecyl sulfate polyacrylamide gel electrophoresis
SH2	Src homology 2
shRNA	small hairpin RNA
SPRY	Sprouty
STAT3	Signal transducer and activator of transcription 3
TBST	Tris buffered saline with tween 20
TCR	T-cell receptor
TERT	Telomerase reverse transcriptase
TIMP	Tissue inhibitor of matrix metalloproteinase
UV	Ultraviolet

Chapter 1

1 Introduction

1.1 Melanocytes as the cells of origin of melanoma

Melanomas are some of the most aggressive human tumours and arise mainly from carcinogenic transformation of epidermal melanocytes. In Canada, the incidence of melanoma has been steadily rising over the past several decades. Of all cancers, melanoma has the 7th highest incidence rate in Canada and about 1.2-1.9 % of cancer deaths in Canada will be due to melanoma (Canadian Cancer Society, 2017).

Melanocytes are melanin-producing cells that originate from the embryonic neural crest. After birth, melanocytes are found in the basal layer of the epidermis (Figure 1.1), in hair follicles, cochlea, iris, meninges and in the heart (Cichorek et al., 2013). A subset of cells that migrates from the neural crest, differentiates into melanoblasts, which are cell precursors that later become melanocyte stem cells and terminally-differentiated melanocytes (Yamaguchi and Hearing, 2014). Melanocytes provide tissue pigmentation by producing melanin within lysosome-like organelles termed melanosomes (Lin and Fisher, 2007). In the skin, melanosomes are transferred from melanocytes to adjacent keratinocytes. The melanin-containing granules are trafficked to perinuclear regions in keratinocytes, forming a protective cap that shields genomic DNA from the harmful effects of solar ultraviolet (UV) radiation (Hearing, 2005). The photoprotective characteristics of melanin include its ability to absorb UV radiation and scavenge reactive oxygen species (ROS) (Brenner and Hearing, 2008). Physiologically, keratinocyte exposure to UV

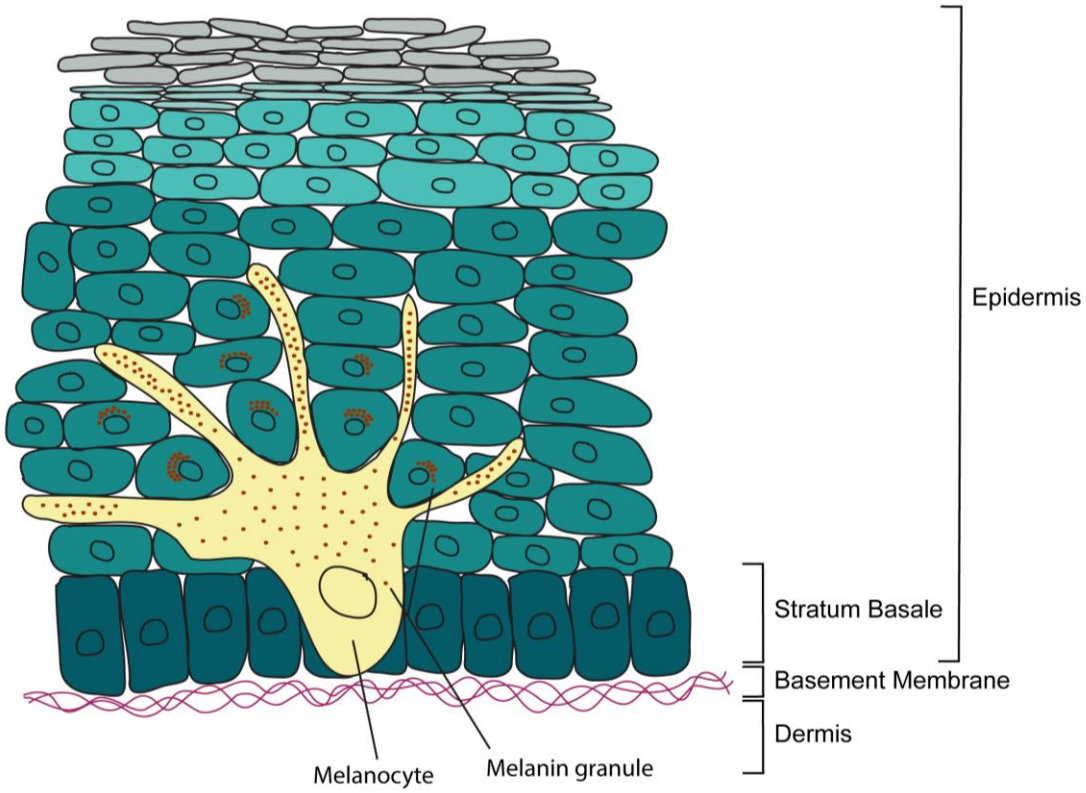

Figure 1.1. Schematic of the epidermis

The epidermis is composed of 5 cell layers. The innermost layer, stratum basale, contains the melanocytes that produce melanin and transfer them in melanosomes to adjacent keratinocytes. The melanin-containing granules (brown dots) form a protective cap over keratinocyte nuclei to shield genomic DNA from solar UV radiation.

radiation results in increased transcription of the pro-opiomelanocortin (POMC) gene, which is required for the production and secretion of melanocyte stimulating hormone (α-MSH). α-MSH released from keratinocytes binds to and activates melanocortin 1 receptors (MC1R) on melanocytes, resulting in intracellular cAMP production followed by protein kinase A (PKA) activation. PKA then activates other proteins and transcription factors, such as the microphthalmia-associated transcription factor (MITF), that are involved in the transcription of enzymes necessary for melanin biosynthesis (D'Orazio et al., 2013).

Excessive exposure to UV radiation is the leading contributor to malignant transformation of melanocytes. Solar UV radiation can be categorized into three types: UVA, UVB and UVC. UVC (100-280 nm) is predominantly absorbed by the atmospheric ozone layer, thus humans are normally not exposed to it. UVA (315-400 nm) can penetrate deep into the dermis of the skin, whereas UVB (280-315) is absorbed predominantly by the epidermis (D'Orazio et al., 2013). UV radiation can lead to direct DNA damage, through the formation of cyclobutene pyrimidine dimers. Additionally, UVA exposure can result in production of ROS, which can cause single or double DNA strand breaks. These DNA lesions can subsequently lead to genetic mutations and tumour formation (Jhappan et al., 2003).

Melanocytes can synthesize two types of melanin, pheomelanin and eumelanin. Eumelanin is a brown/black pigment, whereas pheomelanin is a red/yellow pigment. Both types of melanin are synthesized by the same types of enzymes (Lin and Fisher, 2007). The amount of eumelanin present in the skin determines its colour, and increased eumelanin levels are responsible for darker skin tones (D'Orazio et al., 2013). Pheomelanin is typically found among red-haired individuals (Brenner and Hearing, 2008). The photoprotective properties

of eumelanin are superior to those of pheomelanin. Consequently, light-skinned and red-haired individuals are at a higher risk of developing melanoma (Roider and Fisher, 2016).

Although exposure to UV radiation is the main cause of melanoma, there are subsets of human populations, which develop melanomas not associated with UV exposure. Examples are acral lentiginous melanoma and mucosal melanoma, which have been found in large numbers of individuals in Asian, African and some Latin American countries and develop in body areas not generally exposed to solar UV radiation (Ossio et al., 2017). The recent discovery of germline mutations that influence predisposition to melanoma, suggest that future research should also focus on individuals of non-European descent (Ossio et al., 2017).

1.2 Driver genetic mutations in melanoma

Mutations that directly confer a selective growth or survival advantage to transformed cells are termed driver mutations. In the context of melanoma, a single driver mutation is not sufficient for melanoma formation. Mutations in tumour cell genomes that do not influence cancer development, are termed passenger mutations (Stratton et al., 2009). Several melanoma driver gene mutations have been identified. The most common somatic mutation, which accounts for about 60% of all human melanomas, is in the *BRAF* gene, which encodes the serine/threonine protein kinase B-RAF (Ascierto et al., 2012). The latter functions in the mitogen-activated protein kinase (MAPK) pathway. Over 90% of B-RAF mutations result from a single nucleotide alteration that replaces valine at position 600 for glutamic acid (B-RAF^{V600E}), leading to constitutive activation of B-RAF (Ascierto et al., 2012). The MAPK pathway can be activated by several events. These events include ligand

binding to receptor tyrosine kinases (RTK), such as epidermal growth factor receptor (EGFR), c-KIT and platelet-derived growth factor receptor (PDGFR), with the subsequent activation of RAS, a small GTPase that localizes to the plasma membrane. RAS, in its active GTP-bound form, causes phosphorylation of RAF. RAF phosphorylates MEK, and then MEK phosphorylates and activates ERK, resulting in the activation of several responses, including the transcription of genes involved in cell proliferation and survival (Fecher et al., 2008) (Figure 1.2).

The second most common melanoma driver mutation, observed in about 20 % of tumours, is in the *NRAS* gene. Mutations that replace glutamine at position 61 with lysine or arginine are more prevalently seen, resulting in the synthesis of a constitutively active N-RAS protein (Johnson and Puzanov, 2015). N-RAS belongs to the family of RAS GTPases, and functions as a key component in the MAPK and phosphoinositide 3-kinase (PI3K) signalling pathways (Mehnert and Kluger, 2012). PI3K is activated in response to ligand binding to RTKs, G protein-coupled receptors (GPCRs) or RAS activation through GTP binding, hence mutant N-RAS leads to constitutive activation of PI3K. Active PI3K is responsible for the conversion of phosphatidylinositol-(3,4)-P_2 (PIP_2) to phosphatidylinositol-(3,4,5)-P_3 (PIP_3). PIP_3 interacts with numerous proteins including AKT which is a serine/threonine kinase that becomes activated upon phosphorylation, and then activates other downstream effectors, such as mTOR, which is involved in regulating cell survival and growth. The overall activity of the PI3K pathway is negatively regulated by the phosphatase PTEN, and, significantly, mutations in PTEN are also observed in melanoma (Davies, 2012; Mehnert and Kluger, 2012) (Figure 1.3).

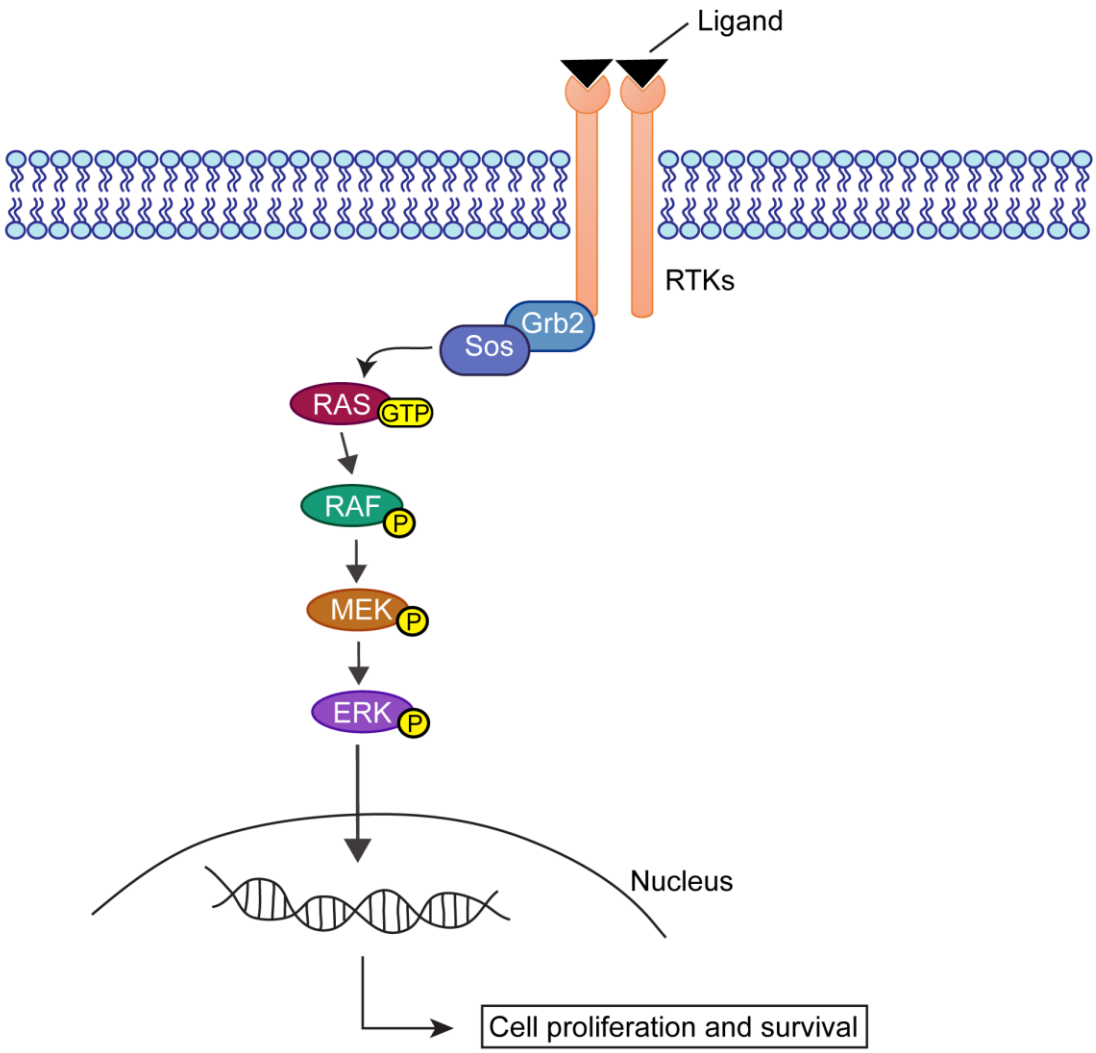

Figure 1.2. MAPK signaling pathway

Receptor tyrosine kinases (RTKs) are activated by ligand binding. Grb2 binds to the activated receptor and to Sos, forming the Grb2/Sos complex. Sos then promotes the activation of RAS by removing GDP. The GTP-bound active RAS causes phosphorylation of RAF. RAF then phosphorylates MEK and MEK phosphorylates ERK. Active ERK promotes the transcription of genes involved in cellular proliferation and survival.

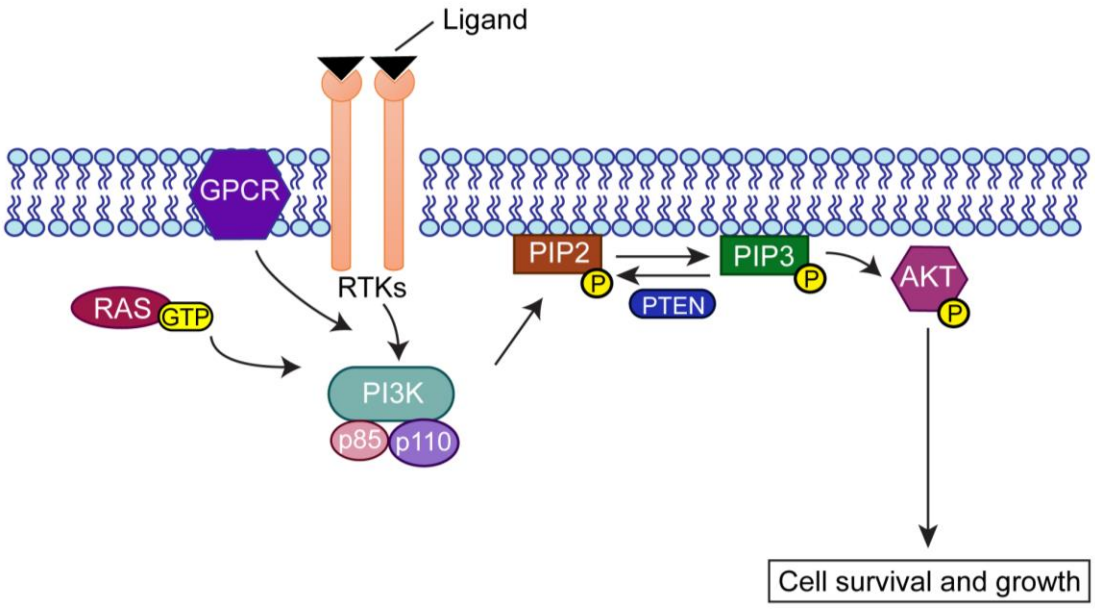

Figure 1.3. PI3K signaling pathway

PI3K is comprised of a regulatory and catalytic subunit termed p85 and p110, respectively. PI3K is activated by ligand-bound receptor tyrosine kinases (RTKs), G protein-coupled receptors (GPCR) or GTP-bound RAS. Active PI3K interacts with lipid substrates on the plasma membrane and results in the formation of PIP_3 from PIP_2. PIP_3 phosphorylates and activates AKT and AKT then activates downstream effectors involved in the regulation of cell survival and growth. PTEN negatively regulates the PI3K pathway by reversing the PIP_2 to PIP_3 conversion.

Mutations in *RAC1* are found in 9% of cutaneous melanomas (Krauthammer et al., 2012). RAC1 belongs to a family of small GTPases, that modulate cell proliferation, migration and cytoskeletal organization (Krauthammer et al., 2012). The driver *RAC1* mutation is a substitution of proline for serine at position 29, which favours the active GTP-bound state of RAC1 (Hodis et al., 2012).

NF1 (neurofibromin 1) mutations are present in 14% of melanomas (Manzano et al., 2016) NF1 is a RAS GTPase-activating protein (GAP), and mutations in this protein lead to sustained activation of RAS and the MAPK and PI3K pathways (Nissan et al., 2014).

1.3 Other common genetic mutations found in melanoma

Other somatic mutations that contribute to melanoma formation and progression include those in the *TERT* and *Kit* genes (Reddy et al., 2017; Mehnert and Kluger, 2012). *TERT* encodes the catalytic subunit of telomerase, a protein that functions in the maintenance of telomere length in chromosomes. The expression of *TERT* in adult human somatic cells is repressed. However, in many human cancers, including melanoma, *TERT* expression is reactivated allowing cells to maintain telomere length and bypass senescence (Horn et al., 2013). *KIT* encodes a transmembrane RTK, and mutations in this gene lead to expression of a constitutively active receptor and subsequent activation of the MAPK and PI3K pathways (Curtin et al., 2006).

Germline mutations that increase susceptibility to melanoma have also been identified. Mutations in the *CDKN2A* gene have been found in 30% - 40% of families that are highly susceptible to melanoma. *CDKN2A* encodes two proteins involved in the regulation of cell

proliferation: $p16^{INK4A}$ and $p14^{ARF}$. $p16^{INK4A}$ is involved in inducing cell cycle arrest in the G1 phase of the cell cycle by inhibiting phosphorylation of the retinoblastoma protein (RB) by cyclin-dependent kinase 4 (CDK4). $p14^{ARF}$ also induces cell cycle arrest and apoptosis through mechanisms that involve p53 (Reddy et al., 2017).

The second most common melanoma germline mutation occurs in the *CDK4* gene, which encodes CDK4, a protein involved in the transition from G1 to the S-phase of the cell cycle. The resulting CDK4 mutant protein is not inhibited by $p16^{INK4A}$, resulting in abnormal cell cycle progression (Potrony et al., 2015).

1.4 Melanoma progression and clinical staging

Cutaneous melanoma can arise from chronically sun-damaged (CSD) and non-CSD skin. Melanomas from CSD skin develop on areas of the body with increased exposure to solar UV radiation, such as the head and neck, and frequently have mutations in *N-RAS*, *KIT* and *B-RAF*. Disease onset for this type of melanoma generally occurs in individuals over 50 years of age. Melanomas from non-CSD skin are found in areas of the body with intermittent UV exposure, such as the torso, arms and legs, and generally exhibit fewer genetic mutations. Melanomas from non-CSD skin predominantly acquire the $B\text{-}RAF^{V600E}$ mutation, and disease onset generally occurs earlier in life (Eggermont et al., 2014; Shain and Bastian, 2016).

Melanoma progression occurs in five stages termed acquired naevus, intermediate neoplasm (or dysplastic naevus), melanoma *in situ*, invasive melanoma and metastatic melanoma. The first stage, acquired naevus, forms as a consequence of benign

hyperproliferation of melanocytes, and is directly responsible for the formation of 20 to 50% of melanomas (Damsky and Bosenberg, 2017). Melanocytic nevi frequently have B-RAF^{V600E} mutations, and are commonly associated with the formation of melanomas in non-CSD skin (Kumar et al., 2004; Roh et al., 2015). Abnormal B-RAF or N-RAS activity leading to constitutive MAPK signalling is observed in acquired naevi (Tan et al., 2017). Although most naevus cells become senescent, a few can acquire additional mutations and retain their ability to proliferate. The accumulation of additional genetic alterations promotes naevus transformation towards malignancy, including the loss of p16^{INK4A} and activation of the PI3K pathway (Roh et al., 2015). Dysplastic naevus is considered a pre-malignant lesion. The distinction between an acquired naevus and dysplastic naevus has often been an area of discussion; however, dysplastic nevi are lesions that have acquired multiple driver mutations in addition to B-RAF (Shain and Bastian, 2016).

The third stage in melanoma progression, melanoma *in situ*, refers to the proliferation of melanoma cells within the epidermis, forming irregularly shaped lesions that can be precursors to invasive melanomas. These lesions are more commonly found in areas of the body chronically exposed to the sun. Additional mutations in genes encoding B-RAF, N-RAS and/or NF1, result in increased activity of the MAPK signalling pathways in these cells. Increased frequency of *TERT* mutations has also been observed in these cells. *In situ* melanomas can become invasive with the acquisition of additional mutations, including those that activate the MAPK pathway, as well as mutations in *CDKN2A*. Melanoma cells that move towards surrounding mesenchymal tissues such as the dermis or submucosa, enter stage four and are termed invasive melanoma (Shain and Bastian, 2016).

The last stage in melanoma progression is metastasis, which involves the migration of melanoma cells from the primary tumour to other organs in the body. Unlike the previously described stages, cells in metastatic melanoma are not distinctly characterized by a given subset of mutations, which contributes to their heterogeneity, unpredictable nature and resistance to treatment (Shain et al., 2015). It is therefore not surprising that prognosis is poor upon diagnosis of metastasis. Patients with metastatic melanoma have an expected 5-year survival rate of only 5-20% (Long et al., 2012; Sandru et al., 2014). For this reason, intense efforts to develop therapies for metastatic melanoma continue at present.

Clinically, melanoma is categorized into one of four stages, with Stage 0 describing melanoma *in situ*. Each stage is further divided to identify differences in primary melanoma tumour thickness, number of affected lymph nodes and distant metastases. Stages I and II encompass localized melanoma, stage III categorizes regional metastatic melanomas and stage IV is used when distant metastases are present (Balch et al., 2009).

Patient survival is partly influenced by the location of melanoma dissemination. For example, regional metastasis within the skin, or to lymph nodes are associated with a higher overall survival in individuals. Patient survival progressively declines with melanoma metastases to the lungs and to the central nervous system (Sandru et al., 2014). Numerous studies have reported that individuals with brain metastasis have the poorest overall survival (Staudt et al., 2010; Flanigan et al., 2011; Davies et al., 2011). These observations outline the importance of early, accurate detection and staging of melanoma.

1.5 Current therapies for melanoma

Surgery is the first line of treatment for cutaneous melanoma in those cases in which the primary tumour and/or metastases can be resected. However, a limitation to this approach is the inability to target melanoma in transit and/or detect microscopic metastases. For this reason, surgical resection is used in conjunction with radiation and/or systemic therapies, such as chemotherapy, targeted therapies and immunotherapies (Maverakis et al., 2015).

Melanoma is known to be inherently resistant to currently used chemotherapeutic agents and radiation, requiring combination of these agents with other therapies (Pak et al., 2004). Proteins involved in the MAPK pathway have been key targets for therapy. There are currently only two clinically used B-RAF inhibitors that target mutant B-RAF: vemurafenib and dabrafenib, that block B-RAF^{V600E} activity. The BRIM-2 Phase II multi-center study with vemurafenib identified a response rate of 53% in patients with B-RAF^{V600E} metastatic melanomas, with a median duration of response of 6.7 months. Adverse effects included the development of cutaneous squamous cell carcinoma in 26% of patients, but these lesions were effectively managed by surgical removal (Sosman et al., 2012). These effects were attributed to the activation of the MAPK pathway in keratinocytes with pre-existing *RAS* mutations (Su et al., 2012). *In vitro* studies have shown that inhibition of B-RAF in cells containing *RAS* mutations result in the dimerization and activation of C-RAF, followed by activation of MAPK signalling and enhanced growth (Hatzivassiliou et al., 2010; Poulikakos et al., 2010). The effectiveness of vemurafenib compared to dacarbazine, a commonly used drug to treat melanoma, was investigated in the BRIM-3 Phase III clinical trial. Overall median progression-free survival was 6.9

months for patients in the vemurafenib treatment and 1.6 for patients taking dacarbazine (Chapman et al., 2011), demonstrating the value of treating with vemurafenib in patients with metastatic melanomas containing $BRAF^{V600E}$ mutations.

Similarly, dabrafenib has shown promising results in Phase I and II clinical trials with 59%-69% of patients exhibiting clinical responses (Falchook et al., 2012; Ascierto et al., 2013). The Phase III BREAK-3 trials later demonstrated median progression-free survival of 5.1 months for patients who received dabrafenib treatment, compared to 2.7 months for patients treated with dacarbazine (Hauschild et al., 2012). Unfortunately, due to the emergence of resistance to the B-RAF inhibitors, these clinical benefits have been short-lived. *In vitro* studies with melanoma cells resistant to B-RAF inhibitors demonstrated sustained activation of the MAPK pathway through alternative mechanisms. For example, the kinase COT can activate the MAPK pathway in a MEK-dependent and RAF-independent manner (Johannessen et al., 2010). Increased COT mRNA expression has also been observed in metastatic $B\text{-}RAF^{V600E}$ melanoma biopsies of individuals undergoing vemurafenib treatment, suggesting that COT may contribute to acquired resistance (Johannessen et al., 2010). Subsets of B-RAF inhibitor-resistant melanoma samples with increased expression of PDGFR and N-RAS mutations have also been identified (Nazarian et al., 2010). For these reasons, other members of the MAPK pathway have become additional targets for therapy.

Trametinib is a clinically used MEK inhibitor. In a Phase III trial (METRIC) of patients with B-RAF-mutated metastatic melanoma, administration of trametinib resulted in median progression-free survival of 4.8 months, compared to 1.5 months for patients treated with dacarbazine (Flaherty et al., 2012). The side effect of developing cutaneous

squamous cell carcinoma as observed with B-RAF inhibitor treatment, was not observed in the individuals who were administered trametinib (Marzuka et al., 2015). To increase efficacy and reduce toxicity, combination therapy with both B-RAF and MEK inhibitors has been investigated. Phase III trials using B-RAF and MEK inhibitors have shown increased progression-free survival, response rate and overall survival with diminished adverse effects compared to B-RAF inhibitor monotherapy (Long et al., 2014; Larkin et al., 2014; Robert et al., 2015). B-RAF and MEK combination therapy has now been recommended as the standard-of-care for patients with BRAF-mutant melanoma.

Immunotherapies harness the ability of the immune system to detect and target tumour cells following antigen presentation. T-cell activation occurs when T-cell receptors bind to an antigen presented on major histocompatibility complex (MHC) proteins. T-cell responses are further regulated by signals transduced through co-stimulatory and co-inhibitory receptors (Grosso and Jure-Kunkel, 2013). Tumour cells can evade immune system responses by expressing ligands that bind to co-inhibitory receptors on T-cells. Upon T-cell activation, the cytotoxic T-lymphocyte-associated antigen 4 (CTLA-4) receptor, is recruited to the T-cell membrane and participates in inhibition of T-cell function. Similarly, programmed death-1 (PD1) is a receptor found on the T-cell membrane with inhibitory T-cell function (Pedoeem et al., 2014) (Figure 1.4). Ipilimumab is a human IgG monoclonal antibody (mAb) that binds to the CTLA-4 receptor and when bound sterically hinders the binding of ligands to the receptor, thereby promoting T-cell activation (Marzuka et al., 2015; Ramagopal et al., 2017). Pembrolizumab and nivolumab are two human monoclonal antibodies, that function to block the PD-1 receptor. Clinical studies have shown improved overall survival in metastatic melanoma patients treated with

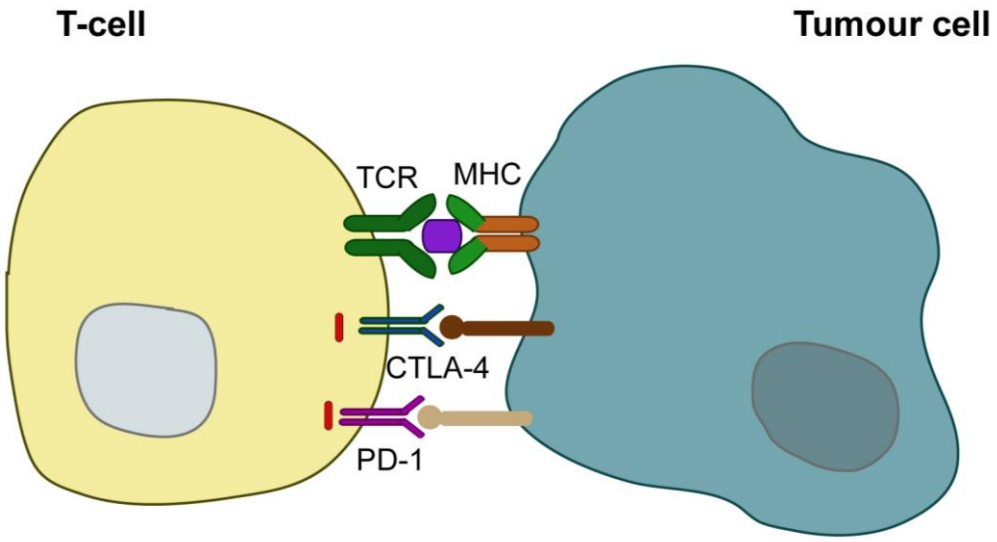

Figure 1.4. T-cell inactivation by tumour cells

T-cells are activated when T-cell receptors (TCR) bind to antigens presented on major histocompatibility complex (MHC) proteins on antigen-presenting cells. Tumour cells can evade immune responses by expressing ligands that bind to co-inhibitory receptors on T-cells, such as CTLA-4 and PD-1, resulting in T-cell inactivation.

ipilimumab, pembrolizumab or nivolumab (Hodi et al., 2010; Robert et al., 2011, 2014; Chmielowski et al., 2013). Additionally, patients receiving both ipilimumab and nivolumab displayed better overall survival compared to those receiving ipilimumab alone, indicating that there are additional benefits from combination therapy (Wolchok et al., 2017). Despite recent progresses in the treatment of metastatic melanoma, tumour cell resistance remains a major clinical challenge, and therefore there is pressing need to identify other therapeutic targets to overcome the emergence of resistance.

1.6 Preclinical models used to study metastatic melanoma

1.6.1 Human melanoma cell lines

Numerous human melanoma cell lines have been used as models to understand human melanoma behaviour. A recent study compared the transcriptional profile of several of these cells lines with primary and/or metastatic melanoma tumours (Vincent and Postovit, 2017). This study found that the expression of about 20, 000 protein-encoding genes was comparable between the melanoma cell lines examined and the tumours. Notably, differential expression was found in genes associated with immune function (Vincent and Postovit, 2017). This was considered an expected limitation of *in vitro* models that lack a microenvironment containing lymphatics, blood vessels and an extracellular matrix (ECM) (Sharma et al., 2015). Despite these limitations, because of the substantial degree of similarity in gene expression between melanoma cell lines and tumours, human melanoma cell lines remain useful models to study certain aspects of melanoma biology using cell culture approaches.

Currently there are numerous human metastatic melanoma cell lines such as SK-MEL-3, RPMI-7951, A375-MA2 and 131/4-5B1, that are being used to model metastatic melanoma. The A375-MA2 cell line was derived from lung metastases of the less metastatic parental A375 cell line (Xu et al., 2008; Chandrasekaran et al., 2016). Similarly, the 131/4-5B1, hereafter termed 5B1, cell line was derived from the human melanoma WM239A cells that acquired the ability to metastasize to the lungs and the brain (Cruz-Munoz et al., 2008). The 5B1 cells are particularly valuable tools for research, as very few melanoma cell lines with brain tropism in xenograft models have been isolated, and metastasis to the brain is associated with poor outcomes in individuals with melanoma (Sandru et al., 2014). Therefore, the 5B1 cells are an excellent preclinical model of spontaneous melanoma brain metastasis. Additionally, the 5B1 cells are resistant to vinblastine and cyclophosphamide, and can therefore model human metastatic melanomas that are similarly resistant to standard chemotherapeutic agents in the clinic.

1.6.2 The chick chorioallantoic membrane (CAM) model

The chick CAM is used to investigate tumour cell behaviour in an *in vivo* setting (Ribatti, 2014; Deryugina and Quigley, 2009). The CAM lines the inner surface of the egg shell and is composed of two epithelial membranes termed chorionic and allantoic epithelium. These two membranes enclose the mesoderm, which contains blood vessels and extracellular matrix proteins. The CAM functions in gas exchange and is highly vascularized, hence it has been an excellent model to use in studies pertaining to angiogenesis (Cepeda et al., 2016; Cheng et al., 2015; Zijlstra et al., 2007). Additionally, tumour cells can be grafted

onto the nutrient rich-CAM to investigate tumour formation and progression (Penuela et al., 2012; Li et al., 2015; Zuo et al., 2015).

Previous studies have used the chick CAM to explore melanoma biology. The CAM supports the development of tumours formed from the mouse metastatic melanoma cell line, B16-F10 (Penuela et al., 2012; Ableser et al., 2014), with some studies specifically investigating B16-F10 tumour angiogenesis (Vandercappellen et al., 2010; Ribatti et al., 2013; Yurlova et al., 2010). Similarly, the chick CAM was used to support tumour growth of human metastatic melanoma cells. A recent study grafted the A375 human metastatic melanoma cells into plastic rings placed on top of the chick CAMs to investigate tumour vessel density (Avram et al., 2017). The SK-MEL-2 melanoma cells were also inoculated into sterile plastic rings placed on CAMs, but to investigate the effects of 2 triterpenoids agents on vascular density surrounding the developing tumours (Caunii et al., 2017). Additionally, the chick CAM model has been used in metastasis assays where upon melanoma tumour formation on the CAM, chick organs such as the brain and liver, were harvested for isolation of genomic DNA and consequent detection of human melanoma cells by qPCR (Sinnberg et al., 2018).

1.6.3 Mouse melanoma models

Established mouse metastatic melanoma cells lines, such as the B16-F10 line, are also commonly used in melanoma research (Brown et al., 2002; Mummert et al., 2003; Winkelmann et al., 2006; Penuela et al., 2012). B16-F10 cells are a metastatic clone of the B16 mouse melanoma cells (Sharma et al., 2015) The B16 cells were passaged *in vivo* through tail vein injections, resulting in the formation of lung metastases, from which the

highly metastatic B16-F10 cells were isolated (Sharma et al., 2015). A limitation to the use of mouse melanoma cell lines to model human melanomas is the differences in the driving mutations found in human and mouse melanomas. While the majority of human melanomas acquire mutations in *B-RAF*, these mutations were not observed in any of the spontaneous or carcinogen-induced mouse melanoma cell lines analysed (Melnikova et al., 2004). Additionally, all mouse melanoma cell lines expressed PTEN, suggesting that loss of PTEN is not involved in mouse melanoma formation (Melnikova et al., 2004). Similar to the use of human melanoma cell lines, *in vitro* culture experiments using mouse melanoma cell lines are limited in their ability to recapitulate tumour interactions with the stromal microenvironment (van der Weyden et al., 2016). To model tumour growth and metastasis *in vivo*, several mouse models have been developed, including those that involve syngeneic or xeno-transplantation of melanoma cells, and genetically engineered mouse models.

Xenografts models involve the subcutaneous engraftment of patient-derived melanoma cells or tumour fragments (Einarsdottir et al., 2014), or of human melanoma cell lines in immunodeficient mice (Kleffel et al., 2015). Xenograft models are often used to explore tumour growth and metastasis, and to investigate therapeutic interventions (Fofaria and Srivastava, 2014; Yang et al., 2015). Genetically engineered mouse models are frequently used to determine the effects of genetic alterations in the initiation and progression of melanoma. Mice have been genetically modified to mimic the B-RAF^{V600E} or N-RAS^{Q61K} mutations. Melanocyte-specific tamoxifen inducible activation of *Braf*^{V600E} in *Tyr::CreER; Braf*$^{CA/+}$ mice only resulted in pigmented melanocytic lesions that did not progress to melanoma (Dankort et al., 2009). This phenotype was consistent with the concept that

melanocyte progression to melanoma requires several mutations in addition to BRAF driver mutations. The combination of B-RAF and PTEN alterations better modeled melanoma formation, as mice with loss of PTEN together with B-RAF^{V600E} expression (*Tyr::CreER; Braf^{CA}; Pten$^{lox/lox}$* mice) developed skin melanomas and metastases to the lymph nodes and lungs (Dankort et al., 2009). Similarly, transgenic mice with melanocyte-specific tamoxifen inducible N-RAS^{Q61K} expression developed benign melanocytic lesions. However, the combination of melanocyte-specific p16^{INK4a} gene inactivation with N-RAS^{Q61K} expression (*Tyr::Nras^{Q61K}; INK4a$^{-/-}$* mice) resulted in melanoma formation and metastasis (Ackermann et al., 2005). These two transgenic lines have been extensively used to study melanoma biology (Lee et al., 2013; Durban et al., 2013; Hennessey et al., 2017; Tormo et al., 2009).

Mice expressing B-RAF^{V600E} or N-RAS^{Q61K} have also been used to investigate the role of additional genetic alterations in melanomas (Damsky et al., 2011; Shah et al., 2010). For example, a recent study examined melanoma formation in mice with melanocyte-specific inactivation of the gene that encodes the non-receptor tyrosine kinase FES, together with *Pten* inactivation and B-RAF^{V600E} expression (*Tyr::CreER; Braf$^{CA/+}$; Pten$^{fl/fl}$*; *Fes$^{-/-}$* mice) (Olvedy et al., 2017). In these animals, loss of FES expression resulted in accelerated melanoma formation and decreased overall survival, suggesting that FES likely functions as a growth suppressor in human melanoma (Olvedy et al., 2017). FES is also known to play a suppressive role in colorectal carcinoma cell anchorage-independent growth and many colorectal tumours express little or no detectable FES protein (Delfino et al., 2006).

FES and FER are members of the FES family of non-receptor tyrosine kinases. Although, the role of FES in melanoma has been investigated, the biological functions of FER in melanoma are not known and will be the focus of my study.

1.7 FER kinase

1.7.1 The FES family of non-receptor tyrosine kinases

Non-receptor tyrosine kinases predominantly function within the cytoplasm of cells to transduce signals from various cell surface receptors to downstream effectors (Hubbard and Till, 2000). In humans, non-receptor tyrosine kinases are grouped into ten main families, which include FES, SRC, JAK, ABL, ACK, CSK, FAK, FRK, TEC and SYK (Robinson et al., 2000).

The FES family is composed of two members, FES and FER (Robinson et al., 2000). Structurally, FES and FER consist of an amino-terminal F-BAR domain, followed by two coiled coil domains, a central SH2 domain and a carboxy-terminal tyrosine kinase domain (Figure 1.5). The conserved F-BAR domain can interact with negatively charged phospholipids on the cell membrane to promote lamellipodia formation and cellular migration (Itoh et al., 2009; McPherson et al., 2009). The SH2 domain mediates interactions with substrates containing phosphotyrosine residues, thereby regulating kinase activity. Finally, the tyrosine kinase domain is responsible for the catalytic activity of these enzymes (Greer, 2002). The amino terminus coiled coil domains are required for the oligomerization of FER (Craig et al., 1999). FER oligomerization promotes autophosphorylation in trans however, it is not essential for kinase activation (Orlovsky et

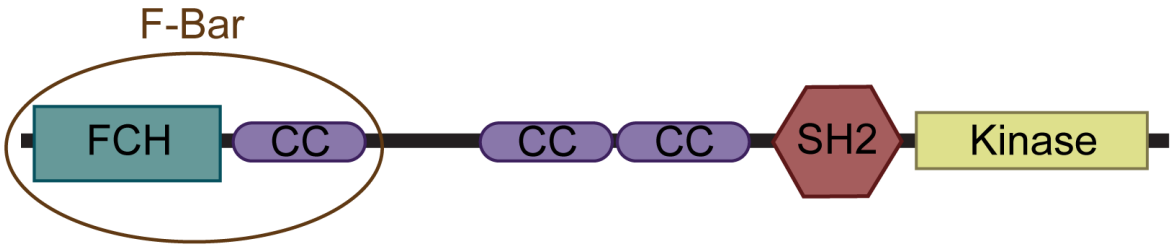

Figure 1.5. FER kinase protein domains

FER kinase is comprised of an amino terminus F-BAR domain followed by two coiled coil domains, a SH2 domain and a carboxy terminus tyrosine kinase domain. The F-BAR domain consists of the conserved FCH domain and the first coiled-coil (CC) domain.

al., 2000; Craig et al., 1999). The amino terminus is also involved in the regulation of FER kinase activity by interacting with other proteins, such as plectin which inhibits FER autophosphorylation (Lunter and Wiche, 2002).

FES has been detected in haematopoietic myeloid lineages, vascular endothelium, epithelial cells, neurons and melanocytes (Haigh et al., 1996; Care et al., 1994; Greer et al., 1994; Easty et al., 1995). FES-null mice are viable and fertile, but exhibit increased activation of the transcription factors, STAT3 and STAT5, in response to interleukin-6 (IL-6) cytokine and granulocyte-macrophage colony-stimulating factor (GM-CSF) (Hackenmiller et al., 2000) and increased sensitivity to lipopolysaccharide (LPS) exposure (Zirngibl et al., 2002), suggesting that FES is involved in innate immune responses, and is necessary for normal myeloid and macrophage function.

In humans, the *FER* locus is on chromosome 5q.21 and encodes a ubiquitous 94-kDa protein (Robinson et al., 2000). FER can localize to both the cytoplasm and nucleus (Hao et al., 1991; Ben-Dor et al., 1999). In mice, there is a testes-specific FER transcript, termed FerT, which encodes a truncated 51-kDa protein expressed in primary spermatocytes. FER and FerT share the SH2 and kinase domains; however, they differ in their amino terminus (Fischman et al., 1990; Keshet et al., 1990). FerT has also recently been reported to localize to the mitochondria of human colon carcinoma cells (Makovski et al., 2012a; Yaffe et al., 2014). Directed mitochondrial expression of FerT in non-malignant fibroblast cells resulted in the formation of tumours *in vivo*, suggesting that FerT may play a novel pro-tumourigenic role (Yaffe et al., 2014).

1.7.2 FER kinase protein-protein interactions

In the cytoplasm, FER is involved in signal transduction and has been shown to interact with and phosphorylate EGFR and PDGFR (Kim and Wong, 1995; Guo and Stark, 2011; Lennartsson et al., 2013). Stimulation of mouse fibroblasts or A431 human squamous carcinoma cells by EGF or PDGF resulted in the formation of FER-p120 catenin complexes, in which the coiled coil domains of FER associates with p120 catenin (Kim and Wong, 1995). FER weakens adherens junctions through phosphorylation of β-catenin, which prevents its interaction with α-catenin (Piedra et al., 2003; Rosato et al., 1998). Conversely, FER phosphorylation of the tyrosine phosphatase PTP1B stabilizes adherens junctions by facilitating PTP1B dephosphorylation of β-catenin (Xu, 2004). In sum, FER modulates adherens junctions and cell-cell adhesion through its association with several proteins.

Stimulation of various cell types by growth factors also promotes phosphorylation of the actin-binding protein cortactin by FER (Kim and Wong, 1998). Cortactin is involved in regulating actin dynamics, as it can bind to the Arp2/3 complex and stabilize branched filamentous actin (Weaver et al., 2001). In addition, phosphorylated cortactin is necessary for migration in various cell types, including mouse melanoma (Huang et al., 1998; Bryce et al., 2005; Huang et al., 2003). In response to actin depolymerization by latrunculin B, there is increased association between FER and cortactin and increased phosphorylation of cortactin (Fan et al., 2004), suggesting that FER may be involved in regulating actin dynamics through its interaction with cortactin.

FER indirectly plays a role in lamellipodia dynamics through its interactions with Rho GDP-dissociation inhibitor (RhoGDI). Lamellipodia formation is necessary for the initiation of directional cell migration and involves various proteins including RAC1 (Steffen et al., 2013). Inactive RAC1 remains in the cytoplasm bound to RhoGDI, however, activation of RAC1 by guanine nucleotide exchange factor (GEF) and dissociation from RhoGD1 allows for the translocation of RAC1 to the cell membrane and consequent interaction with its downstream effectors (Moissoglu et al., 2006). Of the three RhoGDI isoforms, RhoGDIα can be phosphorylated by and forms a complex with FER (Fei et al., 2010). This phosphorylation disrupts RhoGDIα binding to RAC1, thereby promoting RAC1 localization to the cell membrane (Fei et al., 2010; Hodge and Ridley, 2016).

FER kinase is also involved in insulin signalling. The activation of the insulin receptor results in the phosphorylation of IRS1. IRS1 can then bind to and activate PI3K, resulting in activation of other downstream effectors involved in the PI3K signalling pathway (Boucher et al., 2014). Upon insulin stimulation of adipocytes, FER associates with complexes containing IRS1 and PI3K, promoting insulin-mediated signal transduction within the cell (Iwanishi et al., 2000; Iwanishi, 2003).

The *in vivo* biological functions of FER kinase have been examined using knock-in mice with kinase-inactivating FER mutations (Craig et al., 2001). These mice develop normally, display no obvious phenotypical alterations and are fertile, thereby suggesting that FER kinase activity is not essential for development or survival. The formation of adherens junctions or focal adhesions and EGF or PDGF-induced phosphorylation of p120 catenin and β-catenin does not require FER kinase activity. Cortactin phosphorylation however,

was reduced in embryonic fibroblasts isolated from these mice, indicating that FER plays an important role in the regulation of cortactin phosphorylation (Craig et al., 2001).

1.7.3 The role of FER kinase in human tumours

FER is involved in multiple biological processes associated with tumour formation and progression. Specifically, prostate, renal, bladder urothelial, lung and ovarian carcinoma cells exhibit increased FER expression relative to normal cells in those tissues (Allard et al., 2000; Miyata et al., 2013; Hu et al., 2017; Ahn et al., 2013; Fan et al., 2016). FER expression is an independent predictor of survival among patients with renal, bladder urothelial, ovarian and breast cancer, with high FER expression associated with poor prognosis (Miyata et al., 2013; Hu et al., 2017; Fan et al., 2016; Ivanova et al., 2013).

FER promotes the proliferation of prostate, breast, renal and colon carcinoma cells through various mechanisms (Allard et al., 2000; Pasder et al., 2006; Miyata et al., 2013; Makovski et al., 2012b). For example, in prostate carcinoma cells, FER promotes cell cycle progression through RB-mediated mechanisms (Pasder et al., 2006). Specifically, FER phosphorylates the RB phosphatase PP1α and downregulation of FER in prostate cells results in increased activation of PP1α, which dephosphorylates RB. The hypo-phosphorylated form of RB inhibits cell proliferation. Additionally, FER forms complexes with and phosphorylates STAT3 and the androgen receptor upon IL-6 induction in prostate carcinoma cells, resulting in the transcription of genes associated with cell proliferation and survival (Zoubeidi et al., 2009; Rocha et al., 2013). Furthermore, FER silencing in colon carcinoma cells disrupts cell cycle progression and initiates programmed cell death through activation of ATM and its downstream effector p53 (Makovski et al., 2012b). FER

deficiency in primary breast carcinoma cells results in increased EGF-induced EGFR internalization and amplification of the MAPK signalling pathway, paradoxically resulting in cytostasis due to supranormal activation of the EGFR pathways (Sangrar et al., 2015). *In vivo* studies have also demonstrated delayed tumour onset and decreased tumour cell proliferative capacity of FER-deficient breast tumours (Sangrar et al., 2015).

FER has also been shown to mediate resistance to quinacrine, which is a therapy that induces cell apoptosis through inhibition of NF-κB and activation of p53. Overexpression of FER in lung and colon carcinoma cells, results in increased activation of NF-κB and increased phosphorylation of EGFR and ERK in the absence of EGF, resulting in the activation of genes responsible for cell survival and proliferation (Guo and Stark, 2011).

FER kinase has been shown to promote the migratory capacity of tumour cells. In prostate and breast carcinoma cells, FER reduces the expression of laminin-binding glycans, thereby impairing attachment of cells to the extracellular matrix and promoting cell migration (Yoneyama et al., 2012). The absence of FER interferes with the process of epithelial-mesenchymal transition (EMT) in bladder urothelial carcinoma cells, through mechanisms that involve increased expression of E-cadherins, together with decreased expression of N-cadherins, Slug and Snail (Hu et al., 2017). FER-deficient lung carcinoma cells also display decreased migration, due to impaired EGF-induced lamellipodia formation. This impairment is due to decreased phosphorylation of the GEF Vav2, resulting in decreased Vav2-RAC1 activity, reduced lamellipodia formation and cell migration (Ahn et al., 2013). In FER-deficient breast carcinoma cells, decreased motility and invasion are due to increased cell adhesion to the ECM due to elevated β1and α6 integrin levels, promoting focal adhesion formation. Breast carcinoma cells in which FER

is silenced are also more susceptible to anoikis (programmed cell death due to detachment from the ECM) (Ivanova et al., 2013).

FER increases the invasive capacity of bladder urothelial, hepatocellular, breast, lung and ovarian carcinoma cells (Hu et al., 2017; Li et al., 2009; Ivanova et al., 2013; Ahn et al., 2013; Fan et al., 2016). FER-deficient bladder urothelial cells exhibit decreased invasion due to decreased matrix metalloproteinase (MMP) expression (Hu et al., 2017) and FER-deficient lung carcinoma cells are less invasive due to impaired lamellipodia formation (Ahn et al., 2013). Recently a novel signalling pathway involving FER kinase was shown to promote motility and invasion of ovarian carcinoma cells (Fan et al., 2016). Specifically, FER can phosphorylate the receptor tyrosine kinase MET in the absence of ligand binding to this receptor, leading to the phosphorylation of the adaptor protein GAB1 and the tyrosine phosphatase Shp2. These events in turn result in activation of the RAC1 and MAPK pathways, which potentiate cell motility and invasiveness (Fan et al., 2016).

Several studies on FER and cancer cell metastasis have used mouse xenograft models. Sections of mouse organ tissues were analysed for the presence of tumour cells, indicating cell metastasis from the primary tumour. The spontaneous formation of metastases from FER-deficient breast, lung and ovarian tumours to distant organs was decreased, suggesting that FER promotes metastasis in these tumour cell types (Ivanova et al., 2013; Ahn et al., 2013; Fan et al., 2016).

The above studies suggest that targeted inhibition of FER activity may attenuate tumour growth and/or metastasis. Recently, a small molecule inhibitor of FER and FerT kinase activity named E260 was developed using a yeast-based high-throughput screening system.

In colon carcinoma cells, FER and PARP-1 association was disrupted following E260 treatment, causing increased PARP-1 activity and a consequent increase in autophagy. Additionally, treatment of colon, liver, and pancreas carcinoma cells with E260, resulted in selective mitochondrial deformation and dysfunction, resulting in decreased cellular ATP levels. This energy deficit further induced cellular autophagy. Additionally, systemic E260 treatment of mice with colon carcinoma cell xenografts resulted in decreased tumour volume, and histopathological analysis demonstrated necrotic and non-vascularized tumour tissue (Elkis et al., 2017).

This above study demonstrates the pro-tumourigenic effects of FER in various carcinoma cells and the attenuation of these effects following inhibition of FER kinase activity using E260. The therapeutic potentials of E260 further demand the investigation of the role of FER in other cancers, such as melanoma.

1.8 Rationale, hypothesis and aims

In human colorectal and melanoma cancer, FES has been shown to play a tumour suppressive role. However, FER, the other protein family member, plays a pro-tumourigenic role in numerous cancers. This suggests that FER and FES may function in opposite manners during tumourigenesis. The biological functions of FER in human metastatic melanoma have not been explored, and observation of FER function in others cancers suggest that FER may promote melanoma tumourigenesis. I hypothesize that ***FER kinase contributes to the tumourigenic properties of human melanoma cells***. To test this hypothesis, the specific aims of my study are:

1. Determine the role of FER kinase in human melanoma cell proliferation.

2. Investigate the role of FER kinase in melanoma cell susceptibility to apoptosis.
3. Determine the role of FER kinase in human melanoma cell migration.
4. Examine the role of FER kinase in human melanoma cell invasion.

Chapter 2

2 Materials and methods

2.1 Reagents

Table 2.1: Reagents

Reagent	Source	Catalogue No.
Amersham ECL Prime Western Blotting Detection Reagent	GE Healthcare, Mississauga, ON	RPN2232
Aprotinin	BioShop, Burlington, ON	APR200
Bio-Rad Protein Assay Dye Reagent Concentrate	Bio-Rad, Mississauga, ON	5000006
5-bromo-2’-deoxyuridine	Acros Organics, Belgium	22859-5000
Collagen Type 1, rat tail	Corning, Bedford, MA	354236
Cultrex Basement Membrane Matrix, Type 3	Trevigen, Gaithersburg, MD	3632-001-02
Doxycycline hydrochloride	Fisher Scientific, Whitby, ON	BP26531
Eosin Y	Sigma-Aldrich, Oakville, ON	HT11016
Fetal bovine serum (FBS)	Gibco, Burlington, ON	12483-020
Hoeschst 33342	Life Technologies, Burlington, ON	H1399
Leupeptin	Bioshop, Burlington, ON	LEU001
Mayer’s hematoxylin	Sigma-Aldrich, Oakville, ON	MHS16

NaF	Sigma Aldrich, St. Louis, MO	S7920
Na_3VO_4	Bioshop, Burlington, ON	SOV664
Paraformaldehyde (PFA)	Fisher Scientific, Whitby, ON	AC416780030
Pepstatin	Bioshop, Burlington, ON	PEP605
Permount Mounting Medium	Fisher Scientific, Ottawa, ON	SP15-100
Phenylmethylsulfonylfluoride (PMSF)	Bioshop, Burlington, ON	PMS123
Poly-L-lysine (PLL) hydrobromide solution	Sigma Aldrich, St. Louis, MO	P5899
Rhodamine-labeled Lens Culinaris Agglutinin (LCA)	Vector Laboratories, Brockville, ON	VECTRL1042
RPMI 1640 with L-glutamine and sodium bicarbonate	Sigma-Aldrich, Oakville, ON	R8758
Shandon Immu-Mount mounting medium	Thermo Fisher Scientific, Pittsburgh, PA	2860060
TGX Stain-Free FastCast Acrylamide Kit, 7.5%	Bio-Rad, Mississauga, ON	1610181
Triton X-100	EMD, Darmstadt, Germany	CATX-1568
Trypsin, 2.5%	Gibco, Burlington, ON	15090046
Tween-20	Amresco, Solon, OH	0777
Xylene	Anachemia, Montreal, QB	97233-540

2.2 Materials

Table 2.2: Materials

Material	Source	Catalogue No.
Axygen, 1.5-ml Eppendorf tubes	Corning, Bedford, MA	10011-700
BioLite T25-cm^2 Flasks, Cell Culture Treated	Thermo Fisher Scientific, Rockford, IL	130189
BioLite T75-cm^2 Flasks, Cell Culture Treated	Thermo Fisher Scientific, Rockford, IL	130190
BioLite T175-cm^2 Flasks, Cell Culture Treated	Thermo Fisher Scientific, Rockford, IL	130191
CELLSTAR Tissue Culture Dishes, 60 x 15 mm	VWR Scientific, Radnor, PA	82050-546
Conical tubes, 15-ml	Sarstedt, Numbrecht, Germany	62.554.205
Conical tubes, 50-ml	Sarstedt, Numbrecht, Germany	62.547.205
Embedding cassettes	VWR Scientific, Radnor, PA	CA60830-098
Falcon conical tubes, 15-ml	BD Biosciences, Bedford, MA	352097
Glass coverslips, 12mm, No. 1	VWR Scientific, Radnor, PA	031014-9
Greiner Bio-One 6-well cell culture plates	VWR Scientific, Radnor, PA	82050-842
Greiner Bio-One 24-well cell culture plates	VWR Scientific, Radnor, PA	82050-892

Imaging dish, 35 mm μ-Dish	Ibidi, Madison, WI	81156
Immobilon-P membrane (PVDF) transfer membranes, 0.45-μm pore size	EMD Millipore, Billerica, MA	IPVH00010
Micro cover glass, rectangular, 22 x 50 mm	VWR Scientific, Radnor, PA	48393-059-1
Nunclon 4-well MultiDishes	VWR Scientific, Radnor, PA	CA62407-068
Syringe filter, 0.2 μm	Sardtedt, Nümbrecht, Germany	83.1826.001
Teflon cell scraper	Thermo Fisher Scientific, Waltham, MA	08-100-240

2.3 Antibodies

Table 2.3: Antibodies

Antibody	Source	Catalogue No.	Dilution [a]
AlexaFluor 488-conjugated goat anti-chicken IgG (H+L)	Life Technologies, Burlington, ON	A-11039	IHC: 1:500 [b]
AlexaFluor 555-conjugated goat anti-mouse IgG (H+L)	Life Technologies, Burlington, ON	A-21422	IF, IHC:1:500 [b]
AlexaFluor 555-conjugated goat anti-rabbit IgG (H+L)	Life Technologies, Burlington, ON	A-21428	IF: 1:500 [b]
AlexaFluor 647-conjugated goat anti-mouse IgG (H+L)	Life Technologies, Burlington, ON	A-21449	IHC: 1:500 [b]
5-bromo-2'-deoxyuridine (BrdU)	Developmental Studies Hybridoma Bank, Iowa City, IA	G3G4	IF: 1:500 [b]
Cleaved caspase 3	Cell Signalling Technology, Pickering, ON	9661S	IB: 1:1000 [c]
Collagen Type 3	Developmental Studies Hybridoma Bank, Iowa City, IA	3B2	IHC: 1:6 [b]
FER kinase	Cell Signalling Technology, Pickering, ON	4268S	IB: 1:1000 [d]

γ-tubulin	Sigma, St. Louis, MO	T6557	IB: 1:10 000 [e]
GFP	Abcam, Cambridge, MA	13970	IHC: 1:1000 [b]
HRP-conjugated goat anti-mouse IgG	Jackson ImmunoResearch, West Grove, PA	115-038-003	IB: 1:500 [f]
HRP-conjugated goat anti-rabbit IgG	Cell Signalling, Pickering, ON	7074	IB: 1:500 [f]
Ki67	Abcam, Cambridge, MA	15580	IF: 1:200 [b]
Pmel17	Santa Cruz, Dallas, TX	sc-377325	IF: 1:50 [b] IHC: 1:100 [b]

[a] IB: immunoblot

IF: immunofluorescence

IHC: immunohistochemistry

[b] diluted in 1x PBS containing 5% goat serum, for one hour at 22 °C

[c] diluted in 1x TBST containing 5% nonfat milk, overnight at 4 °C

[d] diluted in 1x TBST containing 1% BSA, overnight at 4 °C

[f] diluted in 1x TBST containing 5% nonfat milk, for one hour at 22 °C

[e] diluted in 1x TBST containing 1% BSA, 30 minutes at 22 °C

2.4 Preparation of poly-L-lysine (PLL)-coated glass coverslips

Glass coverslips were washed in 1M HCl for 5 h at 50-60° C. They were cooled to room temperature and then washed with 100% ethanol and dried in the tissue culture laminar flow hood. The coverslips were then incubated with a solution containing 0.1 g/ml of PLL dissolved in 18-MΩ dH_2O for 1 h at 22 °C. They were then washed with deionized dH_2O and allowed to dry in the tissue culture laminar flow hood. The coverslips were stored in a sterile container until used.

2.5 Preparation of poly-HEMA coated dishes

Poly-HEMA solution was made by adding 1.2 g of poly-HEMA to 99.5% (vol/vol) ethanol and dissolving it for 5-6 h at 37 °C, as described in (Kuroda et al., 2013). CELLSTAR tissue culture dishes, 60 x 15 mm, were coated with 1.3 ml of this solution and allowed to dry overnight in the tissue culture laminar flow hood. Coated plates were stored at 22 °C for up to 1 month.

2.6 Laminin 332 matrix production, collection and coating procedures

The laminin 332 matrix producing 804G cells (Tripathi et al., 2008) were cultured in RPMI 1640 medium with L-glutamine and 5% FBS. Once 804G cells reached 90% confluency, the culture medium was removed by aspiration, the cells were washed once with PBS and then cultured in serum-free RPMI 1640 medium. Fourty-eight hours later, conditioned medium was collected and centrifuged at 130 x g for 5 min at 22 °C. The supernatant

containing laminin 332 matrix was filtered through a 0.2 μm syringe filter and stored at 4°C for up to 1 week.

μ-Dishes were coated with 8.6 μg/cm^2 of collagen I (diluted in 0.02 M acetic acid) for 16 h at 22 °C. The dishes were then washed thoroughly with PBS before plating cells. To coat dishes with laminin 332 matrix, 2 ml of the laminin 332-containing 804G conditioned medium was placed in the dish and incubated at 37 °C for 1.5 h. The medium was aspirated and cells were plated. For experiments involving collagen I and laminin 332, dishes were sequentially coated with collagen I and laminin 332-matrix, following the steps described above for the individual extracellular matrix substrates.

2.7 Cell culture and doxycycline treatments

131/4-5B1 cells (Cruz-Munoz et al., 2008), hereafter referred to as 5B1 cells, were a kind gift from Dr. Robert Kerbel (Sunnybrook Health Sciences Centre, Toronto, ON, Canada). A doxycycline (dox)-inducible and lentivirus-based small hairpin RNA (shRNA) system (Herold et al., 2008) was used to downregulate FER kinase levels in these cells. Lentivirus transductions were conducted by Dr. Iordanka Ivanova as follows. The third generation lentivirus packaging plasmids, pHDM.Hgpm2 (which encodes gag-pol), pHDM.G encoding VSV-G, pREV and pTat, were a kind gift from Dr. Patrick Derksen (University Medical Center Utrecht, The Netherlands). 293T cells were transfected with these plasmids, together with either FH1tUTG control, non-targeting or FH1tUTG FER-targeting shRNA plasmids (Ivanova et al., 2013). In this manner, transfected cells were able to package lentiviral particles encoding the appropriate shRNAs. Lentivirus-containing medium was collected 72 h after transfection, centrifuged at 130 x g for 5 min

and filtered through a 0.45-μm filter. The lentiviruses were then re-suspended in RPMI 1640 medium containing 5% FBS and added to 5B1 cells to transduce them. GFP-positive cells were subjected to fluorescence activated cell sorting (FACS), cultured and used in all subsequent experiments as polyclonal melanoma cell populations. The lentivirus-mediated integration of the control (non-targeting) or the FER-targeting shRNA into the genome of the parent 5B1 cells generated two new cell lines, hereafter termed, respectively, Control and FER 9 cells. The FER shRNA targets positions 594 - 614 in the FER kinase mRNA, which correspond to the F-BAR domain of the protein. The nucleotide sequences for the Control, non-targeting shRNA, are as follows:

Control sense:

5’-tcccttctccgaacgtgtcacgtttcaagagaacgtgacacgttcggagaatttttc-3’

Control anti-sense:

5’-tcgagaaaaattctccgaacgtgtcacgttctcttgaaacgtgacacgttcggagaa-3’

The nucleotide sequences for the FER-targeting shRNA are as follows, with the targeting sequences being capitalized:

FER[978-998] sense:

5’-tcccGTATTATGATATCACACTTCCttcaagagaGGAAGTGTGATATCATAATACtttttc-3’

FER[978-998] anti-sense:

5’-tcgagaaaaaGTATTATGATATCACACTTCCtctcttgaaGGAAGTGTGATATCATAATAC-3’

Control and FER 9 5B1 cells were cultured in RPMI 1640 medium with L-glutamine and 5% fetal bovine serum (FBS). A stock solution of doxycycline (dox) was made by dissolving dox in dH_2O to a concentration of 1 mg/ml. To silence FER mRNA and decrease FER protein levels, cells were cultured in the presence of 2 μg/ml of dox for 5

days. Medium was changed every 48 hours and fresh dox was added to maintain shRNA expression, resulting in decreased FER kinase levels. Each experiment was conducted with Control and FER 9 cells treated with 1X PBS (vehicle) or with dox. Cells were cultured at 37°C in a humidified atmosphere containing 5% CO_2.

To investigate the duration of FER knockdown following dox removal, 5B1 cells were cultured in medium containing 2 μg/ml of dox for 5 days, after which the cells were washed with PBS and further cultured with fresh medium without dox. Cells remained in culture for up to 7 days after dox withdrawal. FER levels were measured every day by immunoblot analysis as outlined in section 2.11.

804G rat bladder epithelial cells secrete laminin-332-containing matrix (Langhofer et al., 1993). Therefore, the laminin 332 matrix produced by these cells was used in cell migration studies, as outlined in section 2.6. 804G cells were cultured in RPMI 1640 medium with L-glutamine and 5% FBS at 37 °C in a humidified atmosphere containing 5% CO_2.

2.8 Analysis of cell proliferation

Cells plated at a density of 2.0×10^4 cells/cm^2 on PLL-coated glass coverslips were incubated in growth medium containing 10 μM of 5'-bromo-2-deoxyuridine (BrdU) for 2 h at 37 °C. The cells were then fixed and processed for immunofluorescence microscopy, as described in section 2.12. Fixed cells were incubated with mouse anti-BrdU antibody (Section 2.3), washed thrice with PBS (10 min/wash) and then incubated with secondary goat anti-mouse AlexaFluor 555-conjugated IgG for 1 h, protected from light.

Similarly, cells plated at a density of 2.0×10^4 cells/cm^2 on PLL-coated glass coverslips were fixed and incubated with rabbit anti-Ki67 antibody (Section 2.3), washed thrice with PBS (10 min/wash) and then incubated with secondary goat anti-rabbit AlexaFluor 555-conjugated IgG for 1 h, protected from light.

2.9 Apoptosis and anoikis analysis

Cells were plated at a density of 3.6×10^3 cells/cm^2 on 60-cm culture dishes with or without poly-HEMA coating. Six days after plating, the cells were collected and processed for immunoblotting as outlined in section 2.11, to determine cleaved caspase-3 levels. In order to demonstrate that 5B1 cells were susceptible to apoptosis, adherent control 5B1 cells were treated with 80 μM or 100 μM of cisplatin. And to induce apoptosis in another cell type, adherent 804G cells were irradiated with 75 mJ of UVC light. Cells were collected and processed according to Section 2.11.

2.10 Cell motility assays

Cells were plated on extracellular matrix coated 35-mm μ-Dishes (prepared according to section 2.6) at a density of 8.6×10^3 cells/cm^2. Images were acquired over a 16-h period using an EVOS Cell Imaging System (ThermoFisher Scientific), capturing a phase-contrast image every 10 min. Image sequences were imported into ImageJ (NIH) and the Manual Tracking Plug-in was used to track every cell within the frame. Migration tracks were then analyzed using the Chemotaxis and Migration Tool software (ibidi), where the migration path of each cell was visually outlined, and the accumulated (total) distance, the euclidean

distance (straight linear distance from the initial to the final migration point) and the average speed of each cell were calculated.

2.11 Immunoblot analysis

2.11.1 Preparation of cell lysates

Growth medium was removed from culture dishes by aspiration, and the cells were rinsed once with ice-cold PBS. One ml of PBS was added and a Teflon cell scraper was used to gently scrape the cells from the culture dish. The cell suspension thus obtained was then transferred to a 1.5-ml microfuge tube and centrifuged at 5 000 x g for 5 minutes at 4°C. After centrifugation, the supernatants were removed by aspiration and the cell pellets were either immediately processed or stored at - 20°C to process at a later time.

Cell pellets were resuspended in 50 µl of ice-cold lysis buffer (50 mM Tris pH 7.6, 150 mM NaCl, 1% Triton X-100, 1 mM PMSF, 5 mM Na_3VO_4, 1 µg/ml aprotinin, 1 µg/ml pepstatin, 1 µg/ml leupeptin) and incubated on ice for 30 min. The lysates were then centrifuged at 13 400 x g for 10 min at 4°C. Following centrifugation, supernatants were transferred to new microfuge tubes. The protein concentration in each lysate was determined using the Bradford assay. Lysates were either immediately processed or stored at – 20 °C to process at a later time.

2.11.2 Polyacrylamide gel electrophoresis and immunoblot analysis

Cell lysate samples were prepared with 50 µg of protein, lysis buffer and 6x Laemmli loading buffer (1.2g SDS, 6 mg bromophenol blue, 4.7 ml glycerol, 1.2 ml of 0.5M Tris

pH 6.8, 0.93 g DTT and 2.1 ml 18-MΩ H_2O) and then denatured by heating to 99°C for 5 minutes. For FER kinase analysis, 7.5% polyacrylamide gels were made, using the TGX Stain-Free FastCast Acrylamide Kit. For cleaved caspase-3 analysis, samples were resolved by SDS-polyacrylamide gel electrophoresis (SDS-PAGE), using 12% resolving and 5 % stacking polyacrylamide gels.

Resolved proteins were then transferred onto a 0.45-µm pore size hydrophobic immobilon-P polyvinylidene difluoride (PVDF) membrane using a semi-dry transfer apparatus. Membranes were blocked by gentle rocking in Tris buffered saline containing 0.1% Tween 20 (TBST, 100 mM Tris-HCl pH 7.5, 1.5 M NaCl) and 5% nonfat milk for 1 h at 22 °C. Following a 10-min wash in TBST, the membranes were incubated with primary antibody diluted in TBST at the dilutions specified in section 2.3. After probing with primary antibody, the membranes were washed three times (10 min/wash) with TBST and then incubated with the species-specific, horse-radish peroxidase-conjugated secondary antibody diluted in 5% nonfat milk in TBST solution. Following the secondary antibody incubation, the membranes were washed 3 times with TBST (10 min/wash).

Proteins were detected using 1:1 vol/vol of Amersham ECL Prime Western Blotting Detection Reagent and images were acquired using a VersaDoc Imaging System (Bio-Rad) and Quantity One software (version 4.6.9). To quantify protein levels, densitometric analyses were conducted using Quantity One software, by drawing equally sized rectangular regions of interest over the background and the bands quantified. A volume report consisting of volume, area and density of bands was provided by the software. The density of the background was subtracted from the densities of the bands of interest. Proteins levels were normalized to those of γ-tubulin to correct for differences in protein

loading, and normalized protein levels are presented relative to control conditions in all relevant experiments.

2.12 Immunofluorescence microscopy

Cells were fixed with freshly diluted 4% paraformaldehyde (PFA) in PBS for 20 min at 22 °C and washed three times with PBS (10 min/wash). They were then permeabilized with 0.1% Triton X-100 solution in PBS for 20 min and then washed twice with PBS (10 min/wash). In experiments to detect BrdU incorporation, genomic DNA was denatured by incubating the cells with 2M HCl for 20 min at 22°C. The cells were then thoroughly washed three times with PBS (10 minutes/ wash) at 22°C. All samples were blocked with PBS containing 5% non-fat milk for 1 h at 22 °C with gentle rocking. After three washes with PBS (10 min/wash), the cells were incubated with appropriate primary antibodies (anti-BrdU, anti-Ki67 or anti-Pmel17) as described in section 2.3. The cells were then washed three times with PBS (10 min/wash) and incubated for 1 h with the appropriate AlexaFluor-conjugated secondary antibody. Cells were washed thrice with PBS (10 min/wash) and were then incubated with Hoechst 33342 for 5 min protected from light. Following three 10-min washes with PBS, the samples were mounted onto microscope slides using Immu-mount mounting medium. Slides were allowed to dry overnight protected from light and imaged using a Leica DMIRBE fluorescence microscope (Leica Microsystems, Wetzlar, Germany) equipped with an Orca-ER digital camera (Hamamatsu Photonics, Hamamatsu, Japan) and Volocity 4.3.2 software.

2.13 Chorioallantoic Membrane (CAM) experiments

2.13.1 Chicken embryo incubation

Fertilized chicken eggs (McKinley Hatchery, St. Mary's Ontario) were incubated in a rotary incubator (Berry Hill) at 70% humidity at 37°C for 3 days, after which the eggs were cracked and all contents, including the embryos at day-4 of development, were placed into a weighing boat. Each weighing boat was covered with a plastic lid allowing air circulation, housed in a holed plastic container containing autoclaved water and maintained in a stationary incubator set at 70% humidity and 37°C for a week. The incubator facilities and cracking procedures were kindly provided by Dr. Silvia Penuela and her personnel (Department of Anatomy and Cell Biology). On day 11 of development, one week after cracking, 1.5 x 10^6 5B1 cells re-suspended in 30 µl of Cultrex Basement Membrane Matrix were placed gently on a branching vascular point of the chick chorioallantoic membrane (CAM). The embryos were then returned to the stationary incubator. Seven days post-inoculation, on day 18 of development and just prior to harvesting, rhodamine labeled *lens culinaris agglutinin* (LCA) (1:10 dilution of a 5 mg/ml stock in PBS), was injected into the CAM vasculature by Dr. Mario Cepeda, who kindly helped with this step in the experiments. Immediately after LCA injection, tumours with their surrounding CAM were excised and placed in 4% PFA overnight for further processing.

2.13.2 Tissue sectioning

Excised tumour samples were processed (dehydrated and immersed in paraffin wax) at the Molecular Pathology Core Facility at The Robarts Research Institute and tissues were sectioned (7 μm in thickness) by Mr. Kevin Barr.

2.13.3 Immunohistochemistry analyses

Paraffin-embedded sections were dewaxed and rehydrated by placing them in the following reagents for 5 min each: twice in xylene followed by 100% and 95% ethanol. The slides were then washed twice with deionized water (2 min per wash). For hematoxylin and eosin staining, the slides were first placed in Mayers Hematoxylin for 2 min then washed with tap water for 1 min. Slides were then placed in tap water containing 200 μl of 1M NaOH for 1 min, washed under running tap water for 5 sec, then dipped into 70% ethanol for 30 sec and placed in Eosin Y for 2 min. Next, they were sequentially placed in two staining jars containing 70% ethanol, 1 min in each jar. Slides were dehydrated by sequential immersion in the following solutions: 95% ethanol, 100% ethanol, and then 2 xylene staining jars (1 min per jar). Coverslips were mounted onto the slides, using Permount.

For immunostaining, high-temperature antigen retrieval was conducted by immersing the tissue sections in boiling sodium citrate buffer (10 mM sodium citrate, 0.05% Tween 20, pH 6.0) for 30 min. The sections were then incubated with primary antibody diluted in PBS containing 5% goat serum for 1 h and then washed 3 times with PBS. Next, the sections were incubated for 1 h with the appropriate AlexaFluor-conjugated secondary antibody diluted in PBS containing 5% goat serum. Following 3 washes with PBS, nuclear DNA

was stained with Hoechst 33342 (1:10 000 dilution of a 10 μg/ml stock in PBS) for 5 min, protected from light. The sections were washed three additional times before mounting using Immu-mount medium.

5B1 cells were detected in the CAM section using a chicken anti-GFP antibody followed by goat anti-chicken AlexaFluor 488-conjugated secondary antibody. CAM tissues were visualized using a mouse anti-Collagen type III antibody, which specifically recognizes chicken tissues, followed by the goat anti-mouse AlexaFluor 647-conjugated secondary antibody. Fluorescence images were acquired as described in section 2.12.

2.14 Statistical analyses

GraphPad Prism software (version 6.0) was used for all statistical analyses. Unpaired t-test was applied for two-way comparisons, and one-way analysis of variance (ANOVA) followed by Tukey's post-hoc test was used for multiple comparisons. Significance was set at P values < 0.05. Unless otherwise indicated, all experiments were conducted at least three times, using 3 technical replicates for analysis.

Chapter 3

3 Results

3.1 Characterization of Control and FER 9 human melanoma cells

To investigate the role of FER kinase in melanoma biology, I used a silencing approach in 5B1 human melanoma cells, with a doxycycline-inducible lentivirus-based shRNA system. Upon stable integration of FER-targeting shRNA sequences into genomic DNA, and subsequent transcription following doxycycline (dox) treatment, FER kinase levels can be reduced. The shRNA vectors used also contain a GFP-encoding cassette, allowing for FACS selection of GFP-positive cells. Therefore, transduced 5B1 cells can be identified through GFP fluorescence imaging. Phase-contrast and fluorescence images from passage 1 (P1) Control cells and cells with the inducible FER shRNA (hereafter termed FER 9) were acquired, demonstrating that every cell in the phase-contrast image was also GFP-positive (Figure 3.1A). This shows that both Control and FER 9 cells were successfully transduced with their respective shRNA, to generate polyclonal populations.

To analyse GFP expression in the 5B1 cells upon dox treatment, Control and FER 9 cells were treated with or without dox for 5 days and then examined using fluorescence imaging. The heterogeneity of the Control and FER 9 polyclonal populations accounts for the observed differences in GFP expression from one cell to the next. However, all Control cells were GFP-positive, indicating that dox administration does not affect GFP expression. Similarly, all FER 9 cells, irrespective of FER protein levels, were GFP-positive (Figure

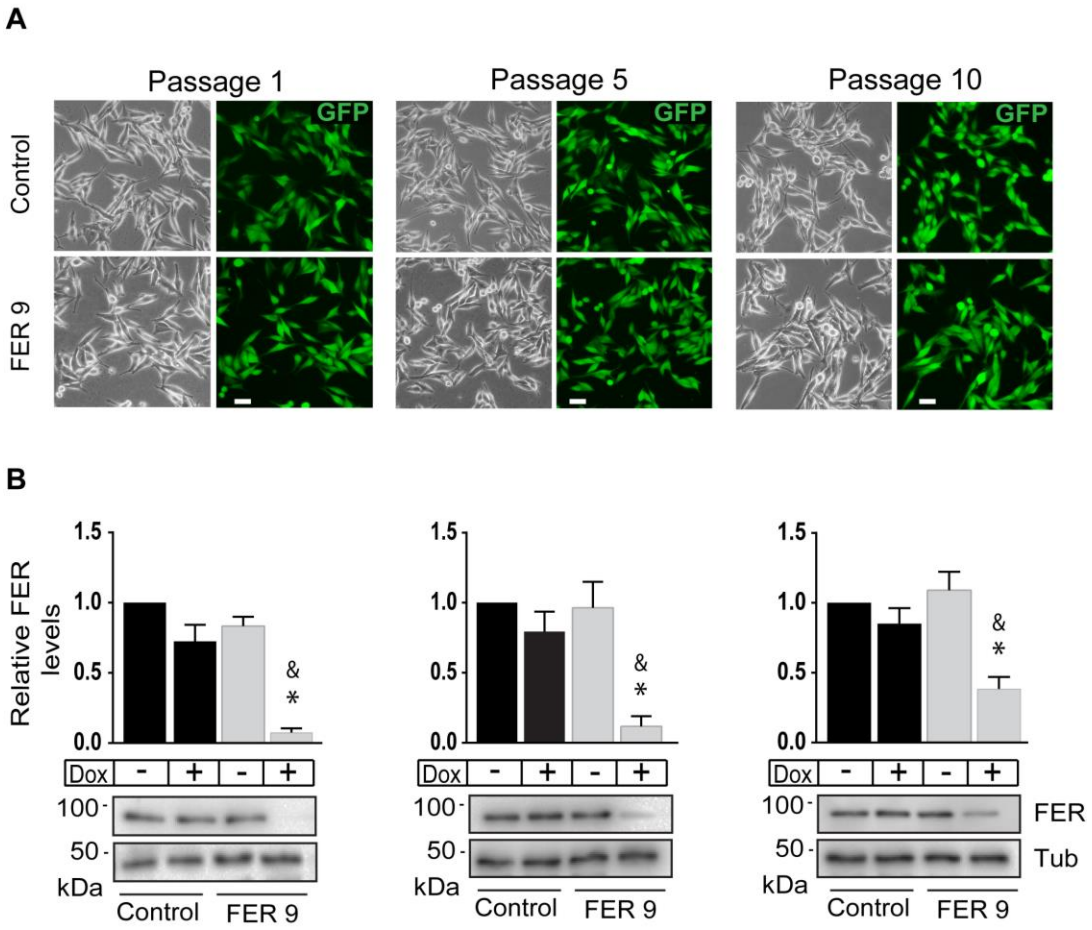

Figure 3.1. FER kinase knockdown of Control and FER 9 cells

Control and FER 9 cells were cultured in medium with or without 2 μg/ml of dox for 5 days. **A.** Phase contrast and fluorescence images were acquired to confirm GFP expression. **B.** FER protein levels of cells at passages 1, 5 and 10 were analysed by immunoblot. Histograms represent mean protein levels ± SEM (N=3) normalized to γ-tubulin (to correct for protein loading) and are expressed relative to Control -dox values, which are set to 1. * represents $P < 0.05$ relative to Control -dox cells, and & indicates $P < 0.05$ relative to FER 9 -dox (ANOVA). Scale bar = 70 μm.

3.2). To reaffirm that the observed GFP expression is specific to the 5B1 melanoma cells, immunofluorescence imaging for premelanosome protein (Pmel) expression was performed. Pmel is a melanocyte-lineage specific type I transmembrane glycoprotein that is mainly located in immature melanosomes Therefore, it is commonly used to detect melanoma cells (Theos et al., 2005). Every GFP-positive Control and FER 9 cell, in Figure 3.2, is correspondingly Pmel-positive indicating that the observed GFP expression is specific to the 5B1 melanoma cells. In addition, no differences in Pmel expression were observed in the Control and FER 9 cells (Figure 3.2).

To determine FER levels in Control and FER 9 cells, P1 cultures were treated with or without dox for 5 days and FER kinase levels were measured by immunoblotting. FER 9 cells treated with dox exhibited about a 90% decrease in FER protein levels compared to untreated FER 9 cells (Figure 3.1B). Control cells showed no significant differences in FER kinase levels irrespective of the presence or absence of dox. In addition, there was no significant difference in FER levels between Control cells and FER 9 cells in the absence of dox. This demonstrates an inducible system, in which only upon doxycycline treatment an efficient reduction in FER kinase levels is observed specifically in cells transduced with FER-targeting shRNA sequences.

I next examined if the inducible nature of the system is maintained throughout cell passaging. Transduced P5 and P10 cells were imaged and FER kinase levels were measured in these cultures. All cells observed were GFP-positive at both P5 and P10, indicating that GFP expression is stable over this period in culture (Figure 3.1A). Dox-treated FER 9 cells showed about an 88% and 65% decrease in FER levels at P5 and P10, respectively (Figure 3.1B). In addition, there was no significant difference in FER levels

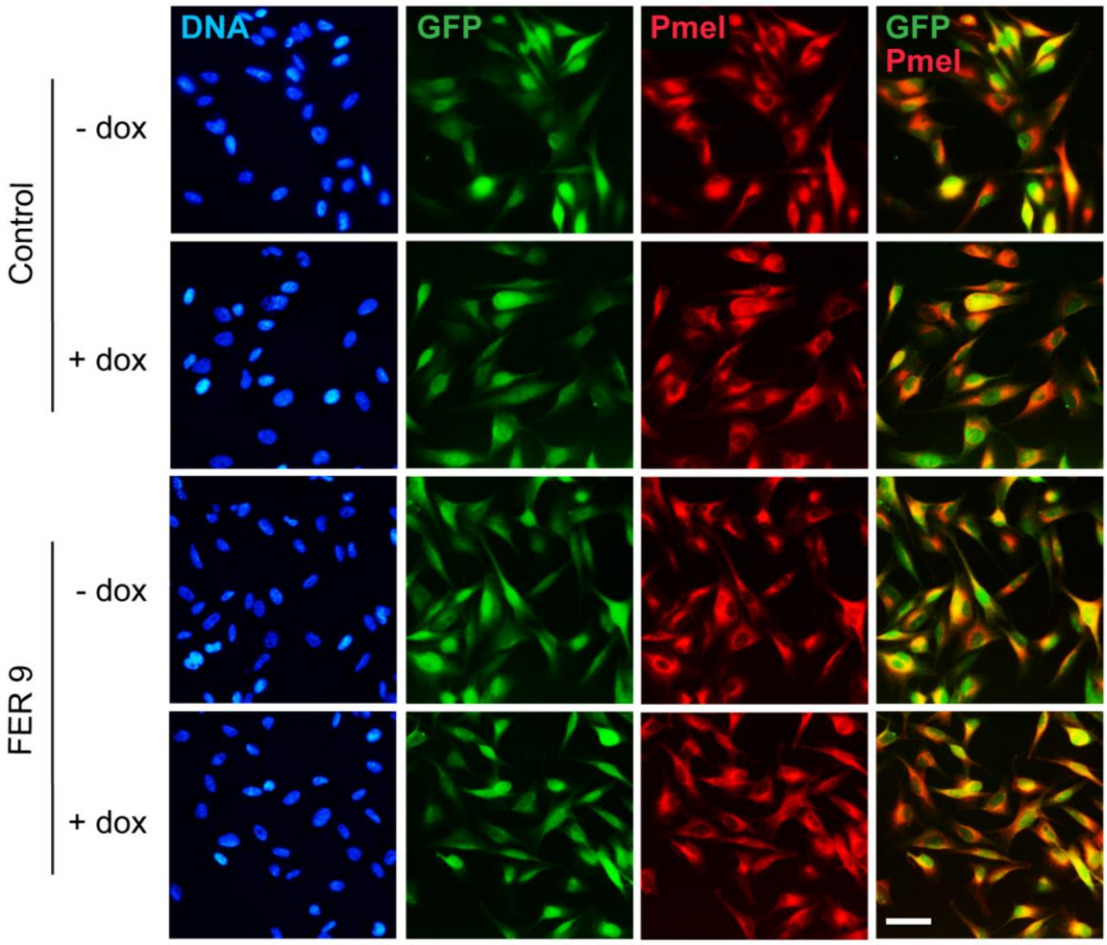

Figure 3.2. Melanocytic lineage confirmation of GFP-positive 5B1 cells

Control and FER 9 cells were cultured in medium with or without 2 μg/ml of dox for 5 days. Immunofluorescence microscopy with an anti- premelanosome (pmel) antibody was used to demonstrate the melanocytic lineage of GFP positive 5B1 cells. White bar = 140 μm.

between Control cells and untreated FER 9 cells. This demonstrates that FER kinase levels can be efficiently reduced in 5B1 clones at least as late as P10. Consequently, all experiments in these studies were conducted with cells between P1 and P5 in which FER 9 cells treated with dox consistently showed an 80-90% decrease in FER protein levels.

To investigate the duration of FER knockdown after dox withdrawal, Control and FER 9 cells were cultured in medium containing dox for 5 days, after which the cells were washed and cultured with fresh medium without dox. The cells were then cultured for 7 days in the absence of dox and FER levels were measured by immunoblot analysis. Figure 3.3 shows that FER levels remained decreased by 63-85% during the 7 days post-dox treatment. This demonstrates that following 5 days of dox treatment, FER kinase levels remain significantly reduced for at least 7 days. In addition, no significant differences were found in the FER protein levels of Control cells in the 7-day time period, indicating that FER levels were not affected by previous dox treatment.

3.2 Effects of FER knockdown on cell proliferation

To determine the effects of reduced FER kinase levels on proliferation, Control and FER 9 cells were cultured in medium containing dox for 5 days and then processed for immunofluorescence microscopy to analyze the fraction of cells expressing Ki67. During interphase of the cell cycle, the Ki67 protein can be found in the nucleus of cells and during mitosis it can be found on the surface of chromosomes (Scholzen and Gerdes, 2000). Therefore, Ki67 can be used to detect actively proliferating cells (i.e. cells in phases G1, S, G2 and M, but not in G0). Through immunofluorescence microscopy I found that, 69 ±

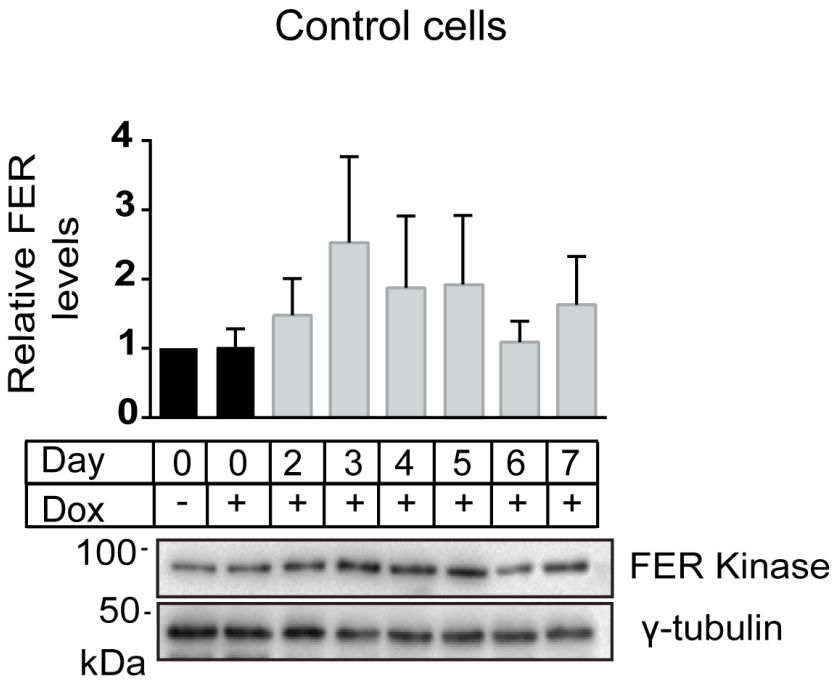
Control cells
Relative FER levels
4
3
2
1
0
Day 0 0 2 3 4 5 6 7
Dox - + + + + + + +
100-
50-
kDa
FER Kinase
γ-tubulin

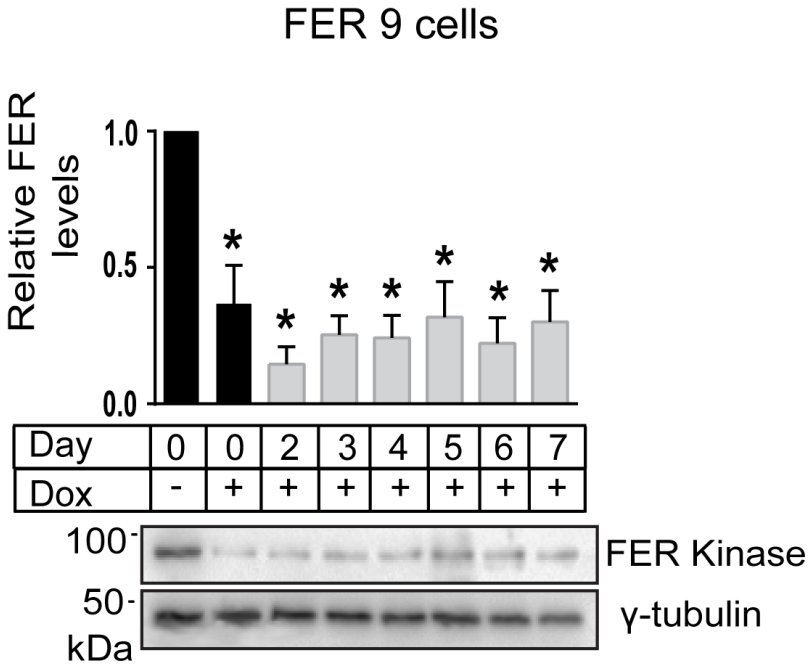
FER 9 cells
Relative FER levels
1.0
0.5
0.0
Day 0 0 2 3 4 5 6 7
Dox - + + + + + + +
100-
50-
kDa
FER Kinase
γ-tubulin

Figure 3.3. Duration of FER kinase knockdown after dox removal in 5B1 cells

Control and FER 9 cells were cultured in medium with or without 2 μg/ml of dox for 5 days. Cultures were then rinsed and incubated with dox-free growth medium. FER levels were measured using immunoblot analysis at the indicated times following dox removal. Histograms represent mean FER protein levels ± SEM (N=3) normalized to γ-tubulin and expressed relative to Control -dox or FER 9 -dox cells, which are set to 1. "Day" indicates the number of days following dox removal and the "Dox" labelling indicates whether cells were pretreated with dox. * represents $P < 0.05$ relative to FER 9 -dox cells (ANOVA).

8% and 70 ± 15% of Control cells without and with dox, respectively, were Ki67-positive. In addition, 73 % ± 13 % of FER 9 cells without dox and 83 ± 5% FER 9 cells with dox were Ki67-positive (Figure 3.4). Therefore, no significant differences were identified suggesting that FER-expressing and FER-deficient cells were actively proliferating.

Although Ki67 is an excellent global marker of proliferating cells, it does not allow for the investigation of cell cycle phase-specific differences between cell populations. Therefore, I opted to determine if S-phase differences result from FER kinase knockdown. Control and FER 9 cells were treated with dox for 5 days after which cells were incubated in medium containing 5-bromo-2-deoxyuridine (BrdU), a thymidine analog that is incorporated into DNA during S-phase. I then determined the proportion of cells showing BrdU immunoreactivity and found that 24 ± 3% and 30 ± 4% of Control cells had incorporated BrdU into their DNA in cultures in the presence and absence of dox, respectively. Therefore, no significant differences in Control cells occurred as a consequence of dox treatment (Figure 3.5). In contrast, whereas the proportion of BrdU-positive FER 9 cells cultured without dox was 29 ± 3%, only 17 ± 4% of FER 9 cells were found to be BrdU-positive when FER was silenced by dox treatment (Figure 3.5). Consequently, FER-deficient cells exhibit a 41% decrease in the proportion of cells in the S-phase of the cell cycle, thereby suggesting that FER kinase plays a role in normal melanoma cell cycle progression.

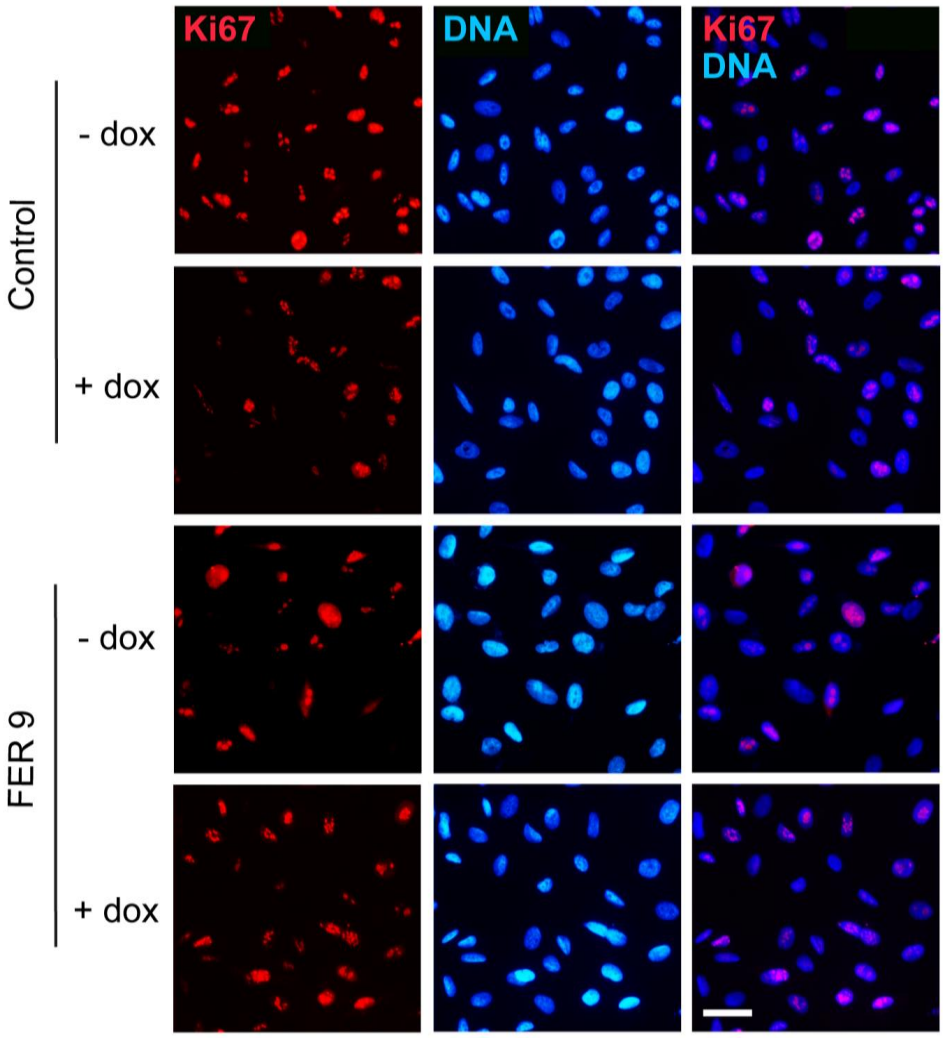
Ki67
DNA
Ki67
DNA
Control
- dox
+ dox
FER 9
- dox
+ dox

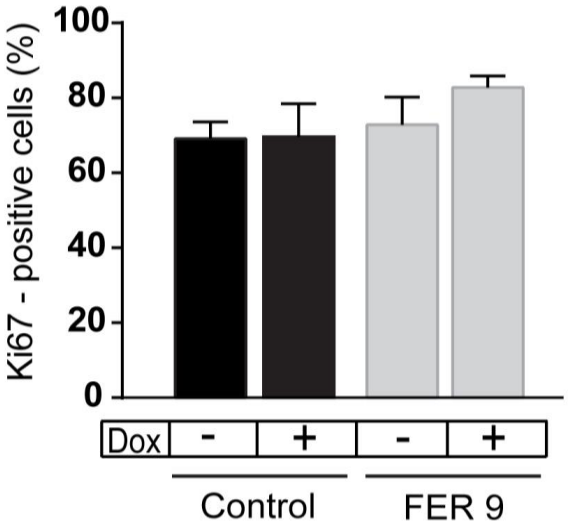
Ki67 - positive cells (%)
100
80
60
40
20
0
Dox
-
+
-
+
Control
FER 9

Figure 3.4. Effect of FER kinase silencing on 5B1 expression of Ki67

Control and FER 9 cells were cultured in medium with or without 2 μg/ml of dox for 5 days and then processed for immunofluorescence microscopy, using an anti-Ki67 antibody. The histogram represents the fraction of Ki67-positive cells in each cell group, expressed as the mean ± SEM (N=3). Scale bar = 140 μm.

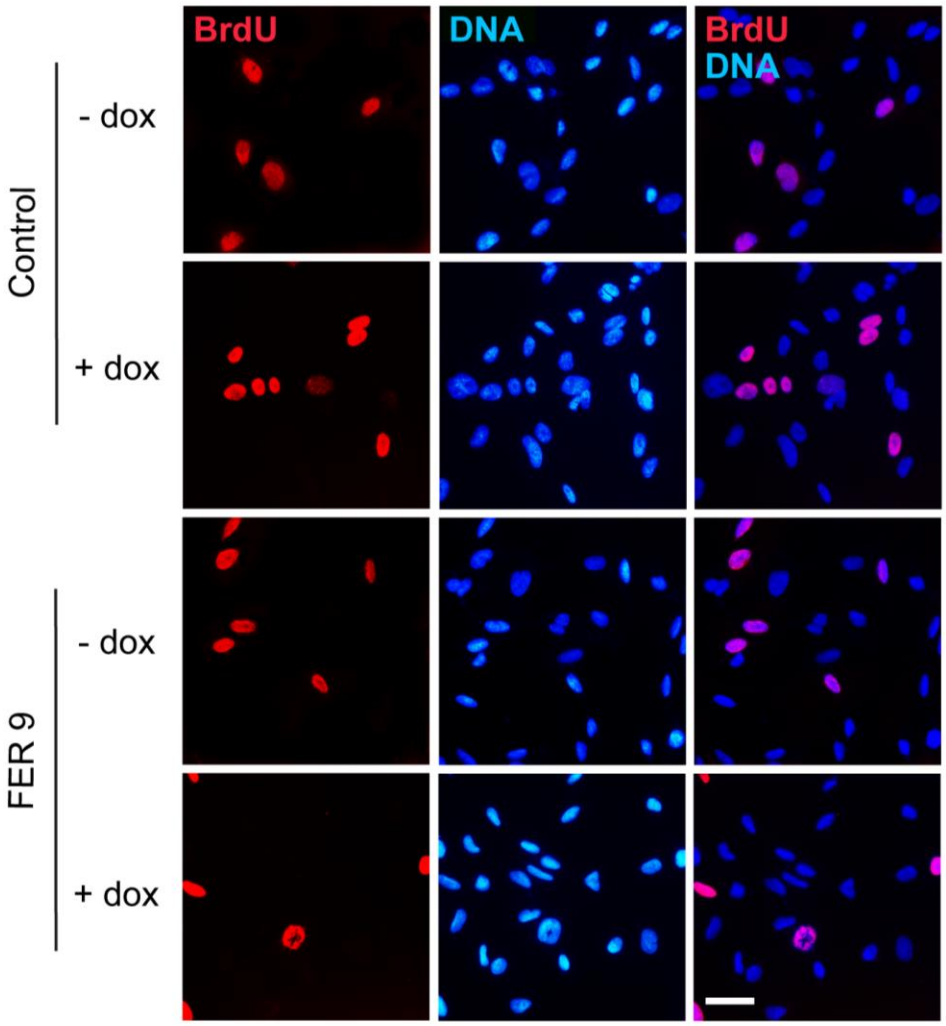
BrdU
DNA
BrdU
DNA
Control
- dox
+ dox
FER 9
- dox
+ dox

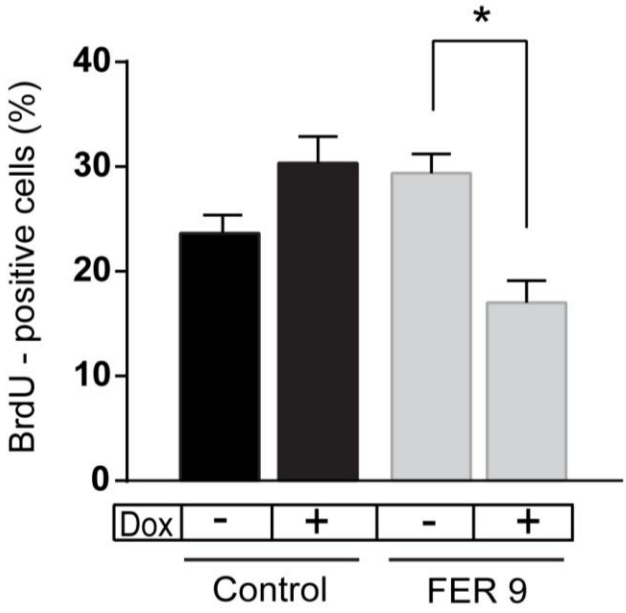
*
BrdU - positive cells (%)
40
30
20
10
0
Dox
-
+
-
+
Control
FER 9

Figure 3.5. Effect of FER kinase silencing on 5B1 cells in S-phase

Control and FER 9 cells were cultured in medium with or without 2 μg/ml of dox for 5 days then incubated in medium containing 10 μM of BrdU for 2 h. The cells were processed for immunofluorescence microcopy using an anti-BrdU antibody. The histogram represents the fraction of BrdU-positive cells, expressed as the mean ± SEM (N=3). * represents $P < 0.05$ (ANOVA). Scale bar = 140 μm.

3.3 Effect of FER kinase silencing on 5B1 susceptibility to anoikis

To investigate the effect of FER kinase knockdown on cell susceptibility to anoikis, a form of apoptosis due to detachment from the extracellular matrix, Control and FER 9 cells were cultured in the presence of dox for 5 days and then plated on normal culture dishes, which allowed cell adhesion, or on dishes coated with poly-HEMA, which prevented cell adhesion to their surface, and thus maintained cells in suspension, for 6 days. Anoikis was analysed by immunoblotting for the presence of the early apoptosis marker, cleaved-caspase 3. Cleaved-caspase 3 was not detected in either FER-expressing or FER-deficient cells plated on either adherent or suspension conditions (Figure 3.6). As a positive control for apoptosis, cleaved caspase 3 was readily detected in adherent Control cells treated with 80 or 100 μM of cisplatin, as well as in G804 rat epithelial bladder cells that were irradiated with 75 mJ of UVC light. This demonstrates that neither Control nor FER 9 cells were susceptible to anoikis irrespective of whether they express FER kinase.

3.4 Effects of FER knockdown on random 5B1 cell motility

In the skin, human melanoma cells metastasize through various mechanisms, including interactions with extracellular matrix proteins such as collagen I (Col I) and laminin 332 (Lam 332). Therefore, I next determined 5B1 random cell motility on these ECM substrates. Control cells were cultured on uncoated μ-Dishes or on dishes coated with Col I, Lam 332 or both. Cells were then imaged for 16 h using time-lapse video microscopy. All cells within the field of view were then tracked to measure migration distance and velocity. Figure 3.7A illustrates migratory cell paths

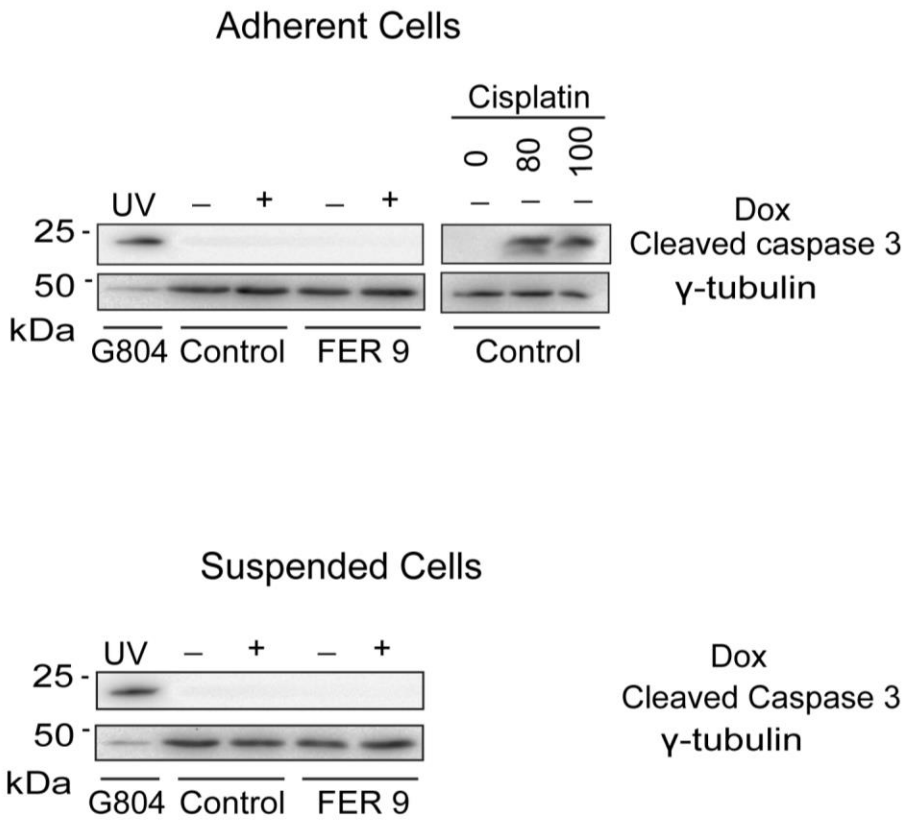

Figure 3.6. FER kinase knockdown on 5B1 cell susceptibility to anoikis

Control and FER 9 cells were cultured in medium with or without 2 μg/ml of dox for 5 days and then plated on dishes coated with (suspended cells) and without (adherent cells) poly-HEMA. As a positive control for 5B1 cell death, adherent Control cells were treated with 80 and 100 μM of cisplatin and adherent G804 cells were irradiated with 75 mJ of UVC as a different cell type control for apoptosis. The presence of cleaved-caspase 3 in cell groups was detected by immunoblot analysis (N=3).

(indicated by closed circles) on the different ECM substrates, as well as, in the absence of exogenously added ECM. The majority of cells cultured with no exogenous matrix or on collagen I, showed minimal migration from their initial point of tracking (0,0). Specifically, in the absence of exogenous ECM the cells migrated a total distance of 182 ± 18 μm, with a speed of 0.19 ± 0.02 μm/min, whereas cells cultured on Col I migrated a total distance of 179 ± 21 μm with a speed of 0.19 ± 0.02 μm/min. In contrast, the migration paths of cells cultured on Lam 332 illustrate movement away from their initial positions. After 16 h, these cells displayed a total migration distance of 278 ± 22 μm, with a speed of 0.28 ± 0.02 μm/min (Figure 3.7). Therefore, a 53% increase in total migration and 47% increase in speed were observed in the cells when plated on Lam 332. Cells cultured on dishes coated with both collagen I and laminin 332 displayed no significant difference in migration or speed, 220 ± 11 μm and 0.23 ± 0.01 μm/min, respectively. Another measure of migration, the Euclidean distance, is a linear measure of the distance between the initial and final migration positions and can therefore be used to quantify directionality in migration. No significant differences were found in the Euclidean distances of Control cells cultured on no ECM, Col I, Col I and Lam 332 and Lam 332, 64 ± 10 μm, 65 ± 17 μm, 61 ± 8 μm and 83± 7 μm, respectively. Thus, irrespective of exogenous ECM, Control cells maintained their normal random migration. In summary, only the addition of exogenous Lam 332 promotes random 5B1 cell migration.

Next, to determine the effects of FER kinase silencing on migration on Lam 332, Control and FER 9 cells were cultured with dox for 5 days and then plated on dishes coated with Lam 332. Cells were imaged for 16 h using time-lapse video microscopy, and the distance and speed were measured as above. The migration paths of FER-expressing cells, as

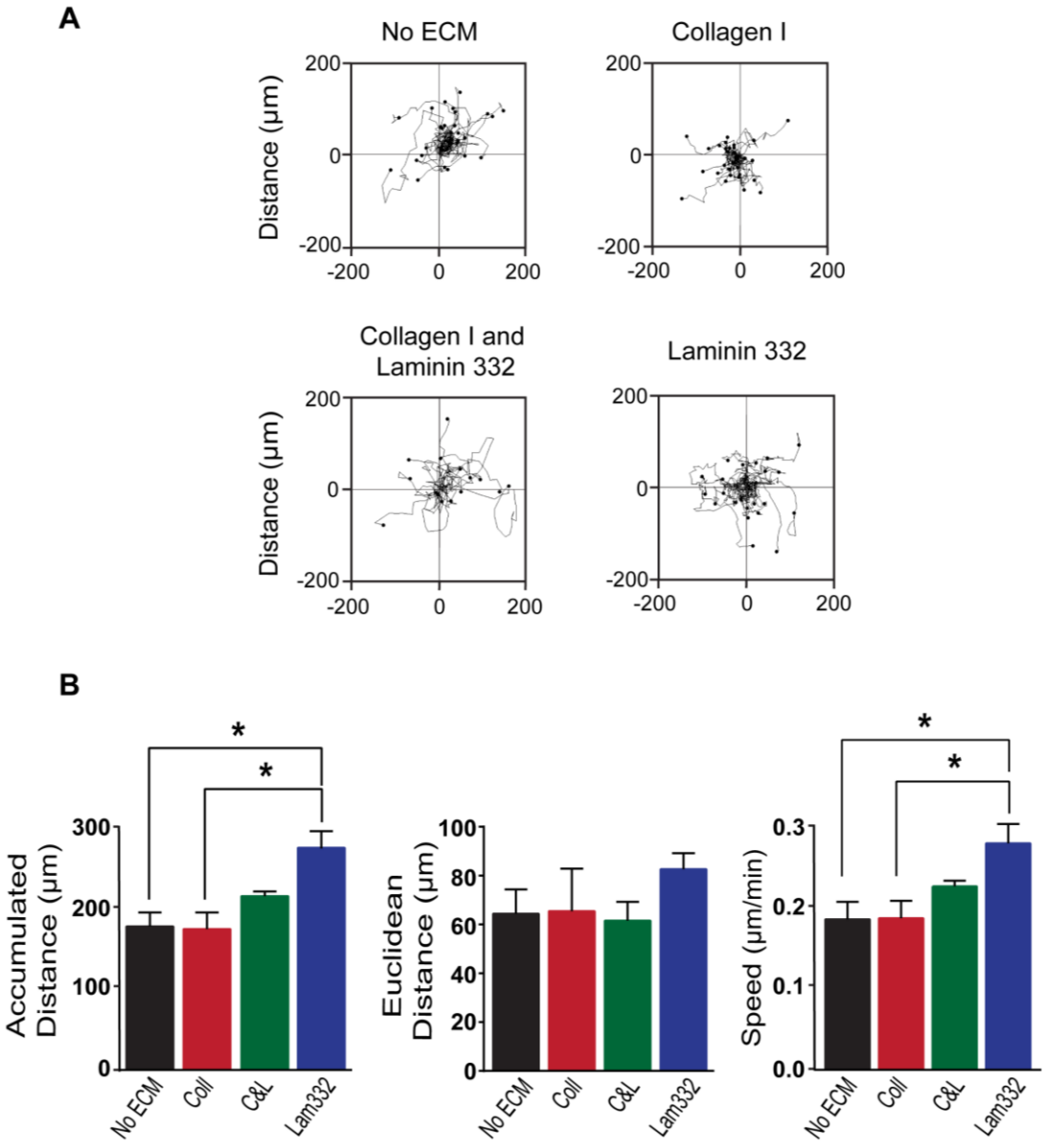
A
No ECM
Collagen I
Collagen I and Laminin 332
Laminin 332
Distance (µm)
200
0
-200
B
Accumulated Distance (µm)
Euclidean Distance (µm)
Speed (µm/min)
No ECM
Coll
C&L
Lam332
*

Figure 3.7. 5B1 migration on different extracellular matrices

Untreated Control cells were plated on μ-Dishes without any exogenous extracellular matrix (No ECM) or coated with collagen I (Coll), laminin 332 (Lam332) or both (C&L). Cells were imaged for 16 h using time-lapse video microscopy and analysed using Image J (NIH) and the Chemotaxis and Migration Tool Software (ibidi). Two hundred cells were tracked in total for each cell group. **A**. Migratory paths of Control cells on varying extracellular matrices. The initial migratory point of a cell is represented as (0,0) and the final point is illustrated as a closed circle. **B.** Histograms represent mean ± SEM (N=3) accumulated (total) distance, Euclidean distance (straight linear distance from the initial to final migratory point) and speed of Control cells. * represents $P < 0.05$ (ANOVA).

illustrated in Figure 3.8A, show that in general their final positions were farther removed from the origin compared to FER-deficient cells. Control cells cultured in the absence of dox migrated a total distance of 278 ± 38 μm with a speed of 0.28 ± 0.04 μm/min, whereas Control cells treated with dox similarly migrated a total distance of 274 ± 80 μm with a speed of 0.32 ± 0.04 μm/min. Thus, dox treatment per se had no significant effect on cell motility. Similarly, FER 9 cells cultured in the absence of dox migrated a total distance of 330 ± 23 μm with a speed of 0.35 ± 0.02 μm/min. In contrast, silencing of FER caused a significant decrease in cell motility, as FER 9 cells treated with dox migrated 228 ± 54 μm with a speed of 0.25 ± 0.07 μm/min (Figure 3.8B). This difference corresponds to a 31% decrease in total distance and a 29% decrease in the migratory speed of FER-deficient cells. The Euclidean distances of Control (no dox: 83 ± 7 μm, dox: 92 ± 15 μm) and FER 9 (no dox: 102 ± 6 μm, dox: 78 ± 12 μm) cells were not significant, indicating random migration of the cells irrespective of their levels of FER. Therefore, the downregulation of FER impairs random cell migration indicating that FER kinase is essential for normal melanoma cell migration on Lam 332.

3.5 The chicken chorioallantoic membrane (CAM) *in vivo* tumour xenograft model to study tumour invasion

Analysis of tumour growth, invasion, and metastasis *in vivo* are often explored using mouse models or the chicken CAM. The CAM is found just underneath the surface of the egg shell and plays a vital role in gas exchange. It is composed of two epithelial membranes, the outermost membrane is called the chorionic epithelium, whereas the innermost membrane, located closer to the chicken embryo, is the allantoic epithelium. These two membranes enclose the mesoderm, which is a highly vascularized stromal tissue containing

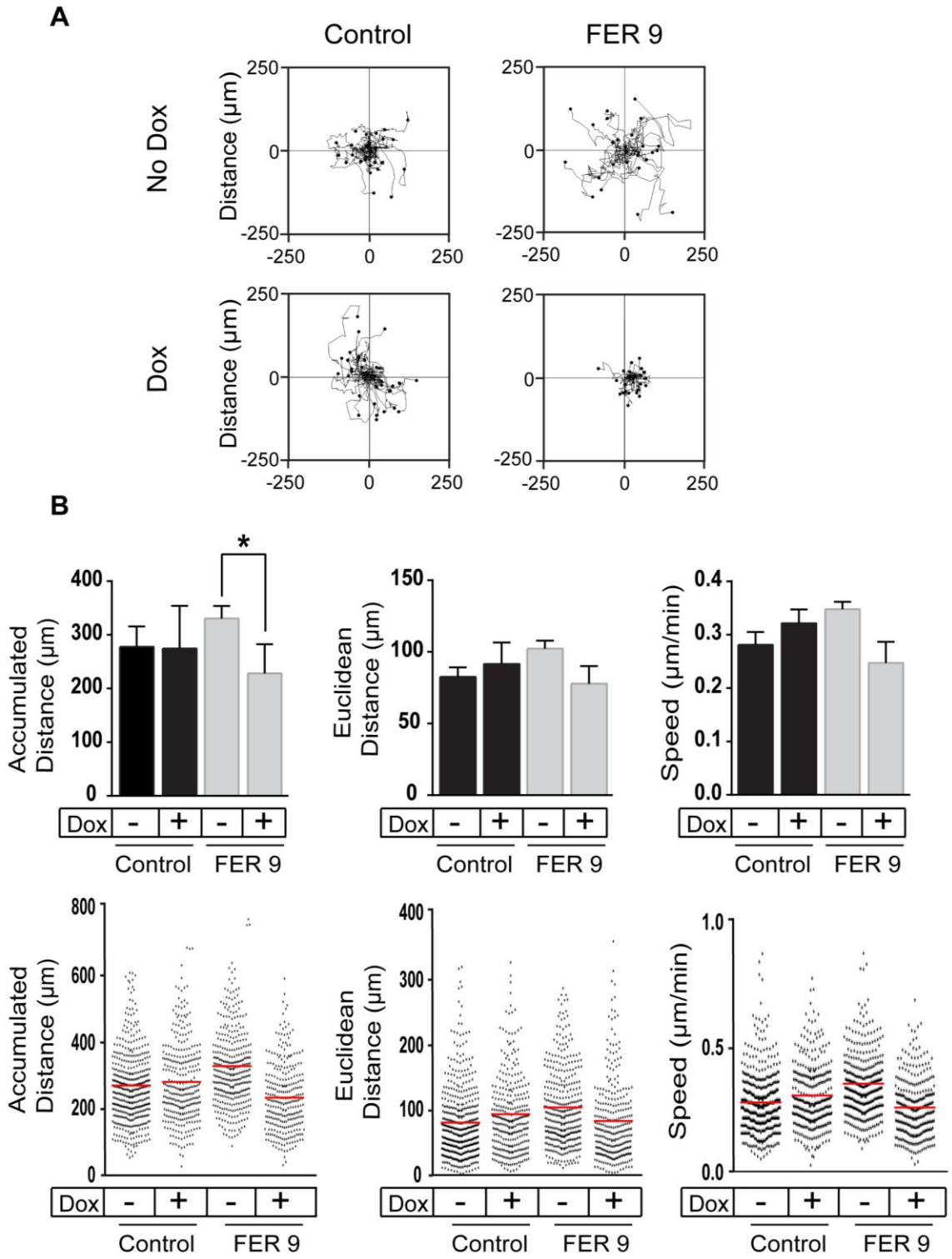
A
Control
FER 9
No Dox
Dox
Distance (µm)
250
0
-250
B
*
Accumulated Distance (µm)
Euclidean Distance (µm)
Speed (µm/min)
Dox
-
+
Control
FER 9

Figure 3.8. Effect of FER kinase knockdown on 5B1 motility

Control and FER 9 cells were cultured in medium with or without 2 μg/ml of dox for 5 days and then cultured on μ-Dishes coated with laminin 332. Cells were imaged for 16 h using time-lapse video microscopy and analysed using Image J (NIH) and the Chemotaxis and Migration Tool Software (ibidi). Three hundred cells were tracked in total for each cell group. **A**. Migratory paths of FER-expressing and FER-deficient cells on laminin 332. The initial migratory point of a cell is represented as (0,0) and the final point is illustrated as a closed circle. **B.** Histograms represent mean ± SEM (N=3) accumulated (total) distance, Euclidean distance (straight linear distance from the initial to final migratory point) and speed of cells. Dot plot illustrates the distribution of 5B1 accumulated distance, Euclidean distance and speed values. * represents $P < 0.05$ (ANOVA).

various extracellular matrix proteins, such as type III collagen. In chicks, CAM growth begins on embryonic day (E) 3 and is completed by E10 (Nowak-Sliwinska et al., 2014). In the CAM tumour xenograft model, fertilized chicken eggs are cracked and their contents are placed in covered dishes. The CAM is then easily accessible for experiments involving grafting of cells or addition of test substances onto the CAM (Figure 3.9A).

To determine if 5B1 cells can form tumours on the CAM, untreated FER 9 cells suspended in Cultrex extracellular matrix extract were grafted onto the CAMs of E11 chick embryos that were isolated by cracking in the manner described above. Seven days post-grafting, rhodamine-labelled *lens culinaris agglutinin* (LCA) was injected into a blood vessel of the CAM and 5-10 min after, the tumours and underlying CAM tissues were harvested and processed for analysis. LCA labels endothelial cells (Deryugina and Quigley, 2009), thus allowing for visualization of the CAM vasculature. Figure 3.9B shows 5B1 tumour growth on the chorionic epithelium of the CAM, indicating that 5B1 cells suspended in Cultrex can grow and form tumours that are readily visible 7 days post-grafting. Immunostaining was then conducted on these tumour sections to determine the best way to distinguish 5B1 cells from CAM tissue. 5B1 cells were clearly visible based on GFP-immunoreactivity, and could be effectively distinguished from the CAM, which was labelled using an antibody that specifically recognizes chicken collagen type III (Melkonian et al., 2000) (Figure 3.9C). The identity of the GFP-positive Control and FER 9 melanoma cells in xenografts was further confirmed by the presence of Pmel, as every GFP-positive cell in tumour tissue also expressed Pmel (Figure 3.9D). I also observed GFP-negative regions within the tumour, which may constitute necrotic tumour tissue. The presence of chicken endothelial cells, indicative of vasculature within the CAM and the tumour was observed,

A

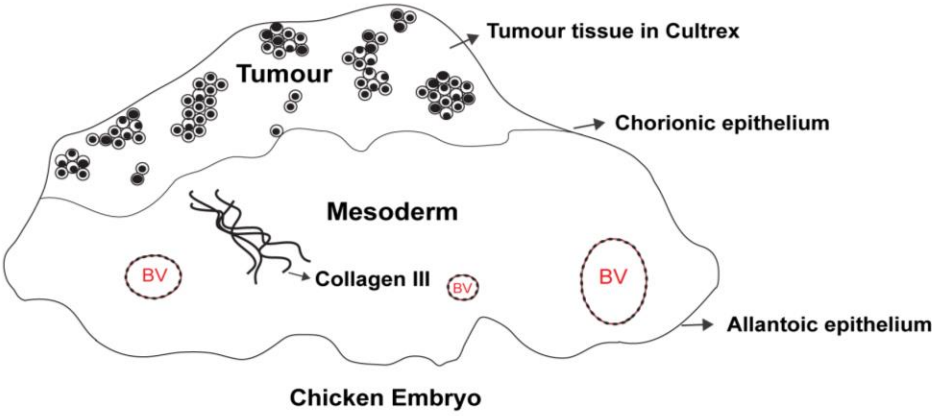
Tumour tissue in Cultrex
Tumour
Chorionic epithelium
Mesoderm
BV
Collagen III
BV
BV
Allantoic epithelium
Chicken Embryo

B

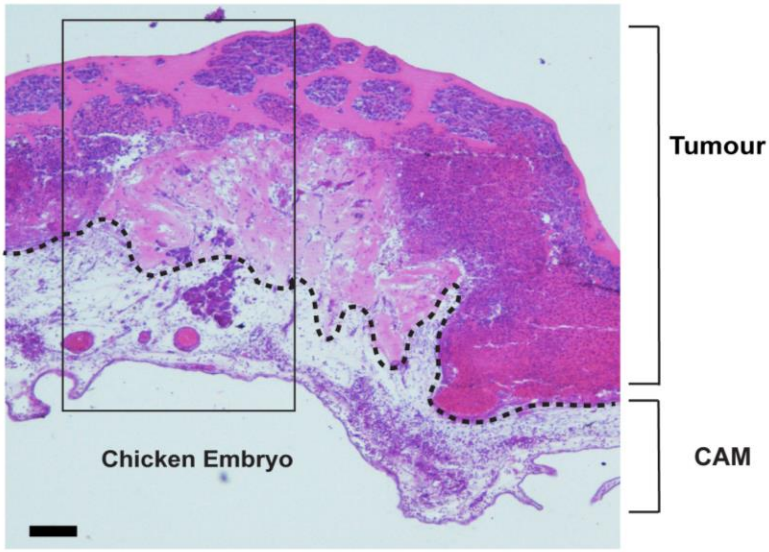
Tumour
CAM
Chicken Embryo

C

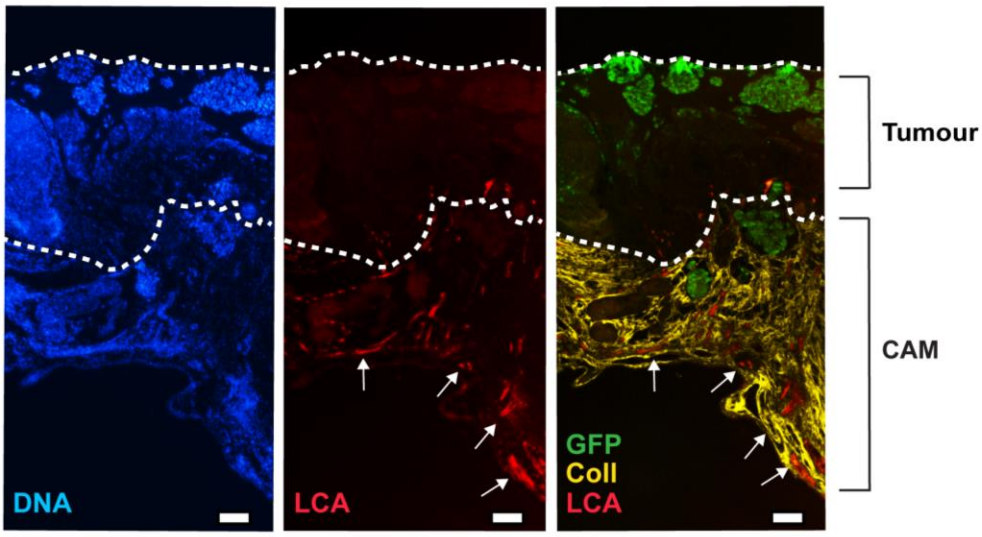
Tumour
CAM
DNA
LCA
GFP
Coll
LCA

D

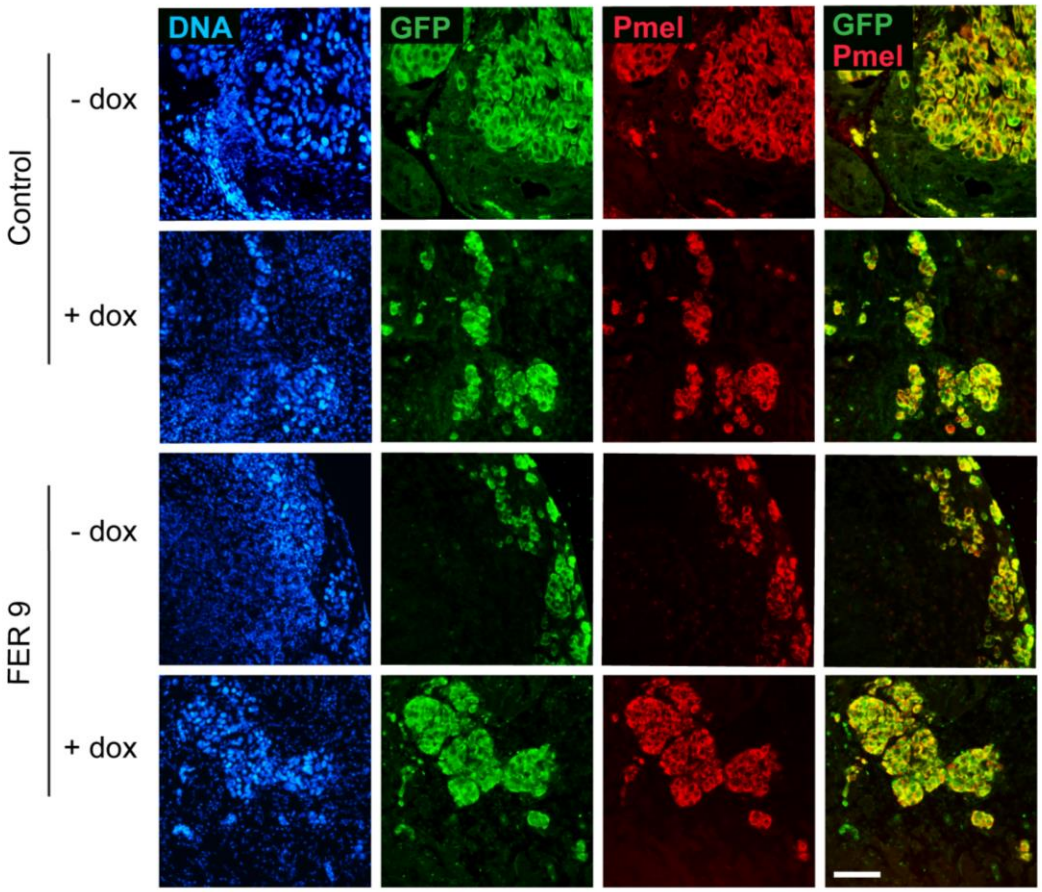

Figure 3.9. Illustration of the chicken chorioallantoic membrane (CAM) used to measure 5B1 cell invasion

FER 9 cells were cultured in medium with or without 2 μg/ml of dox for 5 days. Cells suspended in Cultrex were grafted on the CAMs of embryonic day 11 (E11) embryos and incubated for an additional 7 days to allow for tumour growth. On E18, rhodamine labelled *lens culinaris agglutinin* (LCA) was injected into a blood vessel of the CAM, tumours were excised and processed for further analysis. **A.** Schematic of 5B1 tumour growth on the CAM. BV= blood vessel. **B**. Representative hematoxylin and eosin (H&E) stained tumour tissue section showing 5B1 tumour growth and invasion into CAM mesoderm. Black Bar = 100 μm. The area outlined by the black rectangle is represented in **C**. as fluorescence images demonstrating 5B1 cell detection using GFP immunoreactivity and detection of the CAM using a chicken specific collagen III antibody. Shown in red, are the endothelial cells labelled with rhodamine-LCA. White bar = 100 μm. **D.** GFP and Pmel immunoreactivity in Control and FER 9 tumour tissue to confirm the melanocytic lineage of GFP-positive 5B1 cells. White bar = 64 μm.

based on staining by the rhodamine-labelled LCA, which is known to bind to glycoconjugates on the endothelial lining of blood vessels (Figure 3.9C).

3.6 Comparison of 5B1 tumour growth in Matrigel and Cultrex

Matrigel (Corning) and Cultrex (Trevigen) are mixtures of extracellular matrix proteins secreted by the Engelbreth-Holm Swarm (EHS) mouse sarcoma. They are composed of about 60% laminin, 30% collagen IV and 8% entactin, as well as sulfate proteoglycans and growth factors (Kleinman and Martin, 2005). Matrigel has been frequently used in xenograft experiments (Benton et al., 2011). To compare tumour growth of 5B1 cells suspended in Matrigel or in Cultrex, untreated Control and FER 9 cells were suspended in one of these substrates and grafted onto the CAM of E11 chick embryos. Seven days after grafting, the tumours and underlying CAMs were harvested and processed for analysis. Control and FER 9 cells were able to form tumours on the CAM when suspended in either Matrigel or Cultrex. 5B1 cells were also detectable within the CAM tissue, as evidenced by the presence of GFP immunoreactivity within collagen III-positive CAM tissue (Figure 3.10). 5B1 tumour growth in Matrigel was indistinguishable from that in Cultrex. For all subsequent experiments in this study, cells were suspended in Cultrex.

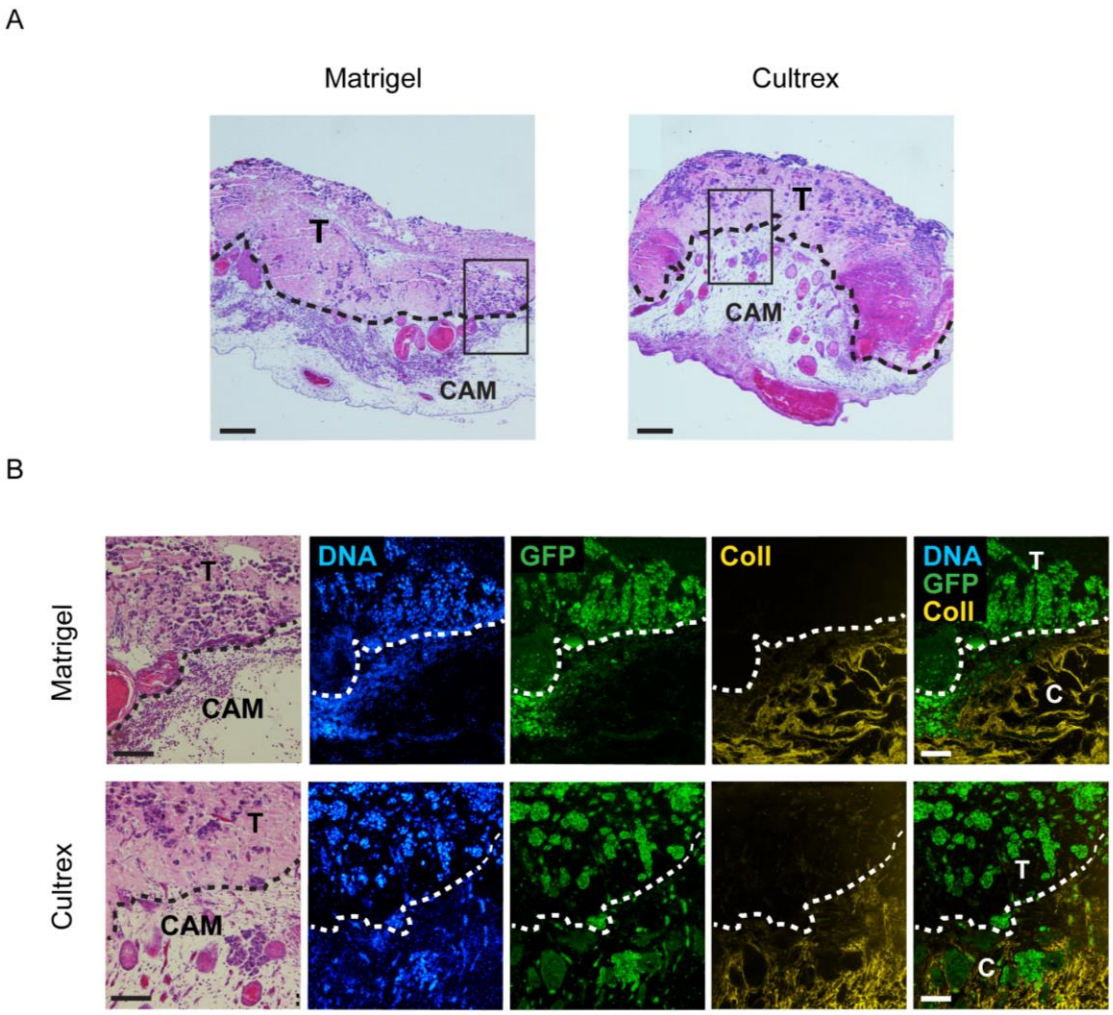

Figure 3.10. Capacity of Matrigel and Cultrex matrices to support 5B1 tumour growth

Untreated Control and FER 9 cells were suspended in either Matrigel or Cultrex and then grafted on the CAMs of E11 embryos. Tumours were excised on E18 and processed for immunohistochemistry analysis. **A.** H & E stained sections of tumours formed from 5B1 cells suspended in Matrigel or Cultrex. T= tumour, black bar = 215 µm. **B.** GFP and collagen III antibodies were used to detect 5B1 cells and delineate the CAM, respectively. T= tumour, C= CAM, black bar = 108 µm and white bar = 100 µm.

3.7 Analysis of 5B1 cell invasion into the CAM mesoderm

To systematically characterize 5B1 tumour growth and invasion, sections throughout the tumour were analyzed. The sections selected were obtained from three areas: near the edge of the tumour, schematically represented by (A) on Figure 3.11, in the middle of the tumour (C, Figure 3.11) and between those two regions (B, Figure 3.11). On average, Control and FER 9 tumours were about 5 mm wide. The distance between the regions indicated as A and B in the schematic was about 0.4 mm, whereas the boundaries indicated as B and C were approximately 2 mm apart. GFP-positive melanoma cells were detected in the sections analyzed from regions A, B and C (Figure 3.11). Invasion into the CAM mesoderm, evidenced by the presence of GFP immunoreactivity embedded within collagen III-positive areas, was also observed in these sections. As melanoma cell growth was consistently observed in these tumour areas, further analysis focused on the core region of the tumour located between regions A and C. For these studies, 10 tissue sections evenly distributed between regions A and C were analysed for each tumour, as previously performed by (Lokman et al., 2012).

3.8 Effect of FER kinase silencing on 5B1 cell invasion into the CAM mesoderm

To determine the role of FER kinase in 5B1 cell invasion into the CAM mesoderm, FER 9 cells were first cultured in medium with or without dox for five days. The cells were rinsed to remove dox, suspended in dox-free Cultrex and grafted onto the CAM as described in section 3.5. Tumours were processed and ten 7-µm sections between regions A and C, (Figure 3.11) were analysed, as mentioned above. Figure 3.12 shows images obtained from

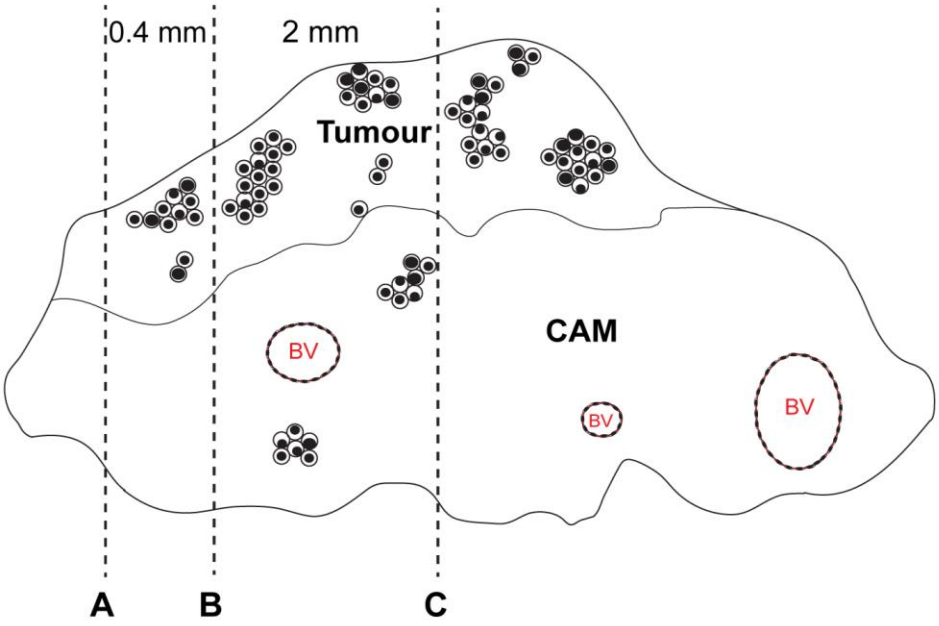
0.4 mm
2 mm
Tumour
CAM
BV
BV
BV
A
B
C

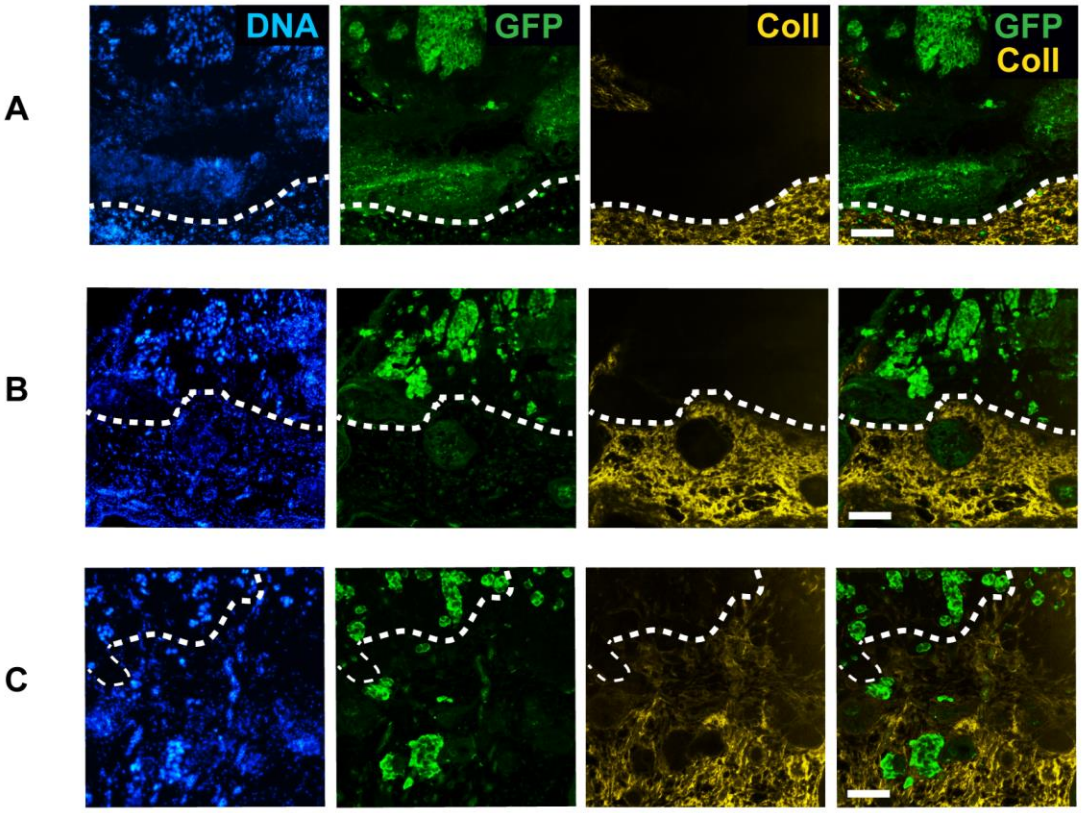
A
B
C
DNA
GFP
Coll
GFP
Coll

Figure 3.11. Systematic analysis of 5B1 cell invasion into the CAM mesoderm

5B1 cell invasion into the CAM was characterized by analysing sections throughout the tumour. GFP and collagen III immunofluorescence was performed on sections obtained from the edge of the tumour (A), middle of tumour (C) and between those two regions (B). White bar = 100 µm. The white dotted line outlines the tumour-CAM interface.

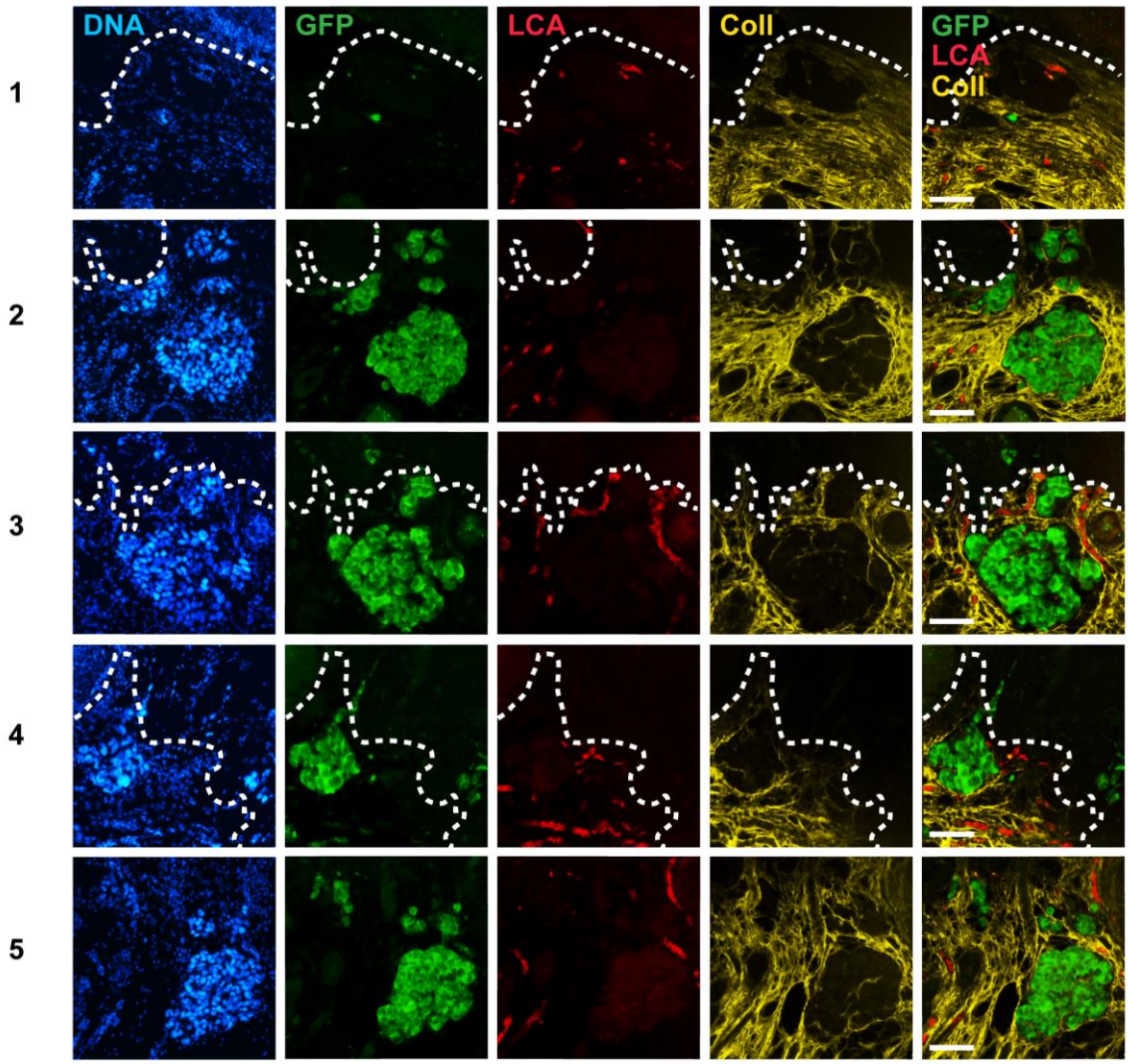
DNA
GFP
LCA
Coll
GFP
LCA
Coll
1
2
3
4
5

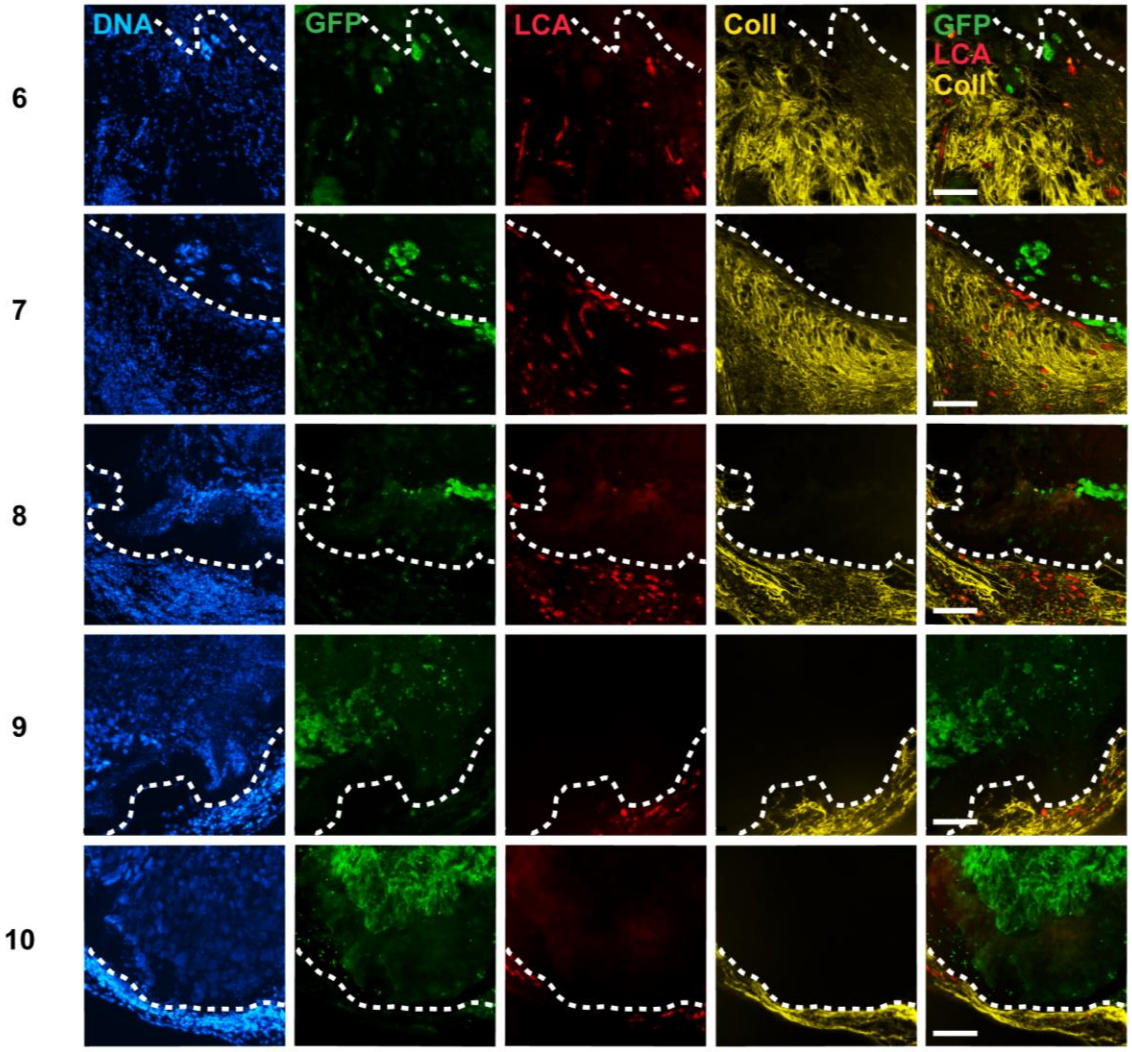
DNA
GFP
LCA
Coll
GFP
LCA
Coll
6
7
8
9
10

Figure 3.12. Analysis of 5B1 invasion into the CAM mesoderm in ten sections of a FER-expressing tumour

Untreated FER 9 cells suspended in Cultrex were grafted on the CAMs of E11 embryos and then cultured for 7 days to promote tumour growth. On E18, rhodamine-labeled *lens culinaris agglutinin* (LCA) was injected into a blood vessel of the CAM, the tumour was subsequently excised and processed for further analysis. Ten serial sections from between regions A and C were examined (Figure 3.11). Sections illustrating GFP immunoreactivity within collagen III-positive areas were categorized as sections showing 5B1 cell invasion. White bar = 64 µm. The white dotted line outlines the tumour-CAM interface.

each of ten sections of a tumour formed by untreated FER 9 cells. In this specimen, sections 1 through 6 show the presence of GFP-positive 5B1 cells within the collagen III-labeled CAM, indicative of invasion. On that basis, the tumour in Figure 3.12 received an invasion score of 6 out of 10. Notably, in this tumour, blood vessels were observed in close proximity to melanoma cells located within the CAM, as evidenced by the rhodamine-LCA fluorescence adjacent to and/or surrounding the GFP positive cells within the CAM. In addition, sections 8 through 10 displayed tumour growth on the CAM surface, and no blood vessels were detected within this tumour region. Similarly, for each tumour analyzed, the number of sections in which invasion was observed was scored.

The invasion of FER-deficient tumours was then analyzed. Figure 3.13 illustrates the 10 sections analysed for a tumour formed by FER 9 cells previously treated with dox (i.e. FER-deficient cells). In this tumour, cell invasion into the CAM mesoderm was observed in sections 1 and 7 through 10, therefore this tumour received an invasion score of 5 out of 10. Similar to the tumour formed by untreated FER 9 cells (Figure 3.12), the presence of vasculature in close proximity to the melanoma cells within the CAM suggests that FER kinase is not essential for the ability of melanoma cells to localize proximal to blood vessels. The tumour sections No. 3 to 6 illustrate tumour cells growing on the CAM. In addition, sections No. 4 and No. 5 exhibit the presence of lectin-labelled chick endothelial cells within the tumour (Figure 3.13).

In total, I grafted 49, 41, 52 and 54 CAMs with Control, Control with dox, FER 9 and FER 9 with dox cells, respectively. The total number of tumours excised at the end of the CAM experiments are outlined in Table 3.1. Of those, the indicated number of “viable” tumours

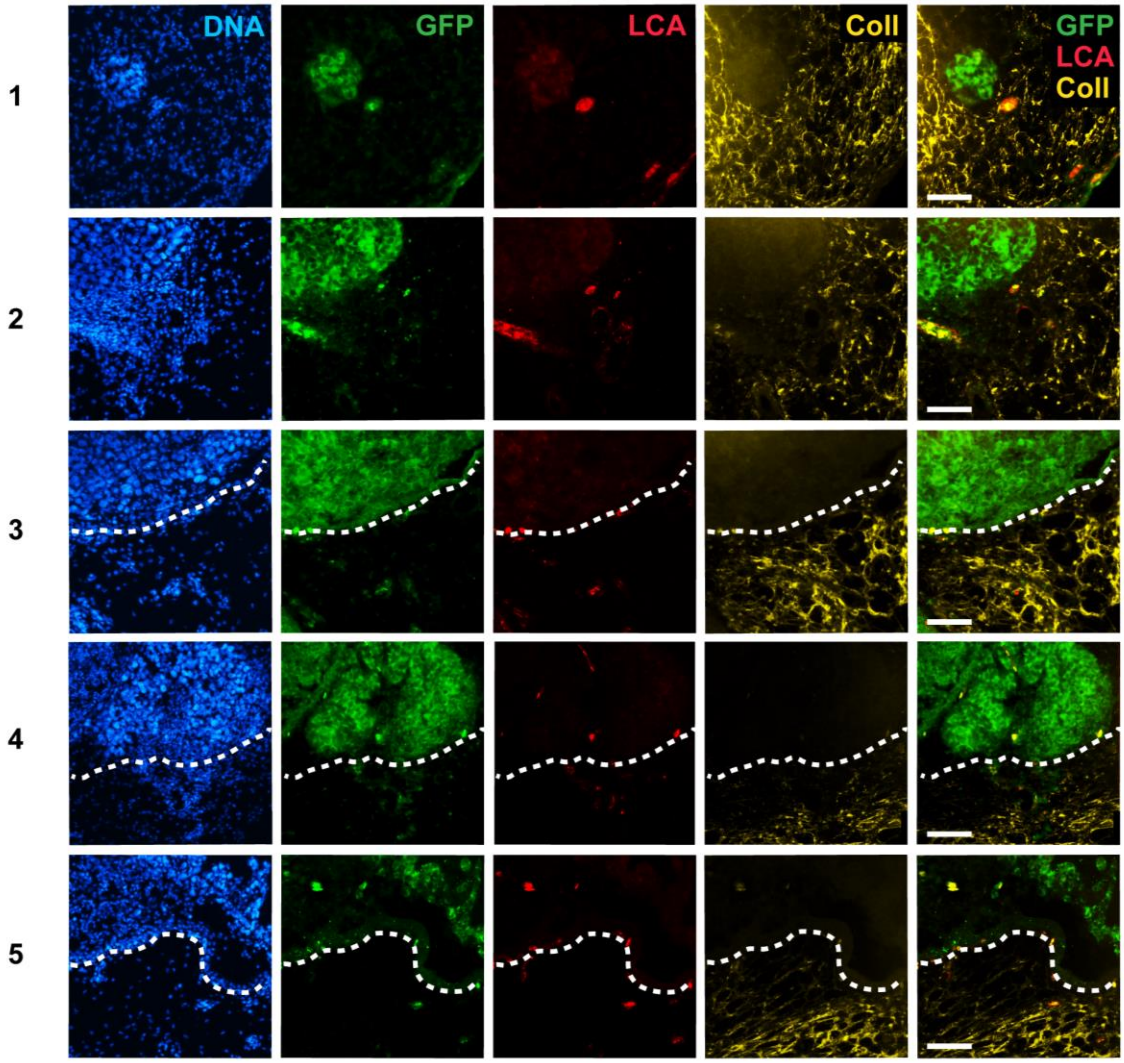
DNA
GFP
LCA
Coll
GFP
LCA
Coll
1
2
3
4
5

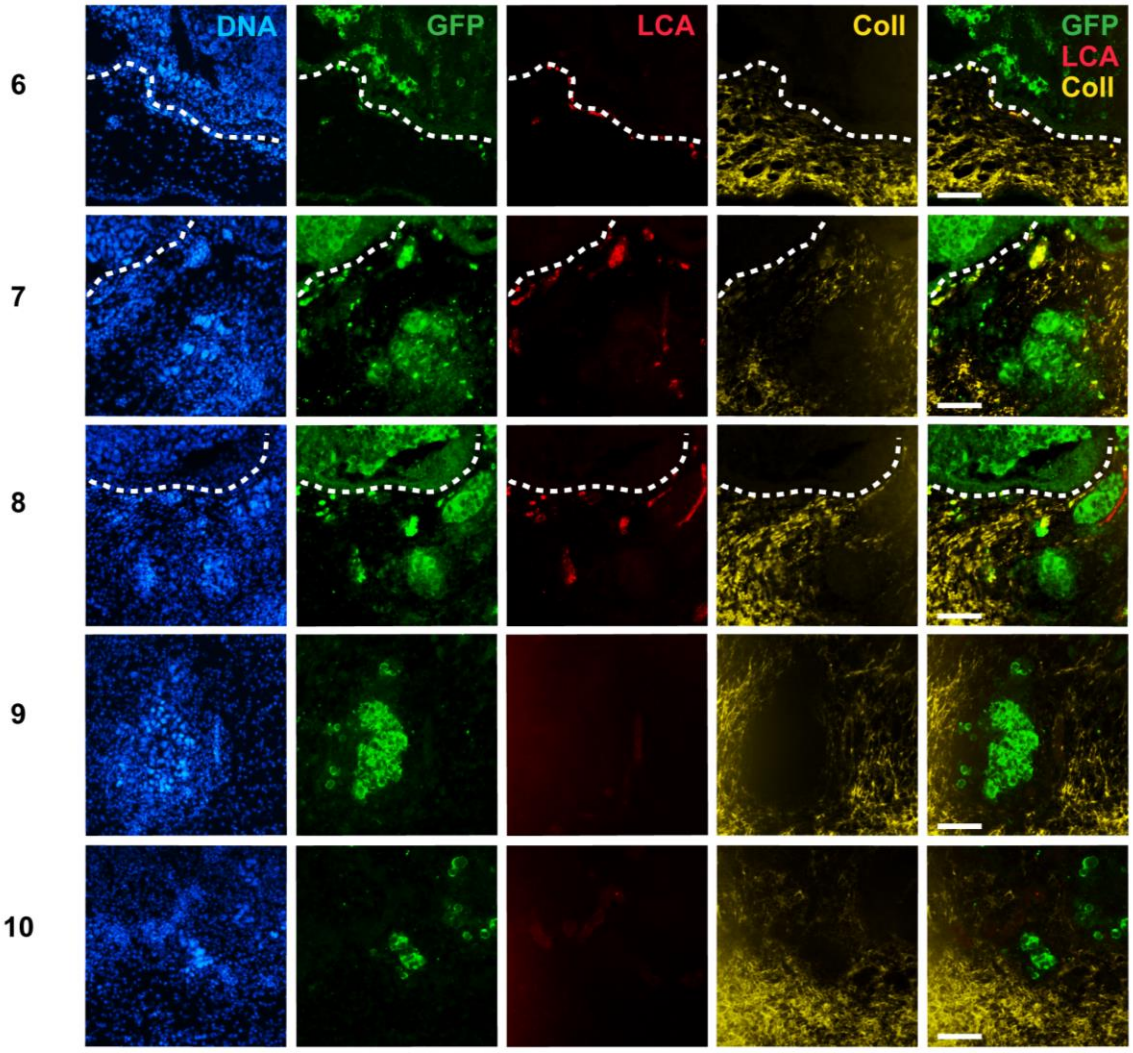
DNA
GFP
LCA
Coll
GFP
LCA
Coll
6
7
8
9
10

Figure 3.13. Analysis of 5B1 invasion into the CAM mesoderm in ten sections of a FER-deficient tumour

Treated FER 9 cells (previously cultured in medium containing dox for 5 days) suspended in Cultrex were grafted onto the CAMs of E11 embryos and then cultured for 7 days to promote tumour growth. On E18, rhodamine-labeled *lens culinaris agglutinin* (LCA) was injected into a blood vessel of the CAM, the tumour was subsequently excised and processed for further analysis. Ten serial sections from between regions A and C were examined (Figure 3.11). Sections illustrating GFP immunoreactivity within collagen III-positive areas were categorized as sections showing 5B1 cell invasion. White bar = 64 µm. The white dotted line outlines the tumour-CAM interface.

were analyzed. Tumour specimens were categorized as “viable” if they exhibited GFP immunoreactivity and Hoechst 33342 immunostaining revealed large round nuclei. Conversely, tumours were classified as necrotic if the cells found above the Collagen III-positive CAM were not GFP-positive and exhibited irregularly shaped condensed chromatin. The invasion scores of the viable tumours are presented in Figure 3.14. Tumours from untreated and dox-treated Control cells have average invasion scores of 2 and 4, respectively. Additionally, tumours formed from untreated FER 9 cells have an average invasion score of 2, whereas FER-deficient tumours (formed from previously dox-treated FER 9 cells) have an average score of 7. This suggests that decreasing levels of FER in 5B1 cells do not impair the capacity of these cells to invade into the chick CAM mesoderm.

Table 3.1: Characteristics of excised tumours *

	Control	**Control with dox**	**FER 9**	**FER 9 with dox**
Total tumours excised	18	12	23	11
Tumours analyzed (“Viable” tumours)	7	10	10	10
“Necrotic” tumours	11	2	13	1

* Of the total tumours excised, only viable tumours were analyzed. Tumour specimens were classified as “viable” if they exhibited GFP immunostaining and even nuclear DNA staining patterns based on Hoechst 33342-fluorescence. Tumours were classified as “Necrotic” if they exhibited condensed chromatin characteristics of non-viable cells, if they were found above and outside of the collagen III-positive CAM tissues and did not exhibit any detectable GFP immunoreactivity.

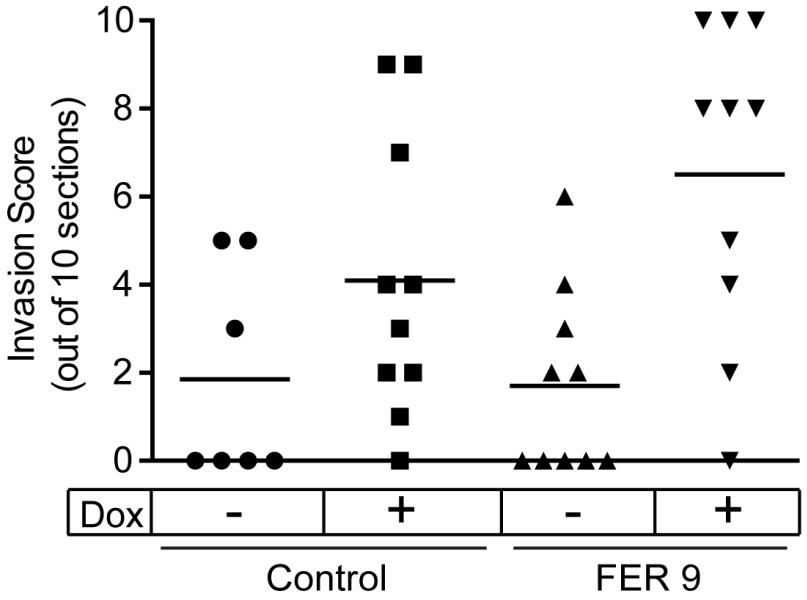

Figure 3.14. Effect of FER kinase on 5B1 cell invasion into the CAM mesoderm

The dot plot illustrates the invasion scores (number of tumour tissue sections, out of 10, showing invasion) of Control and FER 9 tumours. The black lines indicate the average invasion score for each cell group and each black symbol represents a tumour of that cell group.

To evaluate the effects of FER kinase on endothelial cell localization to the tumour, FER 9 cells pretreated with or without dox were suspended in Cultrex and grafted onto the CAM, as described in section 3.5. The tumour-specific regions, identified as regions not expressing collagen III, of the tumour sections were analysed for rhodamine-LCA fluorescence, indicative of endothelial cells. Specifically, 6 out of 7 tumours formed from untreated FER 9 cells and 5 out of 5 tumours formed from treated FER 9 cells showed endothelial cells within the tumour (Figure 3.15). Therefore, localization of endothelial cells within the tumour occurred in both the FER-expressing and FER-deficient tumours, indicating that FER is not essential for endothelial cell recruitment to the tumour.

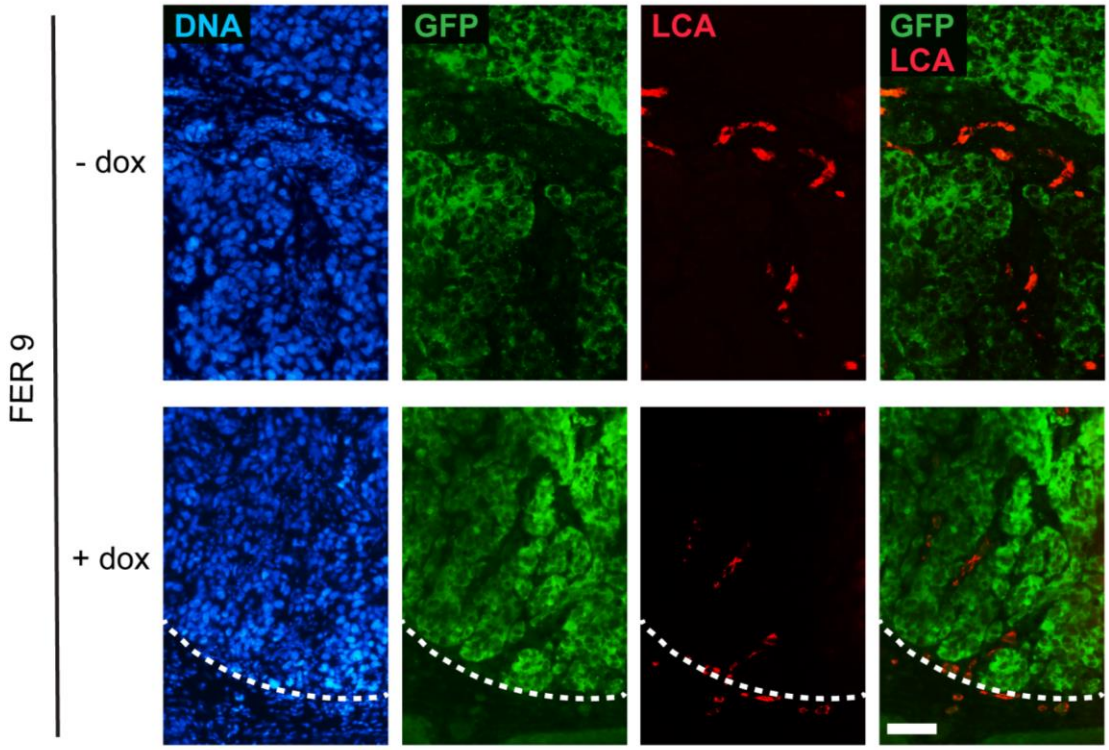

Figure 3.15. Effect of FER kinase on endothelial cell localization to the tumour

Tumour-specific regions, identified as areas not expressing collagen III, of FER 9 tumours were analysed for rhodamine-LCA fluorescence. White bar = 64 µm. The white dotted line outlines the tumour-CAM interface.

Chapter 4

4 Discussion

4.1 Summary

FER kinase contributes towards the tumourigenic properties of various cancers, including breast (Sun et al., 2011), lung (Ahn et al., 2013) and prostate (Allard et al., 2000); however its role in human melanoma has not been explored. This study examined the contributions of FER to proliferation and invasion of human melanoma cells. I showed that FER silencing in 5B1 cells is associated with a decrease in the proportion of cells in S-phase of the cell cycle, suggesting that FER is essential for normal cell cycle progression. In addition, I observed a decrease in the migration of FER-deficient cells seeded on laminin 332. My *ex ovo* CAM studies demonstrated that downregulation of FER resulted in increased 5B1 cell invasion into the CAM mesoderm and that FER is dispensable for the localization of endothelial cells to xenografted tumours.

4.2 FER kinase modulates cell cycle progression

Early subcellular fractionation experiments established that FER kinase localized to both the cytoplasm and the nucleus in various human carcinoma cells (Hao et al., 1991). Significantly, the nuclear localization of FER was found to change depending on the phase of the cell cycle. For example, in quiescent primary mouse fibroblasts, FER is cytoplasmic, and it translocates to the nucleus at the start of and throughout S-phase (Ben-Dor et al., 1999). Similarly, FER nuclear translocation during S-phase was observed in human PC-3 prostate carcinoma cells (Allard et al., 2000). Additionally, flow-cytometry and BrdU-

incorporation studies demonstrated that the downregulation of FER kinase in the PC-3 cells caused an increase in the G0/G1 fraction, with a concomitant decrease in S-phase cells. This observation was attributed to the hypo-phosphorylation of CDK2 and CDK4, resulting in the hypo-phosphorylation of retinoblastoma protein (RB) and consequent activation of its repressing activity in the transcription of genes associated with proliferation (Pasder et al., 2006). These studies suggest that FER translocation to the nucleus is likely important for proper progression from G1 to S-phase. Similarly, in the present study, I have shown a decrease in the proportion of S-phase 5B1 melanoma cells following FER downregulation. Although, I did not investigate the role that changes in FER subcellular localization plays on 5B1 cell cycle progression, it will be important in future experiments to exogenously express FER kinase mutants lacking the nuclear localization signal in FER-deficient cells, to determine if these mutants modulate the ability of the cells to reach and traverse S-phase and, consequently, progress through the cell cycle.

FER kinase also regulates the activity of several transcription factors implicated in cell proliferation. For example, in prostate carcinoma cells, STAT3 phosphorylation by FER is essential for STAT3 activation, nuclear localization and overall proliferation (Zoubeidi et al., 2009). In A375 melanoma cells, inhibition of STAT3 decreased proliferation (Flashner-Abramson et al., 2016), suggesting that STAT3 plays an important role in melanoma growth. The interaction between FER and STAT3 in 5B1 cells will be an important area for further investigation.

4.3 5B1 cell susceptibility to anoikis

Anoikis is a form of programmed cell death induced by detachment from the extracellular matrix. Signals from the microenvironment are important for cellular differentiation, survival, proliferation and migration. Untransformed epithelial and endothelial cells undergo anoikis when detached from the extracellular matrix (Rennebeck et al., 2005). However, many tumour cells, such as those in breast (Eckert et al., 2004) and prostate (Sakamoto and Kyprianou, 2010) carcinoma, are able to survive without attachment. This contributes to tumour progression, invasion into surrounding tissues and metastasis to secondary sites. Anoikis resistance likely arises from constitutive activation of pro-survival signalling pathways, alterations in integrin expression and changes in cell metabolism (Paoli et al., 2013).

Melanoma cells have also been found to resist anoikis through various mechanisms. For example, B-RAF knockdown or MEK inhibition in WM793 melanoma cells cultured in suspension led to an increase in cleaved caspase-3 levels, a marker of apoptosis, and increased levels of two proapoptotic proteins, Bad and Bim (Boisvert-Adamo and Aplin, 2006, 2008). Therefore, the B-RAF signalling pathway and its downstream effectors, Bim and Bad, modulate the susceptibility of WM793 melanoma cells to apoptosis. Other proteins, such as Myeloid Cell Leukemia-1 (Mcl-1) (Boisvert-Adamo et al., 2009) and STAT3, contribute towards melanoma resistance to anoikis. Interestingly, anoikis-resistant melanoma cells exhibit increased STAT3 phosphorylation and increased expression of the anti-apoptotic proteins Bcl-2 and Mcl-1, both of which are STAT3 target genes (Fofaria and Srivastava, 2014).

In this study, I investigated if altering FER kinase levels led to changes in 5B1 cell susceptibility to anoikis and found that 5B1 cells were resistant to anoikis, irrespective of whether or not FER kinase levels were decreased. When cultured in suspension, I noted that 5B1 cells grew in clusters or spheroids, whose size increased during the 6-day culture period of these experiments. This is consistent with the concept that the cells survived and proliferated when cultured in suspension. Cell-to-cell contacts established within the spheroids may have provided growth and survival signals that contributed to 5B1 cell resistance to anoikis. In agreement with this proposal, when suspended colorectal carcinoma cells were dissociated into single cells, an increase in the levels of cleaved caspase-3 and its substrate poly(ADP-ribose) polymerase-1 (PARP-1) occurred, indicative of apoptosis. In contrast, when suspended cells were allowed to remain in spheroids no cleaved caspase-3 or PARP-1 was detected (Kondo et al., 2011). In the same manner, the cellular interactions may have contributed to 5B1 cell survival, and therefore future experiments should consider determining anoikis in a single-cell suspension of 5B1 cells.

4.4 FER is necessary for normal 5B1 cell migration on laminin 332

Melanoma cell interaction with ECM proteins present in the skin, such as collagen I and laminin 332, are important for migration and invasion. Normal melanocytes exhibit different migration phenotypes when cultured on collagen I or laminin 332. Specifically, mouse primary melanocytes show greater migration on laminin-332 compared to collagen I (Crawford et al., 2017). Similarly, I found that 5B1 melanoma cell migration was greater on laminin 332 compared to collagen I or in the absence of any exogenously added ECM substrate. This increase in migration on laminin 332 was also observed in A375 human

melanoma cells (Tsuji et al., 2002), and was abrogated upon inhibition of integrin α3β1. Therefore, interactions between laminin 332 and α3β1 likely mediate these migration responses. Focal adhesion complexes are formed when laminin 332 binds to integrin α3β1, leading to association with actin microfilaments and cell migration (Marinkovich, 2007). The increase in 5B1 cell migration on laminin 332 may follow similar mechanisms.

I have demonstrated that FER-deficient 5B1 cells seeded on laminin-332 show deficits in migration capability. In the same manner, FER is an important player for migration in other cells types through mechanisms that involve modulating cell adhesion to the surrounding ECM (Rosato et al., 1998). For example, the cell surface receptor α-dystroglycan (α-DG) and its interacting glycan ligands are important for cellular interaction with ECM proteins such as laminin. In human prostate and breast carcinoma cells, the downregulation of FER results in increased expression of laminin-binding glycans, due to an increase in the transcription of glycosyltransferases, which are necessary for their synthesis. Moreover, these cells also exhibit a decrease in cell migration (Yoneyama et al., 2012). Thus, by decreasing the expression of genes encoding glycans which bind to laminins, FER contributes to cell migration. In addition, upregulation of integrins α6- and β1 has been reported in FER knockdown breast carcinoma cells, inducing focal adhesion formation and inhibiting cell migration (Ivanova et al., 2013). Together, these studies suggest that FER promotes breast carcinoma cell migration by reducing attachment to the ECM through mechanisms that involve downregulation of adhesion molecules. Whether similar mechanisms are implicated in the positive modulation of 5B1 melanoma cell migration remains to be investigated.

4.5 The study of 5B1 melanoma tumour formation using the *in vivo* chicken chorioallantoic membrane model

The CAM has been used as an excellent model for experiments pertaining to angiogenesis and metastasis. This *in vivo* model offers many advantages for the study of tumourigenesis, tumour invasion and metastasis. First, the highly vascularized and easily accessible CAM allows for easy grafting of tumour cells and provides cells with continued nourishment for survival and growth (Kain et al., 2014). Second, the immune system of the chicken embryo is immature until E18 (Friend et al., 1990). Implantation of tumour cells in this model takes place around E11, minimizing the loss of grafted human tumour cells due to immune defence responses. Using this system, my study demonstrated the ability of the CAM to support the growth of 5B1 human melanoma xenografts.

Although mouse models are frequently used in melanoma research (Sharma et al., 2015), the CAM model has recently gained momentum due to the short duration required for completion of the assays, easy accessibility and visibility. A recent study demonstrated that both the mouse and the CAM *in vivo* models can be used to effectively study human A375 melanoma tumour growth and metastasis (Avram et al., 2017). The increased accessibility and vascularization of the CAM allows research on angiogenesis, whereas the longer periods of tumour growth achievable using mouse xenograft models allow for a detailed analysis of later stages of melanoma progression (Avram et al., 2017). The majority of CAM studies reported on melanoma progression have used mouse melanoma cell lines. For example, altered expression of connexin 43 and pannexin 1 in BL6 mouse melanoma cells grafted onto *ex ovo* CAMs have been used to determine the effect of these proteins on BL6 growth and its metastatic properties (Penuela et al., 2012; Ableser et al., 2014). In

addition, metastasis of mouse melanoma cells from the primary tumour to organs within the chicken embryo was investigated in these studies (Penuela et al., 2012). In a similar manner, I attempted to study 5B1 cell metastasis from the primary tumour grafted onto the CAM to the chick embryo organs, such as liver and lungs, using PCR amplification of human Alu sequences. However, this approach was not successful, as non-specific amplicons were consistently obtained. It is also possible that 5B1 cells do not form substantial metastases within the short, 7-day period in which the CAM experiments must be completed before loss of host viability occurs.

4.6 FER kinase and 5B1 melanoma cell invasion into the CAM

Analysis of 5B1 cell invasion into the CAM was performed only on tumours in which GFP immunoreactivity was detected and there was no evidence of chromatin condensation, consistent with the concept that these specimens contained tumour cells which would have been viable at the time of tissue harvest. Of the total number of tumours assessed, I found that about half of the Control and FER 9 tumours failed to show GFP immunoreactivity and showed condensed chromatin, and I therefore termed them “necrotic” although multiple forms of cell death besides necrosis could have taken place, but were not assessed in these experiments. In contrast, very few “necrotic” FER 9 and Control tumours formed by cells that had been treated with dox for 5 days prior to grafting were observed. This suggests the possibility of a protective dox effect, however, the cells were grafted onto the CAM in the absence of dox. Therefore, the effects from culturing 5B1 cells in medium containing dox may have been maintained through multiple cell divisions in the CAM experiments. In our laboratory, analyses of 5B1 cell lysates cultured in the presence or

absence of dox have indicated changes in the abundance of some proteins due to dox treatment (I. Ivanova, L. Dagnino, unpublished observations). Therefore, this reinforces the necessity of proper controls, such as the Control plus dox condition in my study, for the effective interpretation and characterization of specific effects associated with FER silencing.

Histological analysis demonstrated the capacity of 5B1 cells to invade through the chorionic epithelium into the CAM mesoderm. Similarly, analysis of tissue sections of murine B16-F10 melanoma xenografts demonstrated invasive behaviour in this system (Ribatti et al., 2013). In addition, *in ovo* CAM experiments using metastatic human uveal melanoma cells showed tumour formation and invasion into the CAM (Kalirai et al., 2015). However, studies on the invasive behaviour of human melanoma cells using the CAM model are limited, and therefore my studies now further demonstrate the broad applicability of this approach. My studies also showed that FER-deficient 5B1 tumours may have increased capacity to invade the CAM, suggesting that FER may function to attenuate the invasive ability of 5B1 cells, although additional experiments are needed to rigorously quantify the invasive ability of these cells. If this, indeed, is the case, it would contrast with *in vitro* studies with lung and breast carcinoma cells cultured onto Matrigel which exhibited invasive behaviour only in the presence of normal FER levels (Ahn et al., 2013; Ivanova et al., 2013). FER may modulate invasive potential differently when cells are cultured *in vitro* vs *in vivo*. Alternatively, at least some aspects of FER function may be cell-type specific. One key difference between the environment in culture and that surrounding the CAM is the presence of growth factors, chemoattractants and nutrient gradients. Contrary to *in vitro* conditions, the CAM, rich in growth factors and nutrients, may strongly attract

melanoma cells grafted on its surface. Significantly, FER-deficient neutrophils demonstrated increased motility towards the chemoattractant, WKYMVm, in comparison to FER-expressing neutrophils (Khajah et al., 2013). Similarly, in 5B1 cells, FER deficiency may result in the activation of alternative pathways that stimulate the movement of melanoma cells into the CAM.

Another potential explanation for the apparent increase in FER-deficient 5B1 cell invasion can be attributed to the difference in proliferation that I observed between the FER-expressing and FER-deficient 5B1 cells. I have shown that a decreased number of FER-deficient cells were in the S-phase of the cell cycle, suggesting that these cells have a decreased proliferative capacity. Studies have focused on the interplay between the proliferative and invasive phenotypes of tumour cells (Gao et al., 2005; Tzamali et al., 2014). Hepatocyte growth factor/scatter factor (HGF/SF), which activates the Met receptor tyrosine kinase, induces both proliferative and invasive responses from DBTRG-05MG (DB-P) human glioblastoma cells. The DB-P cells are highly invasive and proliferate less compared to a selected population of DB-P cells, named DB-A2, which are highly proliferative. *In vitro* invasion assays using Matrigel have shown that the DB-A2 cells are less invasive, suggesting that selecting for a highly proliferative phenotype in the DB-P cells resulted in decreased invasive potential. Notably, the more invasive DB-P cells expressed higher levels of RAS and HGF/SF induced increased phosphorylation of ERK (downstream effector in the RAS/MAPK pathway) and Akt (downstream effector of the PI3K pathway), suggesting that the Ras/MAPK and PI3K pathways are associated with the invasive phenotype (Gao et al., 2005). Perhaps the downregulation of FER in 5B1 cells, which resulted in a decrease in their proliferative potential, favoured the activation of

pathways associated with increased invasion, such as MAPK or PI3K, thereby promoting FER-deficient 5B1 cell invasion into the CAM. These possibilities will be important areas for future research.

An important step in tumour cell invasion is the degradation of the extracellular matrix. The matrix metalloproteinases (MMPs) are enzymes that are primarily responsible for the degradation of various ECM components and are grouped as being either soluble or membrane-bound (membrane-type MMP, MT-MMP) MMPs. Their activity is regulated in part by tissue inhibitor of matrix metalloproteinases (TIMPs), which bind to MMPs and inhibit their activity (Hofmann et al., 1999). The balance between levels of activated MMPs and TIMPs plays a key role in melanoma invasion (Hofmann et al., 2000). *In vitro* and mouse xenograft experiments show increased expression of active MMP2 in highly invasive melanoma cell lines (Hofmann et al., 1999). Additionally, overexpression of MT1-MMP stimulated Bowes melanoma invasion in Matrigel (Iida et al., 2004) and expression of MT3-MMP facilitated Bowes melanoma cell invasion into fibrin but not collagen I (Tatti et al., 2011). Therefore, the expression of MMPs varies depending on the surrounding matrix and between the numerous melanoma cell lines (Hofmann et al., 2000). FER deficiency in the 5B1 melanoma cells, may result in the upregulation of certain MMPs that promote the invasion of the cells into the CAM. Consequently, the relationship between FER and MMP and/or TIMP expression requires further investigation.

4.7 FER kinase effects on endothelial cell localization to 5B1 tumours

In addition to investigating invasion into the CAM, I examined the presence or absence of chick endothelial cells within the grafted tumour, indicative of endothelial cell migration from the CAM, which could be evidence of blood vessel formation within the tumour. The endothelial cells were easily detected following injection of *lens culinaris agglutinin* (LCA) into the blood vessels of E18 CAMs prior to harvesting. LCA has been shown to efficiently allow detection of the endothelial lining of arteries, veins and capillaries (Jilani et al., 2003). As a result, LCA has been used in studies pertaining to cancer cell intravasation, extravasation and metastasis (Kim et al., 2016; Deryugina and Quigley, 2009). Significantly, to my knowledge, my study is one of only a handful to histologically examine tumours for the presence of LCA labelled endothelial cells, although this approach does not allow quantitative analyses. I detected endothelial cells within both FER-expressing and FER-deficient tumours, suggesting that FER is not necessary for endothelial cell recruitment to the tumour. This observation is in agreement with a recent study that reported no differences in tissue microvessel density in the stromal cells located within FER-expressing and FER-deficient renal cell carcinoma tumours, suggesting a minimal, if any, role of FER in angiogenesis in this type of tumour (Mitsunari et al., 2017). The mechanisms involved in recruitment of endothelial cells to the 5B1 melanoma tumours, and whether these endothelial cells mark functional vasculature will be important areas for future research.

4.8 Future directions

I have demonstrated that FER kinase promotes 5B1 melanoma cell proliferation and migration, however the downstream effectors responsible for the observed phenotypes remain to be investigated. In addition, I showed using the CAM model that FER is not essential for endothelial cell recruitment to the tumour, however FER-deficient tumours exhibit increased invasion into the CAM. The role of FER in the subsequent metastatic cascade is yet to be elucidated. For example, extravasation of 5B1 cells (with and without FER) from CAM blood vessels could be studied by examining the transit of GFP-labelled FER expressing and FER-deficient melanoma cells through lectin-labelled vessels, using time-lapse video-microscopy (Kim et al., 2016).

4.9 Limitations to the study

This study used an inducible knockdown model to reduce FER kinase levels in the 5B1 cells. An inducible system was used over a constitutive system as it allows to control the onset of shRNA expression. This is beneficial to clearly compare normal cell phenotypes to phenotypes observed at the onset of shRNA expression. Previous studies have shown that FER promotes cancer cell proliferation and survival therefore, constitutive reduction of FER levels in melanoma cells may not be favourable for cell growth. However, the introduction of inducible agents to cells presents as a limitation as it could affect cell behaviour, therefore it is important to have the appropriate controls to decipher the phenotypes presented only due to decreased protein levels.

I have shown that upon dox treatment there is a 65-90% decrease in FER levels, suggesting that a small amount of FER protein remains in the cells. The phenotypes observed in this study may therefore be contingent on the cells having some residual FER activity. It will be important to examine the effects of complete FER knockdown on 5B1 cell behaviour through gene knockout methods such as Crisper/Cas 9.

In this study, 5B1 cell invasion into CAM mesoderm was measured by determining the number of sections that show GFP-expressing 5B1 cells within collagen III-positive CAM. This assay is limited in its ability to determine quantifiable differences in invasion between FER-expressing and FER-deficient cell groups, such as differences in the number of invasive cells or the depth of 5B1 cell invasion into CAM mesoderm. *In vitro* invasion assays such as the Boyden chamber or the vertical gel invasion assay may help address these questions. To better model cell invasion within a tumour microenvironment, Hernandez and others have presented an *in vivo* invasion assay where microneedles filled with ECM extracts like Matrigel are introduced into a primary tumour formed in a mouse/rat. Invasive cells from the tumour can enter the needle over the course of a few hours and thereafter analyzed for the number or type of cells (Hernandez et al., 2009).

Additionally, I observed invasion into the CAM in tumour sections obtained at the end of the experimental timeline, one week after cells were grafted. Perhaps invasive phenotypes are different shortly after tumour formation, with one cell group acquiring a delayed ability to invade. It will be interesting to collect tumour samples at various time points in the 7-day period to observe for any timely differences in invasion.

4.10 Concluding remarks

Currently, treatment options for melanoma range from standard chemotherapy to targeted therapies and immunotherapy (Michielin and Hoeller, 2015). However, the response of patients with metastatic melanoma to chemotherapy and other treatment options is frequently limited due to the emergence of resistance (Nikolaou et al., 2012). Therefore, there is a pressing need to target additional pathways for therapy.

Over 50% of melanomas have a B-RAF mutation (Sosman et al., 2012), including the 5B1 melanoma cells. Therefore, these cells are an excellent model to characterize additional proteins that may promote growth and resistance to therapy in melanoma cells with B-RAF driver mutations. In this study I have shown that 5B1 cell proliferation and migration can be attenuated with the downregulation of FER. Additionally, our laboratory has shown that FER-deficient 5B1 cells are more susceptible to cisplatin cytotoxicity compared to FER-expressing cells (X. Zheng, I. Ivanova, L. Dagnino, unpublished observations). This suggests a potential in targeting FER for combinatorial therapy with current treatments, such as cisplatin. Additionally, mutations in numerous other proteins, such as N-RAS, RAC1 and NF1, account for the heterogeneity of melanoma tumours. Therefore, it will be important to investigate FER function in different subsets of melanomas and determine its contribution to their malignant phenotypes.

I have also shown that FER-deficient 5B1 cells are not susceptible to apoptosis when cultured in suspension and that they form tumours on and invade into the CAM. This suggests that FER may not be essential for melanoma tumour growth. However, a hypothesis to be tested is that FER may cooperate with oncogenic drivers to potentiate

malignant properties. The importance of crosstalk signalling events in the acquisition of carcinoma resistance to targeted drug therapies has recently become an area of intense study. In melanoma cells with $BRAF^{V600E}$ mutations, the administration of the B-RAF inhibitor, vermurafenib, alters the RAS-signalling pathway. Typically, activation of B-RAF leads to the phosphorylation and activation of MEK, which in turn phosphorylates and activates ERK. Phosphorylated ERK then activates the transcription of various genes, including Sprouty (SPRY) (Lito et al., 2012). In humans, there are four SPRY forms, and they selectively interfere with signalling from RTKs, such as the EGFR and FGFR. SPRY interferes with EGFR signalling through various mechanisms, including inhibition of EGFR endocytosis and, consequently, signalling, as well as binding to the adaptor protein, Grb2, and thus preventing the formation of the Grb2 - SOS1 (RAS-specific guanine nucleotide exchange factor) complex, which is required for RAS activation (Hanafusa et al., 2002). In melanoma cells that express a constitutively active B-RAF mutant, inhibition by vemurafenib resulted in increased RAS, together with reduced SPRY levels (Lito et al., 2012). Under these conditions, reduction in SPRY allowed partial restoration of EGFR endocytosis and signalling, resulting in the development of resistance to the vemurafenib treatment.

FER is known to interact with EGFR in various carcinoma cells upon stimulation by either EGF or PDGF (Kim and Wong, 1995; Sangrar et al., 2015). In breast carcinoma cells in which the EGF pathway is amplified due to overexpression of HER2, FER deficiency resulted in increased EGFR internalization, and enhanced RAS signalling. However, this supranormal activation of EGFR pathways was toxic to the cells, resulting in cytostasis, as well as, increased sensitization to the EGFR inhibitor, lapatinib (Sangrar et al., 2015). It

is possible that in cell systems with above normal levels of EGFR signalling, inhibition of FER might interfere with tumour growth and be used in conjunction with targeted therapies, such as lapatinib, to enhance the effect of the treatment and prevent the onset of treatment resistance. Clearly, additional research on FER and its relationship to various oncogenic drivers, and FER as a potential useful target for adjuvant therapy in subsets of melanomas, is needed.

References

Ableser, M.J., S. Penuela, J. Lee, Q. Shao, and D.W. Laird. 2014. Connexin43 reduces melanoma growth within a keratinocyte microenvironment and during tumorigenesis in vivo. *J. Biol. Chem.* 289:1592–1603. doi:10.1074/jbc.M113.507228.

Ackermann, J., M. Frutschi, K. Kaloulis, A.N. Qk, I. Background, T. Mckee, A. Trumpp, and F. Beermann. 2005. Metastasizing Melanoma Formation Caused by Expression of Activated N-Ras Q61K on an INK4a-Deficient Background Metastasizing Melanoma Formation Caused by Expression of. *Cancer Res.* 4005–4011. doi:10.1158/0008-5472.CAN-04-2970.

Ahn, J., P. Truesdell, J. Meens, C. Kadish, X. Yang, A.H. Boag, and A.W. Craig. 2013. Fer protein-tyrosine kinase promotes lung adenocarcinoma cell invasion and tumor metastasis. *Mol. Cancer Res.* 11:952–963. doi:10.1158/1541-7786.mcr-13-0003-t.

Allard, P., A. Zoubeidi, L.T. Nguyen, S. Tessier, S. Tanguay, M. Chevrette, A. Aprikian, and S. Chevalier. 2000. Links between Fer tyrosine kinase expression levels and prostate. *Mol. Cell. Endocrinol.* 159:63–77.

Ascierto, P.A., J.M. Kirkwood, J.-J. Grob, E. Simeone, A.M. Grimaldi, M. Maio, G. Palmieri, A. Testori, F.M. Marincola, and N. Mozzillo. 2012. The role of BRAF V600 mutation in melanoma. *J. Transl. Med.* 10:85. doi:10.1186/1479-5876-10-85.

Ascierto, P.A., D. Minor, A. Ribas, C. Lebbe, A. O'Hagan, N. Arya, M. Guckert, D. Schadendorf, R.F. Kefford, J.J. Grob, O. Hamid, R. Amaravadi, E. Simeone, T. Wilhelm, K.B. Kim, G. V. Long, A.M. Martin, J. Mazumdar, V.L. Goodman, and U. Trefzer. 2013. Phase II trial (BREAK-2) of the BRAF inhibitor dabrafenib (GSK2118436) in patients with metastatic melanoma. *J. Clin. Oncol.* 31:3205–3211. doi:10.1200/JCO.2013.49.8691.

Avram, S., D.E. Coricovac, I.Z. Pavel, I. Pinzaru, R. Ghiulai, F. Baderca, C. Soica, D. Muntean, D.E. Branisteanu, D.A. Spandidos, A.M. Tsatsakis, and C.A. Dehelean. 2017. Standardization of A375 human melanoma models on chicken embryo chorioallantoic membrane and Balb/c nude mice. *Oncol. Rep.* 38:89–99. doi:10.3892/or.2017.5658.

Balch, C.M., J.E. Gershenwald, S.J. Soong, J.F. Thompson, M.B. Atkins, D.R. Byrd, A.C. Buzaid, A.J. Cochran, D.G. Coit, S. Ding, A.M. Eggermont, K.T. Flaherty, P.A. Gimotty, J.M. Kirkwood, K.M. McMasters, M.C. Mihm, D.L. Morton, M.I. Ross, A.J. Sober, and V.K. Sondak. 2009. Final version of 2009 AJCC melanoma staging and classification. *J. Clin. Oncol.* 27:6199–6206. doi:10.1200/JCO.2009.23.4799.

Ben-Dor, I., O. Bern, T. Tennenbaum, and U. Nir. 1999. Cell cycle-dependent nuclear accumulation of the p94fer tyrosine kinase is regulated by its NH2 terminus and is affected by kinase domain integrity and ATP binding. *Cell Growth Differ.* 10:113–29.

Benton, G., H.K. Kleinman, J. George, and I. Arnaoutova. 2011. Multiple uses of basement membrane-like matrix (BME/Matrigel) in vitro and in vivo with cancer cells. *Int. J. Cancer*. 128:1751–1757. doi:10.1002/ijc.25781.

Boisvert-Adamo, K., and a E. Aplin. 2006. B-RAF and PI-3 kinase signaling protect melanoma cells from anoikis. *Oncogene*. 25:4848–56. doi:10.1038/sj.onc.1209493.

Boisvert-Adamo, K., and a E. Aplin. 2008. Mutant B-RAF mediates resistance to anoikis via Bad and Bim. *Oncogene*. 27:3301–3312. doi:10.1038/sj.onc.1211003.

Boisvert-Adamo, K., W. Longmate, E. V Abel, and A.E. Aplin. 2009. Mcl-1 is required for melanoma cell resistance to anoikis. *Mol Cancer Res*. 7:549–556. doi:10.1158/1541-7786.MCR-08-0358.

Boucher, J., A. Kleinridders, and C. Ronald Kahn. 2014. Insulin receptor signaling in normal and insulin-resistant states. *Cold Spring Harb. Perspect. Biol.* 6. doi:10.1101/cshperspect.a009191.

Brenner, M., and V.J. Hearing. 2008. The protective role of melanin against UV damage in human skin. *Photochem. Photobiol.* 84:539–549. doi:10.1111/j.1751-1097.2007.00226.x.

Brown, L.M., D.R. Welch, and S.R. Rannels. 2002. B16F10 melanoma cell colonization of mouse lung is enhanced by partial pneumonectomy. *Clin. Exp. Metastasis*. 19:369–376. doi:10.1023/A:1016345627965.

Bryce, N.S., E.S. Clark, J.L. Leysath, J.D. Currie, D.J. Webb, and A.M. Weaver. 2005. Cortactin promotes cell motility by enhancing lamellipodial persistence. *Curr. Biol.* 15:1276–1285. doi:10.1016/j.cub.2005.06.043.

Canadian Cancer Society. 2017. Canadian Cancer Statistics 2017. 2017. 1-132 pp.

Care, A., G. Mattia, E. Montesoro, I. Parolini, G. Russo, M.P. Colombo, and C. Peschle. 1994. c-fes expression in ontogenetic development and hematopoietic differentiation. *Oncogene*. 9:739–747.

Caunii, A., C. Oprean, M. Cristea, A. Ivan, C. Danciu, C. Tatu, V. Paunescu, D. Marti, G. Tzanakakis, D.A. Spandidos, A. Tsatsakis, R. Susan, C. Soica, and S. Avram. 2017. Effects of ursolic and oleanolic on SK-MEL-2 melanoma cells: In vitro and in vivo assays. *Int. J. Oncol.* 51:1651–1660. doi:10.3892/ijo.2017.4160.

Cepeda, M.A., J.J.H. Pelling, C.L. Evered, K.C. Williams, Z. Freedman, I. Stan, J.A. Willson, H.S. Leong, and S. Damjanovski. 2016. Less is more: low expression of MT1-MMP is optimal to promote migration and tumourigenesis of breast cancer cells. *Mol. Cancer*. 15:65. doi:10.1186/s12943-016-0547-x.

Chandrasekaran, S., U.B.T. Giang, L. Xu, and L.A. DeLouise. 2016. In vitro assays for determining the metastatic potential of melanoma cell lines with characterized in vivo invasiveness. *Biomed. Microdevices*. 18. doi:10.1007/s10544-016-0104-9.

Chapman, P.B., A. Hauschild, C. Robert, J.B. Haanen, P. Ascierto, J. Larkin, R. Dummer, C. Garbe, A. Testori, M. Maio, D. Hogg, P. Lorigan, C. Lebbe, T. Jouary, D. Schadendorf, A. Ribas, S.J. O'Day, J.A. Sosman, J.M. Kirkwood, A.M.M. Eggermont, B. Dreno, K. Nolop, J. Li, B. Nelson, J. Hou, R.J. Lee, K.T. Flaherty, and G.A. McArthur. 2011. Improved Survival with Vemurafenib in Melanoma with BRAF V600E Mutation. *N. Engl. J. Med.* 364:2507–2516. doi:10.1056/NEJMoa1103782.

Cheng, X., R. Luo, G. Wang, C. jun Xu, X. Feng, R. hao Yang, E. Ding, Y. qing He, M. Chuai, K.K.H. Lee, and X. Yang. 2015. Effects of 2,5-hexanedione on angiogenesis and vasculogenesis in chick embryos. *Reprod. Toxicol.* 51:79–89. doi:10.1016/j.reprotox.2014.12.006.

Chmielowski, B., O. Hamid, D.R. Minor, S.P. D'Angelo, G.K. Pennock, K. Grossmann, P.A. Ascierto, A. Daud, R. Dummer, F.S. Hodi, C. Lebbe, C. Robert, J.A. Sosman, A. Yang, A. Lambert, and J.S. Weber. 2013. A phase III open-label study of nivolumab (anti-PD-1; BMS-936558; ONO-4538) versus investigator's choice in advanced melanoma patients progressing post anti-CTLA-4 therapy. *ASCO Meet. Abstr*. 31:TPS9105-.

Cichorek, M., M. Wachulska, A. Stasiewicz, and A. Tymi??ska. 2013. Skin melanocytes: Biology and development. *Postep. Dermatologii i Alergol.* 30:30–41. doi:10.5114/pdia.2013.33376.

Craig, A.W., R. Zirngibl, K. Williams, L.A. Cole, and P.A. Greer. 2001. Mice devoid of fer protein-tyrosine kinase activity are viable and fertile but display reduced cortactin phosphorylation. *Mol. Cell. Biol.* 21:603–13. doi:10.1128/MCB.21.2.603-613.2001.

Craig, A.W.B., R. Zirngibl, and P. Greer. 1999. Disruption of coiled-coil domains in Fer protein-tyrosine kinase abolishes trimerization but not kinase activation. *J. Biol. Chem.* 274:19934–19942. doi:10.1074/jbc.274.28.19934.

Crawford, M., V. Leclerc, and L. Dagnino. 2017. A reporter mouse model for in vivo tracing and in vitro molecular studies of melanocytic lineage cells and their diseases. *Biol. Open*. 6. doi:10.1242/bio.025833.

Cruz-Munoz, W., S. Man, P. Xu, and R.S. Kerbel. 2008. Development of a preclinical model of spontaneous human melanoma central nervous system metastasis. *Cancer Res.* 68:4500–4505. doi:10.1158/0008-5472.CAN-08-0041.

Curtin, J.A., K. Busam, D. Pinkel, and B.C. Bastian. 2006. Somatic activation of KIT in distinct subtypes of melanoma. *J. Clin. Oncol.* 24:4340–4346. doi:10.1200/JCO.2006.06.2984.

D'Orazio, J., S. Jarrett, A. Amaro-Ortiz, and T. Scott. 2013. UV radiation and the skin. *Int. J. Mol. Sci.* 14:12222–12248. doi:10.3390/ijms140612222.

Damsky, W.E., and M. Bosenberg. 2017. Melanocytic nevi and melanoma: unraveling a complex relationship. *Oncogene*. 1–22. doi:10.1038/onc.2017.189.

Damsky, W.E., D.P. Curley, M. Santhanakrishnan, L.E. Rosenbaum, J.T. Platt, B.E. Gould Rothberg, M.M. Taketo, D. Dankort, D.L. Rimm, M. McMahon, and M. Bosenberg. 2011. ??-Catenin Signaling Controls Metastasis in Braf-Activated Pten-Deficient Melanomas. *Cancer Cell*. 20:741–754. doi:10.1016/j.ccr.2011.10.030.

Dankort, D., D.P. Curley, R. a Cartlidge, B. Nelson, N. Anthony, W.E.D. Jr, M.J. You, R. a Depinho, and M. Bosenberg. 2009. BRAF V600E cooperates with PTEN silencing to elicit metastatic melanoma. *Nat. Genet.* 41:544–552. doi:10.1038/ng.356.BRaf.

Davies, M.A., P. Liu, S. McIntyre, K.B. Kim, N. Papadopoulos, W.J. Hwu, P. Hwu, and A. Bedikian. 2011. Prognostic factors for survival in melanoma patients with brain

metastases. *Cancer*. 117:1687–1696. doi:10.1002/cncr.25634.

Davies, M. a. 2012. The Role of the PI3K-AKT Pathway in Melanoma. *Cancer J.* 18:142–147. doi:10.1097/PPO.0b013e31824d448c.

Delfino, F.J., H. Stevenson, and T.E. Smithgall. 2006. A growth-suppressive function for the c-Fes protein-tyrosine kinase in colorectal cancer. *J. Biol. Chem.* 281:8829–8835. doi:10.1074/jbc.M507331200.

Deryugina, E.I., and J.P. Quigley. 2009. Chick embryo chorioallantoic membrane model systems to study and visualize human tumor cell metastasis. *Cell*. 130:1119–1130. doi:10.1007/s00418-008-0536-2.Chick.

Durban, V.M., M.M. Deuker, M.W. Bosenberg, W. Phillips, and M. McMahon. 2013. Differential AKT dependency displayed by mouse models of BRAF V600E-Initiated melanoma. *J. Clin. Invest.* 123:5104–5118. doi:10.1172/JCI69619.

Easty, D.J., M. Herlyn, and D.C. Bennett. 1995. Abnormal protein tyrosine kinase gene expression during melanoma progression and metastasis. *Int J Cancer*. 60:129–136.

Eckert, L.B., G.A. Repasky, A.S. Ulkü, A. McFall, H. Zhou, C.I. Sartor, and C.J. Der. 2004. Involvement of Ras activation in human breast cancer cell signaling, invasion, and anoikis. *Cancer Res.* 64:4585–92. doi:10.1158/0008-5472.CAN-04-0396.

Eggermont, A.M.M., A. Spatz, and C. Robert. 2014. Cutaneous melanoma. *Lancet*. 383:816–827. doi:10.1016/S0140-6736(13)60802-8.

Einarsdottir, B.O., R.O. Bagge, J. Bhadury, H. Jespersen, J. Mattsson, L.M. Nilsson, K. Truvé, M.D. López, P. Naredi, O. Nilsson, U. Stierner, L. Ny, and J.A. Nilsson. 2014. Melanoma patient-derived xenografts accurately model the disease and develop fast enough to guide treatment decisions. *Oncotarget*. 5:9609–18. doi:10.1158/1538-7445.mel2014-b38.

Elkis, Y., M. Cohen, E. Yaffe, S. Satmary-Tusk, T. Feldman, E. Hikri, A. Nyska, A. Feiglin, Y. Ofran, S. Shpungin, and U. Nir. 2017. A novel Fer/FerT targeting compound selectively evokes metabolic stress and necrotic death in malignant cells. *Nat. Commun.* 8:940. doi:10.1038/s41467-017-00832-w.

Falchook, G.S., G. V. Long, R. Kurzrock, K.B. Kim, T.H. Arkenau, M.P. Brown, O. Hamid, J.R. Infante, M. Millward, A.C. Pavlick, S.J. O'Day, S.C. Blackman, C.M. Curtis, P. Lebowitz, B. Ma, D. Ouellet, and R.F. Kefford. 2012. Dabrafenib in patients with melanoma, untreated brain metastases, and other solid tumours: A phase 1 dose-escalation trial. *Lancet*. 379:1893–1901. doi:10.1016/S0140-6736(12)60398-5.

Fan, G., S. Zhang, Y. Gao, P.A. Greer, and N.K. Tonks. 2016. HGF-independent regulation of MET and GAB1 by nonreceptor tyrosine kinase FER potentiates metastasis in ovarian cancer. *Genes Dev.* 30:1542–1557. doi:10.1101/gad.284166.116.

Fan, L., C. Di Ciano-Oliveira, S.A. Weed, A.W.B. Craig, P.A. Greer, O.D. Rotstein, and A. Kapus. 2004. Actin depolymerization-induced tyrosine phosphorylation of cortactin: the role of Fer kinase. *Biochem. J.* 380:581–91. doi:10.1042/BJ20040178.

Fecher, L. a, R.K. Amaravadi, and K.T. Flaherty. 2008. The MAPK pathway in melanoma. *Curr. Opin. Oncol.* 20:183–189. doi:10.1097/CCO.0b013e3282f5271c.

Fei, F., S.-M. Kweon, L. Haataja, P. De Sepulveda, J. Groffen, N. Heisterkamp, A. Ridley, E. Boulter, R. Garcia-Mata, C. Guilluy, A. Dubash, G. Rossi, P. Brennwald, K. Burridge, A. Dovas, J. Couchman, E. Dransart, B. Olofsson, J. Cherfils, C. DerMardirossian, A. Schnelzer, G. Bokoch, N. Knezevic, A. Roy, B. Timblin, M. Konstantoulaki, T. Sharma, A. Malik, D. Mehta, C. DerMardirossian, G. Rocklin, J. Seo, G. Bokoch, R. Unwin, D. Sternberg, Y. Lu, A. Pierce, D. Gilliland, A. Whetton, G. Sun, D. Kemble, M. Mehdi, N. Pandey, S. Pandey, A. Srivastava, J. Rosado, P. Redondo, G. Salido, E. Gomez-Arteta, S. Sage, J. Pariente, W. Sangrar, Y. Gao, M. Scott, P. Truesdell, P. Greer, Z. Wang, D. Thurmond, Q. Hao, D. Ferris, G. White, N. Heisterkamp, J. Groffen, R. Rosato, J. Veltmaat, J. Groffen, N. Heisterkamp, E. Voisset, S. Lopez, A. Chaix, C. Georges, K. Hanssens, T. Prebet, P. Dubreuil, P. De Sepulveda, T. Itoh, J. Hasegawa, K. Tsujita, Y. Kanaho, T. Takenawa, S. Kweon, Y. Cho, P. Minoo, J. Groffen, N. Heisterkamp, Q. Hao, N. Heisterkamp, and J. Groffen. 2010. The Fer tyrosine kinase regulates interactions of Rho GDP-Dissociation Inhibitor a with the small GTPase Rac. *BMC Biochem.* 11:48. doi:10.1186/1471-2091-11-48.

Fischman, K., J.C. Edman, G.M. Shackleford, J.A. Turner, W.J. Rutter, and U. Nir. 1990. A murine fer testis-specific transcript (ferT) encodes a truncated Fer protein. *Mol. Cell. Biol.* 10:146–153.

Flaherty, K.T., C. Robert, P. Hersey, P. Nathan, C. Garbe, M. Milhem, L. V. Demidov, J.C. Hassel, P. Rutkowski, P. Mohr, R. Dummer, U. Trefzer, J.M.G. Larkin, J. Utikal, B. Dreno, M. Nyakas, M.R. Middleton, J.C. Becker, M. Casey, L.J. Sherman, F.S. Wu, D. Ouellet, A.-M. Martin, K. Patel, and D. Schadendorf. 2012. Improved Survival with MEK Inhibition in BRAF-Mutated Melanoma. *N. Engl. J. Med.* 367:107–114. doi:10.1056/NEJMoa1203421.

Flanigan, J.C., L.B. Jilaveanu, M. Faries, M. Sznol, S. Ariyan, J.B. Yu, J.P.S. Knisely, V.L. Chiang, and H.M. Kluger. 2011. Melanoma Brain Metastases: Is It Time to Reassess the Bias? *Curr. Probl. Cancer*. 35:200–210. doi:10.1016/j.currproblcancer.2011.07.003.

Flashner-Abramson, E., S. Klein, G. Mullin, E. Shoshan, R. Song, A. Shir, Y. Langut, M. Bar-Eli, H. Reuveni, and A. Levitzki. 2016. Targeting melanoma with NT157 by blocking Stat3 and IGF1R signaling. *Oncogene*. 35:2675–2680. doi:10.1038/onc.2015.229.

Fofaria, N.M., and S.K. Srivastava. 2014. Critical role of STAT3 in melanoma metastasis through anoikis resistance. *Oncotarget*. 5:7051–64. doi:10.18632/oncotarget.2251.

Friend, J. V., R.W.R. Crevel, T.C. Williams, and W.E. Parish. 1990. Immaturity of the inflammatory response of the chick chorioallantoic membrane. *Toxicol. Vitr.* 4:324–326. doi:10.1016/0887-2333(90)90074-4.

Gao, C.-F., Q. Xie, Y.-L. Su, J. Koeman, S.K. Khoo, M. Gustafson, B.S. Knudsen, R. Hay, N. Shinomiya, and G.F. Vande Woude. 2005. Proliferation and invasion: Plasticity in tumor cells. *Proc. Natl. Acad. Sci. U. S. A.* 102:10528–10533. doi:10.1073/pnas.0504367102.

Greer, P. 2002. Closing in on the biological functions of Fps/Fes and Fer. *Nat. Rev. Mol.*

Cell Biol. 3:278–289. doi:10.1038/nrm783.

Greer, P., J. Haigh, G. Mbamalu, W. Khoo, A. Bernstein, and T. Pawson. 1994. The Fps/Fes protein-tyrosine kinase promotes angiogenesis in transgenic mice. *Mol. Cell. Biol.* 14:6755–63.

Grosso, J.F., and M.N. Jure-Kunkel. 2013. CTLA-4 blockade in tumor models: an overview of preclinical and translational research. *Cancer Immun.* 13:5. doi:CTLA-4;T cell;antibody;co-stimulation;preclinical.

Guo, C., and G.R. Stark. 2011. FER tyrosine kinase (FER) overexpression mediates resistance to quinacrine through EGF-dependent activation of NF- B. *Proc. Natl. Acad. Sci.* 108:7968–7973. doi:10.1073/pnas.1105369108.

Hackenmiller, R., J. Kim, R.A. Feldman, and M.C. Simon. 2000. Abnormal stat activation, hematopoietic homeostasis, and innate immunity in c-fes(-/-) mice. *Immunity*. 13:397–407. doi:10.1016/S1074-7613(00)00039-X.

Haigh, J., J. McVeigh, and P. Greer. 1996. The Fps/Fes tyrosine kinase is expressed in myeloid, vascular endothelial, epithelial, and neuronal cells and is localized in the trans- Golgi network. *Cell Growth Differ.* 7.

Hanafusa, H., S. Torii, T. Yasunaga, and E. Nishida. 2002. Sprouty1 and Sprouty2 provide a control mechanism for the Ras/MAPK signalling pathway. *Nat. Cell Biol.* 4:850–858. doi:10.1038/ncb867.

Hao, Q.L., D.K. Ferris, G. White, N. Heisterkamp, and J. Groffen. 1991. Nuclear and cytoplasmic location of the FER tyrosine kinase. *Mol. Cell. Biol.* 11:1180–1183. doi:10.1128/MCB.11.2.1180.

Hatzivassiliou, G., K. Song, I. Yen, B.J. Brandhuber, D.J. Anderson, R. Alvarado, M.J.C. Ludlam, D. Stokoe, S.L. Gloor, G. Vigers, T. Morales, I. Aliagas, B. Liu, S. Sideris, K.P. Hoeflich, B.S. Jaiswal, S. Seshagiri, H. Koeppen, M. Belvin, L.S. Friedman, and S. Malek. 2010. RAF inhibitors prime wild-type RAF to activate the MAPK pathway and enhance growth. *Nature*. 464:431–435. doi:10.1038/nature08833.

Hauschild, A., J.J. Grob, L. V. Demidov, T. Jouary, R. Gutzmer, M. Millward, P. Rutkowski, C.U. Blank, W.H. Miller, E. Kaempgen, S. Martín-Algarra, B. Karaszewska, C. Mauch, V. Chiarion-Sileni, A.M. Martin, S. Swann, P. Haney, B. Mirakhur, M.E. Guckert, V. Goodman, and P.B. Chapman. 2012. Dabrafenib in BRAF-mutated metastatic melanoma: A multicentre, open-label, phase 3 randomised controlled trial. *Lancet*. 380:358–365. doi:10.1016/S0140-6736(12)60868-X.

Hearing, V.J. 2005. Biogenesis of pigment granules: A sensitive way to regulate melanocyte function. *In* Journal of Dermatological Science. 3–14.

Hennessey, R.C., A.M. Holderbaum, A. Bonilla, C. Delaney, J.E. Gillahan, K.L. Tober, T.M. Oberyszyn, J.H. Zippin, and C.E. Burd. 2017. Ultraviolet radiation accelerates NRas-mutant melanomagenesis: A cooperative effect blocked by sunscreen. *Pigment Cell Melanoma Res.* 30:477–487. doi:10.1111/pcmr.12601.

Hernandez, L., T. Smirnova, J. Wyckoff, J. Condeelis, and E. Jeffrey. 2009. In Vivo Assay for Tumor Cell Invasion. *Methods Mol Biol*. 571:227–238. doi:10.1007/978-1-60761-

198-1.

Herold, M.J., J. van den Brandt, J. Seibler, and H.M. Reichardt. 2008. Inducible and reversible gene silencing by stable integration of an shRNA-encoding lentivirus in transgenic rats. *Proc. Natl. Acad. Sci. U. S. A.* 105:18507–12. doi:10.1073/pnas.0806213105.

Hodge, R.G., and A.J. Ridley. 2016. Regulating Rho GTPases and their regulators. *Nat. Rev. Mol. Cell Biol.* 17:496–510. doi:10.1038/nrm.2016.67.

Hodi, F.S., S.J. O'Day, D.F. McDermott, R.W. Weber, J.A. Sosman, J.B. Haanen, R. Gonzalez, C. Robert, D. Schadendorf, J.C. Hassel, W. Akerley, A.J.M. van den Eertwegh, J. Lutzky, P. Lorigan, J.M. Vaubel, G.P. Linette, D. Hogg, C.H. Ottensmeier, C. Lebbé, C. Peschel, I. Quirt, J.I. Clark, J.D. Wolchok, J.S. Weber, J. Tian, M.J. Yellin, G.M. Nichol, A. Hoos, and W.J. Urba. 2010. Improved survival with ipilimumab in patients with metastatic melanoma. *N. Engl. J. Med.* 363:711–23. doi:10.1056/NEJMoa1003466.

Hodis, E., I.R. Watson, G. V. Kryukov, S.T. Arold, M. Imielinski, J.P. Theurillat, E. Nickerson, D. Auclair, L. Li, C. Place, D. Dicara, A.H. Ramos, M.S. Lawrence, K. Cibulskis, A. Sivachenko, D. Voet, G. Saksena, N. Stransky, R.C. Onofrio, W. Winckler, K. Ardlie, N. Wagle, J. Wargo, K. Chong, D.L. Morton, K. Stemke-Hale, G. Chen, M. Noble, M. Meyerson, J.E. Ladbury, M.A. Davies, J.E. Gershenwald, S.N. Wagner, D.S.B. Hoon, D. Schadendorf, E.S. Lander, S.B. Gabriel, G. Getz, L.A. Garraway, and L. Chin. 2012. A landscape of driver mutations in melanoma. *Cell*. 150:251–263. doi:10.1016/j.cell.2012.06.024.

Hofmann, U.B., J.R. Westphal, G.N. Van Muijen, and D.J. Ruiter. 2000. Matrix metalloproteinases in human melanoma. *J. Invest. Dermatol.* 115:337–344. doi:10.1046/j.1523-1747.2000.00068.x.

Hofmann, U.B., J.R. Westphal, E.T. Waas, A.J.W. Zendman, I.M.H.A. Cornelissen, D.J. Ruiter, and G.N.P. van Muijen. 1999. Matrix metalloproteinases in human melanoma cell lines and xenografts: increased expression of activated matrix metalloproteinase-2 (MMP-2) correlates with melanoma progression. *Br. J. Cancer*. 81:774–782. doi:10.1038/sj.bjc.6690763.

Horn, S., A. Figl, P.S. Rachakonda, C. Fischer, A. Sucker, A. Gast, S. Kadel, I. Moll, E. Nagore, K. Hemminki, D. Schadendorf, and R. Kumar. 2013. TERT promoter mutations in familial and sporadic melanoma. *Science (80-.).* 339:959–61. doi:10.1126/science.1230062.

Hu, X., Z. Zhang, Z. Liang, D. Xie, T. Zhang, D. Yu, and C. Zhong. 2017. Downregulation of feline sarcoma-related protein inhibits cell migration, invasion and epithelial-mesenchymal transition via the ERK/AP-1 pathway in bladder urothelial cell carcinoma. *Oncol. Lett.* 13:686–694. doi:10.3892/ol.2016.5459.

Huang, C., J. Liu, C.C. Haudenschild, and X. Zhan. 1998. The role of tyrosine phosphorylation of cortactin in the locomotion of endothelial cells. *J. Biol. Chem.* 273:25770–25776. doi:10.1074/jbc.273.40.25770.

Huang, J., T. Asawa, T. Takato, and R. Sakai. 2003. Cooperative Roles of Fyn and

Cortactin in Cell Migration of Metastatic Murine Melanoma. *J. Biol. Chem.* 278:48367–48376. doi:10.1074/jbc.M308213200.

Hubbard, S.R., and J.H. Till. 2000. Protein tyrosine kinase structure and function. *Annu. Rev. Biochem.* 69:373–398. doi:10.1146/annurev.biochem.69.1.373.

Iida, J., K.L. Wilhelmson, M.A. Price, C.M. Wilson, D. Pei, L.T. Furcht, and J.B. McCarthy. 2004. Membrane Type-1 Matrix Metalloproteinase Promotes Human Melanoma Invasion and Growth. *J. Invest. Dermatol.* 122:167–176. doi:10.1046/j.0022-202X.2003.22114.x.

Itoh, T., J. Hasegawa, K. Tsujita, Y. Kanaho, and T. Takenawa. 2009. The tyrosine kinase Fer is a downstream target of the PLD-PA pathway that regulates cell migration. *Sci. Signal.* 2:ra52. doi:10.1126/scisignal.2000393.

Ivanova, I. a, J.F. Vermeulen, C. Ercan, J.M. Houthuijzen, F. a Saig, E.J. Vlug, E. van der Wall, P.J. van Diest, M. Vooijs, and P.W.B. Derksen. 2013. FER kinase promotes breast cancer metastasis by regulating α6- and β1-integrin-dependent cell adhesion and anoikis resistance. *Oncogene*. 32:5582–92. doi:10.1038/onc.2013.277.

Iwanishi, M. 2003. Overexpression of Fer increases the association of tyrosine-phosphorylated IRS-1 with P85 phosphatidylinositol kinase via SH2 domain of Fer in transfected cells. *Biochem. Biophys. Res. Commun.* 311:780–785. doi:10.1016/j.bbrc.2003.10.050.

Iwanishi, M., M.P. Czech, and A.D. Cherniack. 2000. The protein-tyrosine kinase fer associates with signaling complexes containing insulin receptor substrate-1 and phosphatidylinositol 3-kinase. *J.Biol.Chem.* 275:38995–39000. doi:10.1074/jbc.M006665200.

Jhappan, C., F.P. Noonan, and G. Merlino. 2003. Ultraviolet radiation and cutaneous malignant melanoma. *Oncogene*. 22:3099–3112. doi:10.1038/sj.onc.1206450.

Jilani, S.M., T.J. Murphy, S.N.M. Thai, A. Eichmann, J. a Alva, and M.L. Iruela-Arispe. 2003. Selective binding of lectins to embryonic chicken vasculature. *J. Histochem. Cytochem.* 51:597–604. doi:10.1177/002215540305100505.

Johannessen, C.M., J.S. Boehm, S.Y. Kim, S.R. Thomas, L. Wardwell, L.A. Johnson, C.M. Emery, N. Stransky, A.P. Cogdill, J. Barretina, G. Caponigro, H. Hieronymus, R.R. Murray, K. Salehi-Ashtiani, D.E. Hill, M. Vidal, J.J. Zhao, X. Yang, O. Alkan, S. Kim, J.L. Harris, C.J. Wilson, V.E. Myer, P.M. Finan, D.E. Root, T.M. Roberts, T. Golub, K.T. Flaherty, R. Dummer, B.L. Weber, W.R. Sellers, R. Schlegel, J.A. Wargo, W.C. Hahn, and L.A. Garraway. 2010. COT drives resistance to RAF inhibition through MAP kinase pathway reactivation. *Nature*. 468:968–972. doi:10.1038/nature09627.

Johnson, D.B., and I. Puzanov. 2015. Treatment of NRAS-mutant melanoma. *Curr. Treat. Options Oncol.* 16:15. doi:10.1007/s11864-015-0330-z.

Kain, K.H., J.W.I. Miller, C.R. Jones-Paris, R.T. Thomason, J.D. Lewis, D.M. Bader, J. V Barnett, and A. Zijlstra. 2014. The chick embryo as an expanding experimental model for cancer and cardiovascular research. *Dev. Dyn.* 243:216–28. doi:10.1002/dvdy.24093.

Kalirai, H., H. Shahidipour, S.E. Coupland, and G. Luyten. 2015. Use of the Chick Embryo Model in Uveal Melanoma. *Ocul. Oncol. Pathol.* 1:133–140. doi:10.1159/000370151.

Keshet, E., A. Itin, K. Fischman, and U. Nir. 1990. The testis-specific transcript (ferT) of the tyrosine kinase FER is expressed during spermatogenesis in a stage-specific manner. *Mol. Cell. Biol.* 10:5021–5. doi:10.1128/MCB.10.9.5021.

Khajah, M., G. Andonegui, R. Chan, A.W. Craig, P.A. Greer, and D.-M. McCafferty. 2013. Fer Kinase Limits Neutrophil Chemotaxis toward End Target Chemoattractants. *J. Immunol.* 190:2208–2216. doi:10.4049/jimmunol.1200322.

Kim, L., and T.W. Wong. 1995. The cytoplasmic tyrosine kinase FER is associated with the catenin-like substrate pp120 and is activated by growth factors. *Mol. Cell. Biol.* 15:4553–4561.

Kim, L., and T.W. Wong. 1998. Growth factor-dependent phosphorylation of the actin-binding protein cortactin is mediated by the cytoplasmic tyrosine kinase FER. *J. Biol. Chem.* 273:23542–23548. doi:10.1074/jbc.273.36.23542.

Kim, Y., K.C. Williams, C.T. Gavin, E. Jardine, A.F. Chambers, and H.S. Leong. 2016. Quantification of cancer cell extravasation in vivo. *Nat. Protoc.* 11:937–948. doi:10.1038/nprot.2016.050.

Kleffel, S., C. Posch, S.R. Barthel, H. Mueller, C. Schlapbach, E. Guenova, C.P. Elco, N. Lee, V.R. Juneja, Q. Zhan, C.G. Lian, R. Thomi, W. Hoetzenecker, A. Cozzio, R. Dummer, M.C. Mihm, K.T. Flaherty, M.H. Frank, G.F. Murphy, A.H. Sharpe, T.S. Kupper, and T. Schatton. 2015. Melanoma Cell-Intrinsic PD-1 Receptor Functions Promote Tumor Growth. *Cell*. 162:1242–1256. doi:10.1016/j.cell.2015.08.052.

Kleinman, H.K., and G.R. Martin. 2005. Matrigel: Basement membrane matrix with biological activity. *Semin. Cancer Biol.* 15:378–386. doi:10.1016/j.semcancer.2005.05.004.

Kondo, J., H. Endo, H. Okuyama, O. Ishikawa, H. Iishi, M. Tsujii, M. Ohue, and M. Inoue. 2011. Retaining cell-cell contact enables preparation and culture of spheroids composed of pure primary cancer cells from colorectal cancer. *Proc. Natl. Acad. Sci. U. S. A.* 108:6235–40. doi:10.1073/pnas.1015938108.

Krauthammer, M., Y. Kong, B.H. Ha, P. Evans, A. Bacchiocchi, J.P. McCusker, E. Cheng, M.J. Davis, G. Goh, M. Choi, S. Ariyan, D. Narayan, K. Dutton-Regester, A. Capatana, E.C. Holman, M. Bosenberg, M. Sznol, H.M. Kluger, D.E. Brash, D.F. Stern, M.A. Materin, R.S. Lo, S. Mane, S. Ma, K.K. Kidd, N.K. Hayward, R.P. Lifton, J. Schlessinger, T.J. Boggon, and R. Halaban. 2012. Exome sequencing identifies recurrent somatic RAC1 mutations in melanoma. *Nat. Genet.* 44:1006–1014. doi:10.1038/ng.2359.

Kumar, R., S. Angelini, E. Snellman, and K. Hemminki. 2004. BRAF Mutations Are Common Somatic Events in Melanocytic Nevi. *J. Invest. Dermatol.* 122:342–348. doi:10.1046/j.0022-202X.2004.22225.x.

Kuroda, Y., S. Wakao, M. Kitada, T. Murakami, M. Nojima, and M. Dezawa. 2013. Isolation, culture and evaluation of multilineage-differentiating stress-enduring (Muse) cells. *Nat. Protoc.* 8:1391–1415. doi:10.1038/nprot.2013.076.

Langhofer, M., S.B. Hopkinson, and J.C. Jones. 1993. The matrix secreted by 804G cells contains laminin-related components that participate in hemidesmosome assembly in vitro. *J. Cell Sci.* 105 (Pt 3:753–764.

Larkin, J., P.A. Ascierto, B. Dréno, V. Atkinson, G. Liszkay, M. Maio, M. Mandalà, L. Demidov, D. Stroyakovskiy, L. Thomas, L. de la Cruz-Merino, C. Dutriaux, C. Garbe, M.A. Sovak, I. Chang, N. Choong, S.P. Hack, G.A. McArthur, and A. Ribas. 2014. Combined vemurafenib and cobimetinib in BRAF-mutated melanoma. *N. Engl. J. Med.* 371:1867–76. doi:10.1056/NEJMoa1408868.

Lee, E.K., Z. Lian, K. D'Andrea, R. Letrero, W. Sheng, S. Liu, J.N. Diehl, D. Pytel, O. Barbash, L. Schuchter, R. Amaravaradi, X. Xu, M. Herlyn, K.L. Nathanson, and J. a. Diehl. 2013. The FBXO4 Tumor Suppressor Functions as a Barrier to BrafV600E-Dependent Metastatic Melanoma. *Mol. Cell. Biol.* 33:4422–4433. doi:10.1128/MCB.00706-13.

Lennartsson, J., H. Ma, P. Wardega, K. Pelka, U. Engström, C. Hellberg, and C.H. Heldin. 2013. The Fer tyrosine kinase is important for platelet-derived growth factor-BB-induced signal transducer and activator of transcription 3 (STAT3) protein phosphorylation, colony formation in soft agar, and tumor growth in vivo. *J. Biol. Chem.* 288:15736–15744. doi:10.1074/jbc.M113.476424.

Li, H., Z. Ren, X. Kang, L. Zhang, X. Li, Y. Wang, T. Xue, Y. Shen, and Y. Liu. 2009. Identification of tyrosine-phosphorylated proteins associated with metastasis and functional analysis of FER in human hepatocellular carcinoma cells. *BMC Cancer*. 9:366. doi:10.1186/1471-2407-9-366.

Li, M., R.R. Pathak, E. Lopez-Rivera, S.L. Friedman, J.A. Aguirre-Ghiso, and A.G. Sikora. 2015. The In Ovo Chick Chorioallantoic Membrane (CAM) Assay as an Efficient Xenograft Model of Hepatocellular Carcinoma. *J. Vis. Exp.* 1–6. doi:10.3791/52411.

Lin, J.Y., and D.E. Fisher. 2007. Melanocyte biology and skin pigmentation. *Nature*. 445:843–850. doi:10.1038/nature05660.

Lito, P., C.A. Pratilas, E.W. Joseph, M. Tadi, E. Halilovic, M. Zubrowski, A. Huang, W.L. Wong, M.K. Callahan, T. Merghoub, J.D. Wolchok, E. de Stanchina, S. Chandarlapaty, P.I. Poulikakos, J.A. Fagin, and N. Rosen. 2012. Relief of Profound Feedback Inhibition of Mitogenic Signaling by RAF Inhibitors Attenuates Their Activity in BRAFV600E Melanomas. *Cancer Cell*. 22:668–682. doi:10.1016/j.ccr.2012.10.009.

Lokman, N.A., A.S.F. Elder, C. Ricciardelli, and M.K. Oehler. 2012. Chick chorioallantoic membrane (CAM) assay as an in vivo model to study the effect of newly identified molecules on ovarian cancer invasion and metastasis. *Int. J. Mol. Sci.* 13:9959–9970. doi:10.3390/ijms13089959.

Long, G. V., D. Stroyakovskiy, H. Gogas, E. Levchenko, F. de Braud, J. Larkin, C. Garbe, T. Jouary, A. Hauschild, J.J. Grob, V. Chiarion Sileni, C. Lebbe, M. Mandalà, M. Millward, A. Arance, I. Bondarenko, J.B.A.G. Haanen, J. Hansson, J. Utikal, V. Ferraresi, N. Kovalenko, P. Mohr, V. Probachai, D. Schadendorf, P. Nathan, C. Robert, A. Ribas, D.J. DeMarini, J.G. Irani, M. Casey, D. Ouellet, A.-M. Martin, N.

Le, K. Patel, and K. Flaherty. 2014. Combined BRAF and MEK Inhibition versus BRAF Inhibition Alone in Melanoma. *N. Engl. J. Med.* 371:1877–1888. doi:10.1056/NEJMoa1406037.

Long, G. V., U. Trefzer, M. a. Davies, R.F. Kefford, P. a. Ascierto, P.B. Chapman, I. Puzanov, A. Hauschild, C. Robert, A. Algazi, L. Mortier, H. Tawbi, T. Wilhelm, L. Zimmer, J. Switzky, S. Swann, A.M. Martin, M. Guckert, V. Goodman, M. Streit, J.M. Kirkwood, and D. Schadendorf. 2012. Dabrafenib in patients with Val600Glu or Val600Lys BRAF-mutant melanoma metastatic to the brain (BREAK-MB): A multicentre, open-label, phase 2 trial. *Lancet Oncol.* 13:1087–1095. doi:10.1016/S1470-2045(12)70431-X.

Lunter, P.C., and G. Wiche. 2002. Direct binding of plectin to Fer kinase and negative regulation of its catalytic activity. *Biochem. Biophys. Res. Commun.* 296:904–910. doi:10.1016/S0006-291X(02)02007-7.

Makovski, A., E. Yaffe, S. Shpungin, and U. Nir. 2012a. Intronic promoter drives the BORIS-regulated expression of FerT in colon carcinoma cells. *J. Biol. Chem.* 287:6100–6112. doi:10.1074/jbc.M111.327106.

Makovski, A., E. Yaffe, S. Shpungin, and U. Nir. 2012b. Down-regulation of Fer induces ROS levels accompanied by ATM and p53 activation in colon carcinoma cells. *Cell. Signal.* 24:1369–1374. doi:10.1016/j.cellsig.2012.03.004.

Manzano, J.L., L. Layos, C. Bugés, M. de los Llanos Gil, L. Vila, E. Martínez-Balibrea, and A. Martínez-Cardús. 2016. Resistant mechanisms to BRAF inhibitors in melanoma. *Ann. Transl. Med.* 4:237–237. doi:10.21037/atm.2016.06.07.

Marinkovich, M.P. 2007. Tumour microenvironment: Laminin 332 in squamous-cell carcinoma. *Nat. Rev. Cancer*. 7:370–380. doi:10.1038/nrc2089.

Marzuka, A., L. Huang, N. Theodosakis, and M. Bosenberg. 2015. Melanoma Treatments: Advances and Mechanisms. *J. Cell. Physiol.* 230:2626–2633. doi:10.1002/jcp.25019.

Maverakis, E., L.A. Cornelius, G.M. Bowen, T. Phan, F.B. Patel, S. Fitzmaurice, Y. He, B. Burrall, C. Duong, A.M. Kloxin, H. Sultani, R. Wilken, S.R. Martinez, and F. Patel. 2015. Metastatic melanoma – A review of current and future treatment options. *Acta Derm. Venereol.* 95:516–524. doi:10.2340/00015555-2035.

McPherson, V.A., S. Everingham, R. Karisch, J.A. Smith, C.M. Udell, J. Zheng, Z. Jia, and A.W.B. Craig. 2009. Contributions of F-BAR and SH2 Domains of Fes Protein Tyrosine Kinase for Coupling to the Fc RI Pathway in Mast Cells. *Mol. Cell. Biol.* 29:389–401. doi:10.1128/MCB.00904-08.

Mehnert, J.M., and H.M. Kluger. 2012. Driver mutations in melanoma: Lessons learned from bench-to-bedside studies. *Curr. Oncol. Rep.* 14:449–457. doi:10.1007/s11912-012-0249-5.

Melkonian, G., C. Le, W. Zheng, P. Talbot, and M. Martins-Green. 2000. Normal patterns of angiogenesis and extracellular matrix deposition in chick chorioallantoic membranes are disrupted by mainstream and sidestream cigarette smoke. *Toxicol. Appl. Pharmacol.* 163:26–37. doi:10.1006/taap.1999.8789.

Melnikova, V.O., S. V Bolshakov, C. Walker, and H.N. Ananthaswamy. 2004. Genomic alterations in spontaneous and carcinogen-induced murine melanoma cell lines. *Oncogene*. 23:2347–2356. doi:10.1038/sj.onc.1207405.

Michielin, O., and C. Hoeller. 2015. Gaining momentum: New options and opportunities for the treatment of advanced melanoma. *Cancer Treat. Rev.* doi:10.1016/j.ctrv.2015.05.012.

Mitsunari, K., Y. Miyata, S.-I. Watanabe, A. Asai, T. Yasuda, S. Kanda, and H. Sakai. 2017. Stromal expression of Fer suppresses tumor progression in renal cell carcinoma and is a predictor of survival. *Oncol. Lett.* 13:834–840. doi:10.3892/ol.2016.5481.

Miyata, Y., S. Kanda, H. Sakai, and P.A. Greer. 2013. Feline sarcoma-related protein expression correlates with malignant aggressiveness and poor prognosis in renal cell carcinoma. *Cancer Sci.* 104:681–686. doi:10.1111/cas.12140.

Moissoglu, K., B. Slepchenko, N. Meller, A. Horwitz, and M. Schwartz. 2006. In Vivo Dynamics of Rac-Membrane Interactions. *Mol. Biol. Cell*. 17:2770–2779. doi:10.1091/mbc.E06-01-0005.

Mummert, M.E., D.I. Mummert, L. Ellinger, and A. Takashima. 2003. Functional roles of hyaluronan in B16-F10 melanoma growth and experimental metastasis in mice. *Mol. Cancer Ther.* 2:295–300. doi:#.

Nazarian, R., H. Shi, Q. Wang, X. Kong, R.C. Koya, H. Lee, Z. Chen, M.-K. Lee, N. Attar, H. Sazegar, T. Chodon, S.F. Nelson, G. McArthur, J.A. Sosman, A. Ribas, and R.S. Lo. 2010. Melanomas acquire resistance to B-RAF(V600E) inhibition by RTK or N-RAS upregulation. *Nature*. 468:973–977. doi:10.1038/nature09626.

Nikolaou, V.A., A.J. Stratigos, K.T. Flaherty, and H. Tsao. 2012. Melanoma: New Insights and New Therapies. *J. Invest. Dermatol.* 132:854–863. doi:10.1038/jid.2011.421.

Nissan, M.H., C.A. Pratilas, A.M. Jones, R. Ramirez, H. Won, C. Liu, S. Tiwari, L. Kong, A.J. Hanrahan, Z. Yao, T. Merghoub, A. Ribas, P.B. Chapman, R. Yaeger, B.S. Taylor, N. Schultz, M.F. Berger, N. Rosen, and D.B. Solit. 2014. Loss of NF1 in cutaneous melanoma is associated with RAS activation and MEK dependence. *Cancer Res.* 74:2340–2350. doi:10.1158/0008-5472.CAN-13-2625.

Nowak-Sliwinska, P., T. Segura, and M.L. Iruela-Arispe. 2014. The chicken chorioallantoic membrane model in biology, medicine and bioengineering. *Angiogenesis*. 17:779–804. doi:10.1007/s10456-014-9440-7.

Olvedy, M., J.C. Tisserand, F. Luciani, B. Boeckx, J. Wouters, S. Lopez, F. Rambow, S. Aibar, B. Thienpont, J. Barra, C. Köhler, E. Radaelli, S. Tartare-Deckert, S. Aerts, P. Dubreuil, J.J.V. Den Oord, D. Lambrechts, P. De Sepulveda, and J.C. Marine. 2017. Comparative oncogenomics identifies tyrosine kinase FES as a tumor suppressor in melanoma. *J. Clin. Invest.* 127:2310–2325. doi:10.1172/JCI91291.

Orlovsky, K., I. Ben-Dor, S. Priel-Halachmi, H. Malovany, and U. Nir. 2000. N-terminal sequences direct the autophosphorylation states of the FER tyrosine kinases in vivo. *Biochemistry*. 39:11084–11091. doi:10.1021/bi0005153.

Ossio, R., R. Roldán-Marín, H. Martínez-Said, D.J. Adams, and C.D. Robles-Espinoza.

2017. Melanoma: A global perspective. *Nat. Rev. Cancer*. 17:393–394. doi:10.1038/nrc.2017.43.

Pak, B.J., J. Lee, B.L. Thai, S.Y. Fuchs, Y. Shaked, Z. Ronai, R.S. Kerbel, and Y. Ben-David. 2004. Radiation resistance of human melanoma analysed by retroviral insertional mutagenesis reveals a possible role for dopachrome tautomerase. *Oncogene*. 23:30–38. doi:10.1038/sj.onc.1207007.

Paoli, P., E. Giannoni, and P. Chiarugi. 2013. Anoikis molecular pathways and its role in cancer progression. *Biochim. Biophys. Acta - Mol. Cell Res.* 1833:3481–3498. doi:10.1016/j.bbamcr.2013.06.026.

Pasder, O., S. Shpungin, Y. Salem, a Makovsky, S. Vilchick, S. Michaeli, H. Malovani, and U. Nir. 2006. Downregulation of Fer induces PP1 activation and cell-cycle arrest in malignant cells. *Oncogene*. 25:4194–4206. doi:10.1038/sj.onc.1209695.

Pedoeem, A., I. Azoulay-Alfaguter, M. Strazza, G.J. Silverman, and A. Mor. 2014. Programmed death-1 pathway in cancer and autoimmunity. *Clin. Immunol.* 153:145–152. doi:10.1016/j.clim.2014.04.010.

Penuela, S., L. Gyeniss, A. Ablack, J.M. Churko, A.C. Berger, D.W. Litchfield, J.D. Lewis, and D.W. Laird. 2012. Loss of pannexin 1 attenuates melanoma progression by reversion to a melanocytic phenotype. *J. Biol. Chem.* 287:29184–29193. doi:10.1074/jbc.M112.377176.

Piedra, J., S. Miravet, J. Castaño, H.G. Pálmer, N. Heisterkamp, A. García de Herreros, and M. Duñach. 2003. p120 Catenin-associated Fer and Fyn tyrosine kinases regulate beta-catenin Tyr-142 phosphorylation and beta-catenin-alpha-catenin Interaction. *Mol. Cell. Biol.* 23:2287–97.

Potrony, M., C. Badenas, P. Aguilera, J.A. Puig-Butille, C. Carrera, J. Malvehy, and S. Puig. 2015. Update in genetic susceptibility in melanoma. *Ann. Transl. Med.* 3:210. doi:10.3978/j.issn.2305-5839.2015.08.11.

Poulikakos, P.I., C. Zhang, G. Bollag, K.M. Shokat, and N. Rosen. 2010. RAF inhibitors transactivate RAF dimers and ERK signalling in cells with wild-type BRAF. *Nature*. 464:427–430. doi:10.1038/nature08902.

Ramagopal, U.A., W. Liu, S.C. Garrett-Thomson, J.B. Bonanno, Q. Yan, M. Srinivasan, S.C. Wong, A. Bell, S. Mankikar, V.S. Rangan, S. Deshpande, A.J. Korman, and S.C. Almo. 2017. Structural basis for cancer immunotherapy by the first-in-class checkpoint inhibitor ipilimumab. *Proc. Natl. Acad. Sci.* 114:E4223–E4232. doi:10.1073/pnas.1617941114.

Reddy, B.Y., D.M. Miller, and H. Tsao. 2017. Somatic driver mutations in melanoma. *Cancer*. 123:2104–2117. doi:10.1002/cncr.30593.

Rennebeck, G., M. Martelli, and N. Kyprianou. 2005. Anoikis and survival connections in the tumor microenvironment: Is there a role in prostate cancer metastasis? *Cancer Res.* 65:11230–11235. doi:10.1158/0008-5472.CAN-05-2763.

Ribatti, D. 2014. The chick embryo chorioallantoic membrane as a model for tumor biology. *Exp. Cell Res.* 328:314–324. doi:10.1016/j.yexcr.2014.06.010’.

Ribatti, D., B. Nico, A.M. Cimpean, M. Raica, E. Crivellato, S. Ruggieri, and A. Vacca. 2013. B16-F10 melanoma cells contribute to the new formation of blood vessels in the chick embryo chorioallantoic membrane through vasculogenic mimicry. *Clin. Exp. Med.* 13:143–147. doi:10.1007/s10238-012-0183-8.

Robert, C., B. Karaszewska, J. Schachter, P. Rutkowski, A. Mackiewicz, D. Stroiakovski, M. Lichinitser, R. Dummer, F. Grange, L. Mortier, V. Chiarion-Sileni, K. Drucis, I. Krajsova, A. Hauschild, P. Lorigan, P. Wolter, G. V. Long, K. Flaherty, P. Nathan, A. Ribas, A.-M. Martin, P. Sun, W. Crist, J. Legos, S.D. Rubin, S.M. Little, and D. Schadendorf. 2015. Improved Overall Survival in Melanoma with Combined Dabrafenib and Trametinib. *N. Engl. J. Med.* 372:30–39. doi:10.1056/NEJMoa1412690.

Robert, C., A. Ribas, J.D. Wolchok, F.S. Hodi, O. Hamid, R. Kefford, J.S. Weber, A.M. Joshua, W.J. Hwu, T.C. Gangadhar, A. Patnaik, R. Dronca, H. Zarour, R.W. Joseph, P. Boasberg, B. Chmielowski, C. Mateus, M.A. Postow, K. Gergich, J. Elassaiss-Schaap, X.N. Li, R. Iannone, S.W. Ebbinghaus, S.P. Kang, and A. Daud. 2014. Anti-programmed-death-receptor-1 treatment with pembrolizumab in ipilimumab-refractory advanced melanoma: A randomised dose-comparison cohort of a phase 1 trial. *Lancet*. 384:1109–1117. doi:10.1016/S0140-6736(14)60958-2.

Robert, C., L. Thomas, I. Bondarenko, S. O'Day, J. Weber, C. Garbe, C. Lebbe, J.-F. Baurain, A. Testori, J.-J. Grob, N. Davidson, J. Richards, M. Maio, A. Hauschild, W.H. Miller, P. Gascon, M. Lotem, K. Harmankaya, R. Ibrahim, S. Francis, T.-T. Chen, R. Humphrey, A. Hoos, and J.D. Wolchok. 2011. Ipilimumab plus Dacarbazine for Previously Untreated Metastatic Melanoma. *N. Engl. J. Med.* 364:2517–2526. doi:10.1056/NEJMoa1104621.

Robinson, D.R., Y.M. Wu, and S.F. Lin. 2000. The protein tyrosine kinase family of the human genome. *Oncogene*. 19:5548–5557. doi:10.1038/sj.onc.1203957.

Rocha, J., F.Z. Zouanat, A. Zoubeidi, L. Hamel, T. Benidir, E. Scarlata, F. Brimo, A. Aprikian, and S. Chevalier. 2013. The Fer tyrosine kinase acts as a downstream interleukin-6 effector of androgen receptor activation in prostate cancer. *Mol. Cell. Endocrinol.* 381:140–149. doi:10.1016/j.mce.2013.07.017.

Roh, M.R., P. Eliades, S. Gupta, and H. Tsao. 2015. Genetics of melanocytic nevi. *Pigment Cell Melanoma Res.* 28:661–672. doi:10.1111/pcmr.12412.

Roider, E., and D. Fisher. 2016. Red hair, light skin, and uv-independent risk for melanoma development in humans. *JAMA Dermatology*. 152:751–753. doi:10.1001/jamadermatol.2016.0524.Conflict.

Rosato, R., J.M. Veltmaat, J. Groffen, and N. Heisterkamp. 1998. Involvement of the tyrosine kinase fer in cell adhesion. *Mol. Cell. Biol.* 18:5762–70.

Sakamoto, S., and N. Kyprianou. 2010. Targeting anoikis resistance in prostate cancer metastasis. *Mol. Aspects Med.* 31:205–214. doi:10.1016/j.mam.2010.02.001.

Sandru, A., S. Voinea, E. Panaitescu, and A. Blidaru. 2014. Survival rates of patients with malignant melanoma. *J. Med. Life*. 7:572–576.

Sangrar, W., C. Shi, G. Mullins, D. LeBrun, B. Ingalls, and P. a Greer. 2015. Amplified

Ras-MAPK signal states correlate with accelerated EGFR internalization, cytostasis and delayed HER2 tumor onset in Fer-deficient model systems. *Oncogene*. 1–9. doi:10.1038/onc.2014.340.

Scholzen, T., and J. Gerdes. 2000. The Ki-67 protein: From the known and the unknown. *J. Cell. Physiol.* 182:311–322. doi:10.1002/(SICI)1097-4652(200003)182:3<311::AID-JCP1>3.0.CO;2-9.

Shah, M., A. Bhoumik, V. Goel, A. Dewing, W. Breitwieser, H. Kluger, S. Krajewski, M. Krajewska, J. DeHart, E. Lau, D.M. Kallenberg, H. Jeong, A. Eroshkin, D.C. Bennett, L. Chin, M. Bosenberg, N. Jones, and Z.A. Ronai. 2010. A role for ATF2 in regulating MITF and melanoma development. *PLoS Genet.* 6:1–21. doi:10.1371/journal.pgen.1001258.

Shain, A.H., and B.C. Bastian. 2016. From melanocytes to melanomas. *Nat. Rev. Cancer*. 16:345–358. doi:10.1038/nrc.2016.37.

Shain, A.H., I. Yeh, I. Kovalyshyn, A. Sriharan, E. Talevich, A. Gagnon, R. Dummer, J. North, L. Pincus, B. Ruben, W. Rickaby, C. D'Arrigo, A. Robson, and B.C. Bastian. 2015. The Genetic Evolution of Melanoma from Precursor Lesions. *N. Engl. J. Med.* 373:1926–1936. doi:10.1056/NEJMoa1502583.

Sharma, A., O.F. Kuzu, F.D. Nguyen, A. Sharma, and M. Noory. 2015. Current State of Animal (Mouse) Modeling in Melanoma Research. *Cancer Growth Metastasis*. 81. doi:10.4137/CGM.S21214.

Sinnberg, T., M.P. Levesque, J. Krochmann, P.F. Cheng, K. Ikenberg, F. Meraz-Torres, H. Niessner, C. Garbe, and C. Busch. 2018. Wnt-signaling enhances neural crest migration of melanoma cells and induces an invasive phenotype. *Mol. Cancer*. 17:59. doi:10.1186/s12943-018-0773-5.

Sosman, J. a., K.B. Kim, L. Schuchter, R. Gonzalez, A.C. Pavlick, J.S. Weber, G. a. McArthur, T.E. Hutson, S.J. Moschos, K.T. Flaherty, P. Hersey, R. Kefford, D. Lawrence, I. Puzanov, K.D. Lewis, R.K. Amaravadi, B. Chmielowski, H.J. Lawrence, Y. Shyr, F. Ye, J. Li, K.B. Nolop, R.J. Lee, A.K. Joe, and A. Ribas. 2012. Survival in BRAF V600–Mutant Advanced Melanoma Treated with Vemurafenib. *N. Engl. J. Med.* 366:707–714. doi:10.1056/NEJMoa1112302.

Staudt, M., K. Lasithiotakis, U. Leiter, F. Meier, T. Eigentler, M. Bamberg, M. Tatagiba, P. Brossart, and C. Garbe. 2010. Determinants of survival in patients with brain metastases from cutaneous melanoma. *Br. J. Cancer*. 102:1213–1218. doi:10.1038/sj.bjc.6605622.

Steffen, A., M. Ladwein, G.A. Dimchev, A. Hein, L. Schwenkmezger, S. Arens, K.I. Ladwein, J.M. Holleboom, F. Schur, J. V. Small, J. Schwarz, R. Gerhard, J. Faix, T.E.B. Stradal, C. Brakebusch, and K. Rottner. 2013. Rac function is crucial for cell migration but is not required for spreading and focal adhesion formation. *J. Cell Sci.* 126:4572–4588. doi:10.1242/jcs.118232.

Stratton, M.R., P.J. Campbell, and P. Andrew F. 2009. The cancer genome. *Nature*. 458:719–724. doi:10.1038/nature07943.

Su, F., A. Viros, C. Milagre, K. Trunzer, G. Bollag, O. Spleiss, J.S. Reis-Filho, X. Kong,

and R.C. Koya. 2012. RAS Mutations in Cutaneous Squamous-Cell Carcinomas in Patients Treated with BRAF Inhibitors. *N. Engl. J. Med.* 306:9. doi:10.1056/NEJMoa1105358.

Sun, T., N. Aceto, K.L. Meerbrey, J.D. Kessler, C. Zhou, I. Migliaccio, D.X. Nguyen, N.N. Pavlova, M. Botero, J. Huang, R.J. Bernardi, E. Schmitt, G. Hu, M.Z. Li, N. Dephoure, S.P. Gygi, M. Rao, C.J. Creighton, S.G. Hilsenbeck, C.A. Shaw, D. Muzny, R.A. Gibbs, D.A. Wheeler, C.K. Osborne, R. Schiff, M. Bentires-Alj, S.J. Elledge, and T.F. Westbrook. 2011. Activation of multiple proto-oncogenic tyrosine kinases in breast cancer via loss of the PTPN12 phosphatase. *Cell*. 144:703–718. doi:10.1016/j.cell.2011.02.003.

Tan, J., L. Tom, K. Jagirdar, D. Lambie, H. Schaider, R. Sturm, H. Soyer, and M. Stark. 2017. The BRAF and NRAS mutation prevalence in dermoscopic subtypes of acquired naevi reveals constitutive mitogen-activated protein kinase pathway activation. *Br. J. Dermatol.* doi:10.1111/bjd.15809.

Tatti, O., M. Arjama, A. Ranki, S.J. Weiss, J. Keski-Oja, and K. Lehti. 2011. Membrane-type-3 matrix metalloproteinase (MT3-MMP) functions as a matrix composition-dependent effector of melanoma cell invasion. *PLoS One*. 6:19–22. doi:10.1371/journal.pone.0028325.

Theos, A.C., D. Tenza, J. Martina, I. Hurbain, A. Peden, E. Sviderskaya, A. Stewart, M. Robinson, D. Bennett, D. Cutler, J. Bonifacino, M. Marks, and G. Raposo. 2005. Functions of Adaptor Protein (AP)-3 and AP-1 in Tyrosinase Sorting from Endosomes to Melanosomes. *Mol. Biol. Cell*. 16:5356–5372. doi:10.1091/mbc.E05-07-0626.

Tormo, D., A. Chęcińska, D. Alonso-Curbelo, E. Pérez-Guijarro, E. Cañón, E. Riveiro-Falkenbach, T.G. Calvo, L. Larribere, D. Megías, F. Mulero, M.A. Piris, R. Dash, P.M. Barral, J.L. Rodríguez-Peralto, P. Ortiz-Romero, T. Tüting, P.B. Fisher, and M.S. Soengas. 2009. Targeted Activation of Innate Immunity for Therapeutic Induction of Autophagy and Apoptosis in Melanoma Cells. *Cancer Cell*. 16:103–114. doi:10.1016/j.ccr.2009.07.004.

Tripathi, M., S. Nandana, H. Yamashita, R. Ganesan, D. Kirchhofer, and V. Quaranta. 2008. Laminin-332 is a substrate for hepsin, a protease associated with prostate cancer progression. *J. Biol. Chem.* 283:30576–30584. doi:10.1074/jbc.M802312200.

Tsuji, T., Y. Kawada, M. Kai-Murozono, S. Komatsu, S.A. Han, K. Takeuchi, H. Mizushima, K. Miyazaki, and T. Irimura. 2002. Regulation of melanoma cell migration and invasion by laminin-5 and alpha3beta1 integrin (VLA-3). *Clin. Exp. Metastasis*. 19:127–134. doi:10.1023/A:1014573204062.

Tzamali, E., G. Grekas, K. Marias, and V. Sakkalis. 2014. Exploring the competition between proliferative and invasive cancer phenotypes in a continuous spatial model. *PLoS One*. 9. doi:10.1371/journal.pone.0103191.

Vandercappellen, J., S. Liekens, A. Bronckaers, S. Noppen, I. Ronsse, C. Dillen, M. Belleri, S. Mitola, P. Proost, M. Presta, S. Struyf, and J. Van Damme. 2010. The COOH-Terminal Peptide of Platelet Factor-4 Variant (CXCL4L1/PF-4var47-70) Strongly Inhibits Angiogenesis and Suppresses B16 Melanoma Growth In vivo. *Mol.*

Cancer Res. 8:322–334. doi:10.1158/1541-7786.MCR-09-0176.

Vincent, K.M., and L.-M. Postovit. 2017. Investigating the utility of human melanoma cell lines as tumour models. *Oncotarget*. 8:10498–10509. doi:10.18632/oncotarget.14443.

Weaver, A.M., A. V. Karginov, A.W. Kinley, S.A. Weed, Y. Li, J.T. Parsons, and J.A. Cooper. 2001. Cortactin promotes and stabilizes Arp2/3-induced actin filament network formation. *Curr. Biol.* 11:370–374. doi:10.1016/S0960-9822(01)00098-7.

van der Weyden, L., E.E. Patton, G.A. Wood, A.K. Foote, T. Brenn, M.J. Arends, and D.J. Adams. 2016. Cross-species models of human melanoma. *J. Pathol.* 238:152–165. doi:10.1002/path.4632.

Winkelmann, C.T., S.D. Figueroa, T.L. Rold, W.A. Volkert, and T.J. Hoffman. 2006. Microimaging characterization of a B16-F10 melanoma metastasis mouse model. *Mol. Imaging*. 5:105–114. doi:10.2310/7290.2006.00011.

Wolchok, J.D., V. Chiarion-Sileni, R. Gonzalez, P. Rutkowski, J.-J. Grob, C.L. Cowey, C.D. Lao, J. Wagstaff, D. Schadendorf, P.F. Ferrucci, M. Smylie, R. Dummer, A. Hill, D. Hogg, J. Haanen, M.S. Carlino, O. Bechter, M. Maio, I. Marquez-Rodas, M. Guidoboni, G. McArthur, C. Lebbé, P.A. Ascierto, G. V. Long, J. Cebon, J. Sosman, M.A. Postow, M.K. Callahan, D. Walker, L. Rollin, R. Bhore, F.S. Hodi, and J. Larkin. 2017. Overall Survival with Combined Nivolumab and Ipilimumab in Advanced Melanoma. *N. Engl. J. Med.* NEJMoa1709684. doi:10.1056/NEJMoa1709684.

Xu, G. 2004. Continuous association of cadherin with -catenin requires the non-receptor tyrosine-kinase Fer. *J. Cell Sci.* 117:3207–3219. doi:10.1242/jcs.01174.

Xu, L., S.S. Shen, Y. Hoshida, A. Subramanian, K. Ross, J.-P. Brunet, S.N. Wagner, S. Ramaswamy, J.P. Mesirov, and R.O. Hynes. 2008. Gene Expression Changes in an Animal Melanoma Model Correlate with Aggressiveness of Human Melanoma Metastases. *Mol. Cancer Res.* 6:760–769. doi:10.1158/1541-7786.MCR-07-0344.

Yaffe, E., E. Hikri, Y. Elkis, O. Cohen, A. Segal, A. Makovski, A. Varvak, S. Shpungin, and U. Nir. 2014. Oncogenic properties of a spermatogenic meiotic variant of Fer kinase expressed in somatic cells. *Cancer Res.* 74:6474–6485. doi:10.1158/0008-5472.CAN-14-0058.

Yamaguchi, Y., and V.J. Hearing. 2014. Melanocytes and their diseases. *Cold Spring Harb. Perspect. Med.* 4:1–18. doi:10.1101/cshperspect.a017046.

Yang, X., Y. Yang, S. Tang, H. Tang, G. Yang, Q. Xu, and J. Wu. 2015. EphB4 inhibitor overcome the acquired resistance to cisplatin in melanomas xenograft model. *J. Pharmacol. Sci.* 129:65–71. doi:10.1016/j.jphs.2015.08.009.

Yoneyama, T., K. Angata, X. Bao, S. Courtneidge, S.K. Chanda, and M. Fukuda. 2012. Fer kinase regulates cell migration through alpha-dystroglycan glycosylation. *Mol. Biol. Cell*. 23:771–780. doi:10.1091/mbc.E11-06-0517.

Yurlova, E.I., K.A. Rubina, V.Y. Sysoeva, G.V. Sharonov, E.V. Semina, E.V. Parfenova, and V.A. Tkachuk. 2010. T-cadherin suppresses the cell proliferation of mouse

melanoma B16F10 and tumor angiogenesis in the model of the chorioallantoic membrane. *Russ. J. Dev. Biol.* 41. doi:10.1134/S1062360410040028.

Zijlstra, A., D. Mikolon, and D.G. Stupack. 2007. Angiogenesis Assays in the Chick. *In* Angiogenesis Assays: A Critical Appraisal of Current Techniques. 183–201.

Zirngibl, R.A., Y. Senis, and P.A. Greer. 2002. Enhanced Endotoxin Sensitivity in Fps/Fes-Null Mice with Minimal Defects in Hematopoietic Homeostasis. *Mol. Cell. Biol.* 22:2472–2486. doi:10.1128/MCB.22.8.2472-2486.2002.

Zoubeidi, A., J. Rocha, F.Z. Zouanat, L. Hamel, E. Scarlata, A.G. Aprikian, and S. Chevalier. 2009. The Fer tyrosine kinase cooperates with interleukin-6 to activate signal transducer and activator of transcription 3 and promote human prostate cancer cell growth. *Mol. Cancer Res.* 7:142–155. doi:10.1158/1541-7786.MCR-08-0117.

Zuo, Z., T. Syrovets, F. Genze, A. Abaei, G. Ma, T. Simmet, and V. Rasche. 2015. High-resolution MRI analysis of breast cancer xenograft on the chick chorioallantoic membrane. *NMR Biomed.* 28:440–447. doi:10.1002/nbm.3270.

Appendices

Appendix A: Additional representative fluorescence micrographs depicting Control and FER 9 cell invasion into the CAM mesoderm

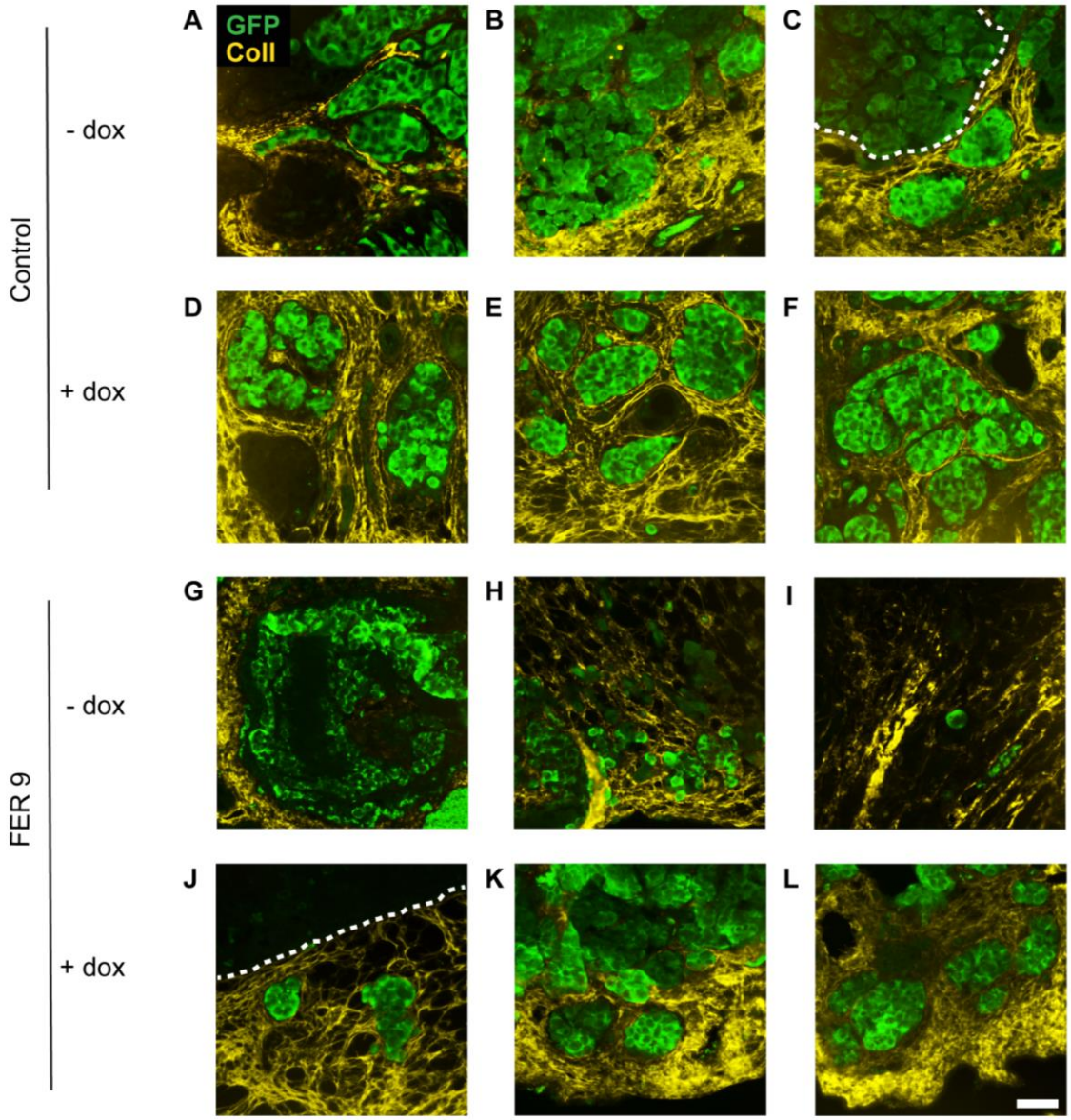
A
GFP
Coll
B
C
Control
- dox
D
E
F
+ dox
G
H
I
FER 9
- dox
J
K
L
+ dox

Figure A1. Control and FER 9 tumour cell invasion into the CAM mesoderm

Control and FER 9 cells (previously cultured in the presence or absence of dox) were grafted on E11 CAMs and then cultured for 7 days to promote tumour growth. On E18, tumours were excised and processed for immunohistochemistry analysis. Ten serial sections for each tumour were analysed for GFP immunoreactivity within collagen III-positive areas, indicative of 5B1 cell invasion into the CAM mesoderm. Micrographs illustrate Control and FER 9 tumour cell invasion into the CAM. **A-C** are micrographs of 3 different Control -dox tumours (tumours formed from Control cells cultured in the absence of dox). **D-F** are micrographs of 3 different Control +dox tumours (tumours formed from Control cells cultured in the presence of dox). **G-I** are micrographs of 3 different FER 9 -dox tumours (tumours formed from FER 9 cells cultured in the absence of dox). **J-L** are micrographs of 3 different FER 9 +dox tumours (tumours formed from FER 9 cells cultured in the presence of dox). The white dotted line outlines the tumour-CAM interface. White bar = 64 µm.

Appendix B: Additional representative fluorescence micrographs depicting endothelial cell localization to FER 9 tumours

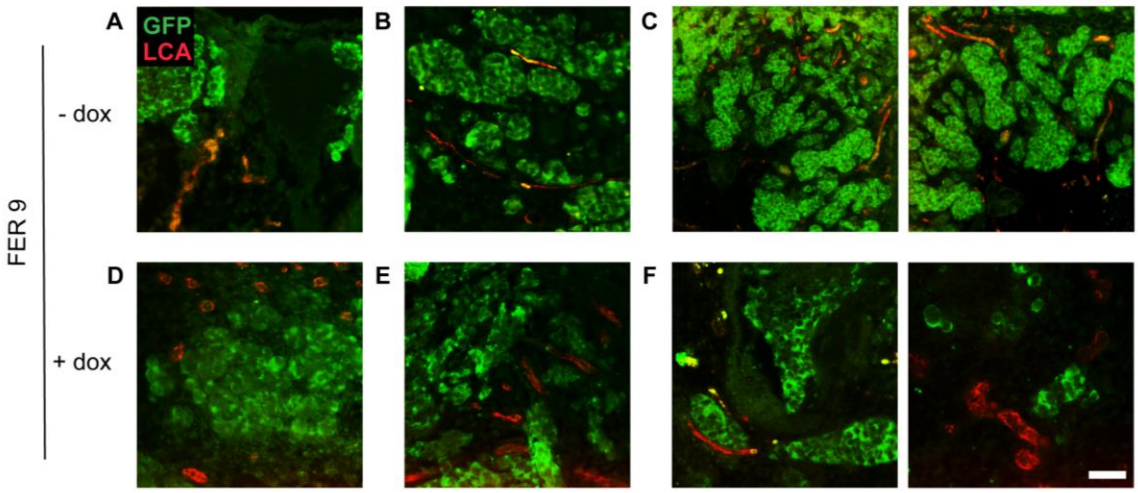

Figure B1. Endothelial cell localization to FER 9 tumours.

FER 9 cells (previously cultured in the presence or absence of dox) were grafted on E11 CAMs and then cultured for 7 days to promote tumour growth. On E18, rhodamine-labeled LCA was injected into a blood vessel of the CAM, tumours were excised and processed for immunohistochemistry analysis. Tumour specific regions, identified as areas not expressing collagen III, were analysed for rhodamine-LCA fluorescence, indicative of endothelial cells. Micrographs illustrate endothelial cell localization to FER 9 tumours. **A-C** are micrographs of 3 different FER 9 -dox tumours (tumours formed from FER 9 cells cultured in the absence of dox) and **D-F** are micrographs of 3 different FER 9 +dox tumours (tumours formed from FER 9 cells cultured in the presence of dox). **C.** Micrographs of 2 different areas of the same FER 9 -dox tumour. **F.** Micrographs of 2 different areas of the same FER 9 +dox tumour. White bar = 64 µm.

Curriculum Vitae

Name:	Shinthujah Arulanantham
Post-secondary Education and Degrees:	Western University London, Ontario, Canada 2016-2018 M.Sc. Western University London, Ontario, Canada 2012-2016 B.MSc.
Honours and Awards:	Ontario Graduate Scholarship 2016-2017 Physiology and Pharmacology Research Day Poster Presentation Winner in the Cancer Biology Category 2017
Related Work Experience:	Teaching Assistant Western University 2016-2017

Presentations:

Arulanantham S., Ivanova I and Dagnino L. The role of FER kinase in melanoma metastasis. London Health Research Day: March 2016 and March 2017. London, ON, Canada.

Arulanantham S., Ivanova I and Dagnino L. The role of FER kinase in melanoma growth and invasion. Oncology Research and Education Day: June 2016 and June 2017. London, ON, Canada.

Arulanantham S., Ivanova I and Dagnino L. The role of FER kinase in melanoma growth and invasion. Physiology and Pharmacology Research Day: November 2016 and November 2017. Western University, London, ON, Canada.